AD_____

Award Number: DAMD17-97-1-7344

TITLE: Pathogenesis of Germline and Somatic NF1 Gene Rearrangements

PRINCIPAL INVESTIGATOR: Karen Stephens, Ph.D.

CONTRACTING ORGANIZATION: University of Washington
Seattle, Washington 98105-6613

REPORT DATE: October 2000

TYPE OF REPORT: Final

PREPARED FOR: U.S. Army Medical Research and Materiel Command
Fort Detrick, Maryland 21702-5012

REPORT DOCUMENTATION PAGE

OMB No. 074-0188

1. AGENCY USE ONLY (Leave blank)	2. REPORT DATE	3. REPORT TYPE AND DATES COVERED
	October 2000	Final (30 Sep 97 - 29 Sep 00)

4. TITLE AND SUBTITLE
Pathogenesis of Germline and Somatic NF1 Gene Rearrangements

5. FUNDING NUMBERS
DAMD17-97-1-7344

6. AUTHOR(S)
Karen Stephens, Ph.D.

7. PERFORMING ORGANIZATION NAME(S) AND ADDRESS(ES)
University of Washington
Seattle, Washington 98105-6613

E-MAIL:
millie@u.washington.edu

8. PERFORMING ORGANIZATION REPORT NUMBER

9. SPONSORING / MONITORING AGENCY NAME(S) AND ADDRESS(ES)
U.S. Army Medical Research and Materiel Command
Fort Detrick, Maryland 21702-5012

10. SPONSORING / MONITORING AGENCY REPORT NUMBER

11. SUPPLEMENTARY NOTES
This report contains colored photos

12a. DISTRIBUTION / AVAILABILITY STATEMENT
Approved for public release; Distribution unlimited

12b. DISTRIBUTION CODE

13. ABSTRACT *(Maximum 200 Words)*

We have identified novel rearrangements of the NF1 gene in germline and somatic tissues of patients with neurofibromatosis type 1. Germline microdeletions are caused by recombination between repeated elements flanking the NF1 gene. Our data provide strong support for a novel gene within 1 Mb of NF1 that potentiates neurofibromagenesis. Our clinical and molecular analyses of NF1 deletion patients suggest that at least some NF1 microdeletions may be predictive for an early age at onset and heavy burden of cutaneous neurofibromas. We identified a patient who is mosaic for an NF1 microdeletion, which proves that these rearrangements can occur in somatic tissues and that mosaicism may be more prevalent than expected. We have identified novel somatic rearrangements in leukemic cells of NF1 children that arise by double mitotic recombination with clustered breakpoints. Because both the germline and somatic rearrangements involve not only the NF1 gene but many other contiguous genes, our data implicate other elements/loci that play an important role in sporadic cases of NF1 and in somatic inactivation of NF1 during leukemogenesis and possibly during other NF1-associated neoplasms. In addition, these results have direct implications for rationale design of putative therapies.

14. SUBJECT TERMS	15. NUMBER OF PAGES
Neurofibromatosis	75
	16. PRICE CODE

17. SECURITY CLASSIFICATION OF REPORT	18. SECURITY CLASSIFICATION OF THIS PAGE	19. SECURITY CLASSIFICATION OF ABSTRACT	20. LIMITATION OF ABSTRACT
Unclassified	Unclassified	Unclassified	Unlimited

Table of Contents

INTRODUCTION

Neurofibromatosis type 1 is a common autosomal dominant tumor-susceptibility disorder. Virtually every affected individual develops benign cutaneous neurofibromas, while the development of other tumors such as plexiform neurofibromas, malignant myeloid disorders, and neurofibrosarcomas are a less common complication (Friedman and VM, 1999; Shannon *et al.*, 1994). The subject of this research project is to investigate the genetic mechanisms and pathology underlying both germline and somatic microdeletions involving the NF1 gene. Two hypotheses will be tested. In 1994, we hypothesize that the early age at onset of cutaneous neurofibromas observed in patients with a germline NF1 microdeletion (Kayes *et al.*, 1994; Kayes *et al.*, 1992; Leppig *et al.*, 1997; Leppig *et al.*, 1996) was caused by co-deletion of NF1 and a gene that potentiates neurofibromagenesis (NPL). To test this hypothesis, we will ascertain additional deletion patients, construct a fine map of the region, map each patient's deletion breakpoints, and look for genotype/phenotype correlations. Secondly, children with NF1 are at increased risk of malignant myeloid disorders (Miles *et al.*, 1997; Mulvihill, 1994; Shannon *et al.*, 1994). Among such cases, approximately 50% of the primary leukemic cells showed loss of constitutional heterozygosity (LOH) at the NF1 locus (Shannon *et al.*, 1994). We recently identified a patient whose LOH resulted from the novel somatic rearrangement of interstitial isodisomy, presumably due to double mitotic recombination. The novelty of this rearrangement led us to hypothesize that it may be a frequent mechanism of LOH at the NF1 locus and/or contribute directly to leukemogenesis. To test this hypothesis, we proposed to ascertain additional patients, map the loci on chromosome 17 that showed LOH, determine parental origin of allelic loss, and determine the underlying molecular mechanism of the somatic rearrangements and their contribution to malignancy.

BODY

We posited two hypotheses in this research project:

1. Deletion of a critical region contiguous to the *NF1* gene predisposes to an early onset and/or large numbers of cutaneous neurofibromas.
2. A novel chromosomal rearrangement in a precursor cell, which results in somatic uniparental disomy of the NF1 region, may be a frequent even that contributes to development of malignant myeloid disorders in NF1 patients.

Technical Objective 1. To identify additional patients with large germline *NF1* deletions.

The timeline for accomplishing Objective 1 was altered for two important reasons. We chose to first focus on and complete Objective 2 and 3 (see below) because samples were available earlier than expected and the results were so exciting. In addition, the identification of multiple low copy repeat elements flanking the NF1 gene (see Objective 2) presented serious unanticipated problems in choosing markers 5' and 3' of NF1 for gene dosage assay. The rational and optimal design of primers for single copy loci for gene dosage assays depended upon completing our mapping and sequence analysis of all the repeats.

Task 1 (months 1-6): Develop and optimize an *NF1* gene dosage PCR assay for detecting deletions at the 5' end of the gene.

Our previous PCR gene dosage assay for exon 32 of the NF1 gene was performed manually with radioactive labeling, co-amplification of cloned control sequences, gel electrophoresis, and product quantitation by phosphorimage analysis. To bypass the significant time required to construct and clone the proper control sequences for each locus, and the time consuming aspects of the assay, we developed an

automated fluorescent PCR gene dosage assay that can quickly be adapted for NF1 or even anonymous loci across the deleted region.

Automated gene dosage assay. The first automated assay we developed was using the ABI 7700 instrument. The accumulation of PCR product during amplification can be quantitated by measuring the increase in fluorescence of a dye such as SYBR green I when bound to double-stranded DNA. Real-time detection of PCR is accomplished with the use of an ABI sequence detection system 7700, which has a built-in thermal cycler. Fluorescence emissions are guided through 96 individual fiber optic cables after excitation by a laser and detected by a CCD camera. The amount of SYBR green fluorescence is compared to an internal passive reference, ROX, during each PCR cycle. During the initial cycles of amplification, little or no change in fluorescence is detected, which represents a baseline. When the fluorescence signal reaches a fixed threshold above the baseline, a fractional CT (threshold cycle) can be determined. The comparison of CT values between a control disomic locus and a target locus can be used to determine the relative quantity or starting copy number of a given template.

We have developed a SYBR green gene dosage assay to detect NF1 microdeletions from genomic DNA. Primers designed to amplify a 55 bp fragment of exon 32 of the NF1 gene and another set specific to a 53 bp segment of exon 8 of the LIS1 (Lisencephaly 1) locus are used to determine the copy number of the NF1 gene. LIS1 is used as the disomic control because all living individuals would be disomic at this locus. To determine whether a patient is disomic or monosomic for NF1, a comparative CT calculation is made. First, the difference of CT values for LIS1 and NF1 is determined for a sample known to be disomic for NF1. Second, the same calculation is made for an "unknown" sample. These "difference" values are used in the standard formula, $2^{-\Delta\Delta CT}$ (Figure 1-1.). Values near 0.5 would represent NF1 monosomy, while values approaching 1.0 would designate disomy. We have established reference ranges for monosomy ranging from 0.35 to 0.65 and disomy from 0.85 to 1.15. A sample of the ABI SDS 7700 data output and comparative CT calculation for the NF1 exon 32 assay is shown in Figure 1-1.

The second automated gene dosage assay employed the LightCycler instrument, which we found required fewer replicate samples and was better at quantitation of copy number for the "intermediate" or mosaic cases (see below). Our exciting research on NF1 microdeletion was instrumental in the Division of Medical Genetics purchasing the LightCycler instrument. Real-time detection of PCR product is accomplished by the LightCycler™ , which measures fluorescence by exciting a fluorophore with a light-emitting diode and detecting the emitted flourescent light. At the end of each amplification cycle, the amount of flourescence is measured, recorded, and plotted in an amplification curve. Figure 1-2 displays the amplification curves for five samples that were used to generate the standard curve below. The LightCycler™ software, using the second derivative maximum algorithm, calculates a fractional cycle or "crossing point" (Cp) value at which the rate of fluorescence increase is the fastest. This is typically the cycle when the fluorescence rises above background. The Cp values from a set of external DNA standards of known copy number analyzed with each set of unknown reactions are used to construct a standard curve. The starting copy number of unknown samples can be determined by simply plotting their respective Cp values on the standard curve (Figure 1-2).

Based on our map of the NF1 region and the identification of single copy loci, we chose 3 loci that were 5' to NF1 and 3 loci 3' to NF1 to convert into gene dosage assays. From these, the loci FB12A2 (5')and N25049 (3') were was optimal for technical reasons and because they were located the closest to the NF1 gene. A sample of the results of gene dosage assays for FB12A2, NF1 exon 32, and N25049 for 10 known microdeletion patients is shown in Figure 2-2. All loci gave gene dosage values near 1.0 for normal control individuals. These are the 3 assays that are currently being used to test our NF1 patient population for deletions (see below).

Task 2 (months 4-7): assay the ~105 DNA samples currently in the lab for 3' *NF1* deletions.

We began screening our collection of NF1 patients and have identified 5 patients with NF1 microdeletions. This screening was performed using the manual NF1 PCR gene dosage assay developed in

my laboratory. These 5 patients were included in our detailed deletion analysis described in Objective 2. A manuscript detailing both the gene dosage PCR assays and the patient phenotypes was submitted (K. Maruyama, M. Weaver, K.A. Leppig, R. Farber, A. Aylsworth, Michael Dorschner, J. Ortenberg, A. Rubenstein, L. Immken, E. Haan, C. Curry and K. Stephens. Quantitative PCR gene dosage assay for detection of NF1 contiguous gene deletions). However, the manuscript reviewers did not like having both gene dosage and clinical data in one manuscript. We think this is critical to understanding the results. This manuscript is not being re-written for submission to another journal. In summary, 30 patients with early onset neurofibromas, atypical facial features, mental retardation, and/or other findings suggestive of a contiguous gene deletion were screened with a gene dosage assay of NF1 exon 32. The assay predicted that 21 patients were disomic at *NF1*, 6 monosomic at *NF1*, and 3 were of "intermediate" *NF1* zygosity. Fluorescent *in situ* hybridization and somatic cell hybrid analyses provided physical confirmation that the 6 apparent monosomic patients were deleted for about 1- 2 Mb, which spanned an entire *NF1* allele and contiguous flanking regions. Clinical features and photographs of the patient's facies document their phenotypes. The patients with "intermediate *NF1* zygosity" are currently being analyzed by the more sensitive gene dosage assays to determine if they are mosaic for an NF1 microdeletion.

Task 3 (months 1-25): Obtain pathological tissue samples or purified DNA from NF1 clinic patients: perform the 5' and 3' NF1 gene dosage PCR assays for all samples; calculate the NF1 gene dosage to identify deletion patients.

We are currently completing this task. It was necessary to delay the development of, and subsequent screening with, the gene dosage assays for FB12A2, NF1 exon 32, and N25049 due to the complexity of repeated sequences in the region. In addition, we discovered that it was necessary to re-purify all of the DNA sample to get optimal assay results. We are currently screening about 200 patient from our NF1 population with each assay using the LightCycler as described above. We anticipate that this major screening effort will be complete by the end of November, 2000.

The results of assay of NF1 exon 32 in 54 patients are intriguing. In these cases, 42 (77%) patients are predicted to be disomic at exon 32 of NF1, 2 (4%) monosomic, and 11 (20%) of "intermediate zygosity". Patients showing "intermediate zygosity" values will be re-assayed and analyzed further. These patients may represent deletion mosaics. This is quite possible based on the gene dosage value of 0.7 obtained from the one documented deletion mosaic patient identified to date (see below).

Task 4 (months 20-25): Determine the frequency of *NF1* deletions. Write a manuscript on deletion screening protocol and frequency.

Upon completion of Task 3, we anticipate two manuscripts regarding the frequency of NF1 deletions. One will address the frequency and phenotype of patients with germline deletions. In addition, our preliminary work suggests that there may be a significant number of patients that are mosaic for NF1 deletions.

Technical Objective 2: Identify a critical deletion region associated with early onset of neurofibromas.

Manuscripts appended describing the final results of Objective 2 studies:

1. Shen S, Battersby S, Weaver M, Clark E, Stephens K, Harmar AJ. 2000. Refined mapping of the human serotonin transporter (SLC6A4) gene within 17q11 adjacent to the CPD and NF1 genes. Eur J Hum Genet 8:75-78.
2. Dorschner MO, Sybert VP, Weaver M, Pletcher BA, Stephens K. NF1 microdeletion breakpoints are clustered at flanking repetitive sequences. Hum Mol Genet 9:35-46, 2000.

All of the following tasks were completed. The results are described in (Dorschner *et al.*, 2000), (Shen *et al.*, 2000), and below.

Task 1 (months 1-12): Map the location of additional loci to the *NF1* region by somatic cell hybrid analysis; identify any physical intervals that lack markers.

Task 2 (month 13-14): Write a manuscript describing the physical map of the *NF1* region; assess the need for identification and mapping of new marker loci to certain physical intervals. If necessary, obtain YACs, PACs, cosmids of the intervals.

Task 3 (months 14-20): Perform FISH to confirm that the large physical clones map to the interval of interest. Make a plasmid library, screen for single copy clones, sequence, and design primers to map new markers on somatic cell hybrid panels to the critical interval.

Task 4 (months 1-30): Construct hybrid cell lines from lymphoblasts of newly identified deletion patients; delineate the extent of the deletions by genotyping of regional markers on hybrid lines.

Task 5 (months 20-36): Determine if there is a correlation between deletion extent and age of onset of neurofibromas; write a manuscript of study results; assess whether an *NF1* gene dosage PCR assay or FISH assay to detect deletion of the critical region has sufficient predictive value to warrant development of a diagnostic test.

Tasks 1,2, 3, 4. To accomplish this objective and identify a critical deletion region associated with early onset of neurofibromas, it was essential to construct a physical map of the NF1 region that was involved in the deletion. Therefore, significant effort was committed to map construction. Our progress in this objective is best depicted graphically. Figure 2-1 shows the state of the 1st generation physical map we had constructed in 1997, when the grant application was submitted. The 2nd generation map was published in the year 2000 (Dorschner *et al.*, 2000). The current status of the map (3rd generation) is shown in Figure 2-2. Construction of this map required the work outlined in Tasks 1,2,3,and 4; details of our results were published (Dorschner *et al.*, 2000). In addition, details of map construction centromeric to the NF1 deletion region were published elsewhere (Shen *et al.*, 2000).

Tasks 4 and 5. This physical map facilitated our mapping of the deletion breakpoints in somatic hybrid cell lines carrying the deleted chromosome 17 for each of 21 unrelated patients. As detailed in our manuscript (Dorschner *et al.*, 2000) and including additional patients, the centromic and telomeric deletion breakpoints of 17 (80%) patients were clustered in low copy repeat elements that we termed NF1REPs. These elements are ~75 kb in length, share >97% sequence identity, and are in direct orientation as shown in the abbreviated map in Figure 2-3. In these patients, the deletions were 1.5 Mb in length. We proposed that these deletions arose by homologous recombination between the proximal element, NF1REP-P, and the medial element, NF1REP-M (Dorschner *et al.*, 2000). Recombination could occur by unequal sister chromatid exchange or by intrachromosomal "looping out". The remaining 4 patients had at least one breakpoint outside of an NF1REP element; one (UWA113-1) had a smaller deletion thereby narrowing the critical region harboring the putative neurofibroma-potentiating locus (NPL) to 1 Mb (Dorschner *et al.*, 2000). The physical features of the 17 NF1 microdeletion patients were summarized (Dorschner *et al.*, 2000). All patients showed an early onset of cutaneous neurofibromas or excessive number of such tumors in adults in whom the age at onset could not be determined. There were no obvious differences detected between the features present in those individuals with the common NF1 deletion and the three with deletions of different lengths. No single feature was present or absent consistently within either group. The location of the putative NPL gene was narrowed to an interval of 1 Mb between FB12A2 and SH3GLP1, as defined by the deletion of patient UWA113-1 (Dorschner *et al.*, 2000). This critical region is known to harbor 4 genes, 2 pseudogenes, and 7 ESTs.

Consistent with our observations it was possible that the NPL locus was interrupted by the breakpoints of the 17 clustered deletions and completely deleted in the remaining patients. For this reason, and for an understanding of how these deletions occur, it was important to map the breakpoints in the NF1REP. Our strategy, outlined in Figure 2-4, was to design primers about every 10 kb using the known

sequence of NF1REP-P, amplify and sequence the deleted chromosome of the patients and search for sequence differences that suggest we had "walked" into NF1REP-M. Simultaneously, we were sequencing BACs harboring the NF1REP-M. This strategy was successful and we identified two paralogous recombination sites (PRS; see Figure 2-5). Four recombination events occurred at PRS-1, while 13 occurred at PRS-2. Sites PRS-1 and –2 were 3 and 6 kb in length, respectively, and located about 20 kb apart within the NF1REPs. Therefore, deletions occurred by homologous recombination between PRS in each REP as shown in Figure 2-5. Breakpoints at the PRS-2 were analyzed in detail using single nucleotide polymorphisms (SNP) specific for NF1REP-P and –M that we identified by sequence analysis of patients and normal controls. In Figure 2-5A, the black bar represents the region in which the recombination occurred between NF1REP-P (green) and NF1-REP-M (hatched green). Eight of nine recombinations occurred in a 2 kb region near two GA rich regions (blue). We speculate that these regions may predispose the region to recombination via changes in secondary structure. The unusual pattern for patient UWA156-1 shown in Figure 2-5A is most likely due to gene conversion, which occurred during the double strand break repair. No genes were found at or near the breakpoints in the NF1REP. It is notable that despite ~ 50 kb of near identical DNA sequence between the two NF1REPs, the breakpoints occur preferentially at PRS-1 and –2. Figure 2-6 shows a cartoon comparing the structures of NF1REPS-P and –M and the location of the PRS.

We have also identified additional low copy repeats in the NF1 region that facilitate deletions in two other important patients (Figure 2-7). First, NF1REP-P2, the second proximal paralogs, is located near the NF1 gene. The deletion of patient UWA113-1 occurred by recombination between NF1REP-P2 and –M. Based on this smallest deletion, we narrowed the location of NPL as detailed above. Because this was based on a single case, it was important to demonstrate that this conclusion was valid. Our findings above validate our narrowing of the NPL region by demonstrating that the deletion in UWA113-3 was a simple deletion of contiguous sequences, rather than a complex rearrangement. Second, two repeats whose sequences are unrelated to NF1REP have been identified; these are shown as blue boxes adjacent to NF1REP-P1 and –M (Figure 2-7). These are the site of the *somatic* deletion breakpoint in an NF1 patient. This patient had no findings of the disorder until her mid-20s when she had a dramatic and rapid onset of hundreds of cutaneous neurofibromas. Delayed onset would be predicted in a patient who is mosaic for an NF1 microdeletion. These data provide strong support for our hypothesis that co-deletion of NF1 and the putative NPL gene exacerbates neurofibromagenesis. By age 80, this patient was virtually covered with tumors.

During the construction of the physical map of the NF1 deleted region, we also identified other NF1REP elements in the genome. The location of these elements is depicted in Figure 2-8. The homology of NF1REP-D at 17q24 to other elements is shown in Figure 2-6.

Task 5. Three lines of evidence show a correlation between deletion extent and age of onset of neurofibromas: the germline deletion patients we, and others, have analyzed (Correa *et al.*, 1999; Dorschner *et al.*, 2000), the mosaic deletion patient we identified with delayed onset of cutaneous neurofibromas, and a single patient with a deletion confined to NF1 that does not show early tumor onset (Correa *et al.*, 1999). The correlation between early age at onset of neurofibromas and microdeletion can, at this time, only apply to those patients that are known to have NF1REP-mediated deletions. This indicates that FISH with an NF1 probe, which is being offered at some institutions as a diagnostic test, is probably not very specific. In collaboration with Dr. Eric Legius (University Hospital Gasthuisberg, Leuven, Belgium), we have developed oligonucleotide primers for amplification of deletion breakpoint junctions that occur in a portion of the PRS-2. In addition, Dr. Dorschner in my laboratory has developed primers for specific amplification of junction fragments for deletions anywhere in PRS-1 and in PRS-2. Further work to confirm the sensitivity and specificity of these assays is needed before they can be used for clinical diagnostic testing. In addition, we need to complete the screening of non-selected NF1 patients by gene dosage PCR (Objective 1) and with the PRS-1 and –2 specific assays to determine if some patients carrying deletions present with conflicting phenotype. Furthermore, we do not know if these rearrangements may occur in the blood cells of normal individuals. Therefore, while our results are

exciting and we hope that our work will provide a basis for a rapid, sensitive and specific test for NF1 patients, the scientific groundwork for such a test has yet to be firmly laid.

Technical Objective 3: To determine if somatic uniparental disomy (UPD) of the *NF1* region is a frequent event in leukemic tumor tissue and to investigate somatic mechanisms of uniparental disomy.

Manuscripts appended describing the final results of Objective 3 studies:

1. Stephens K, Weaver M, Leppig KA, Maruyama K, Emanuel PD, Davis EM, Espinosa III R, Le Beau MM, Shannon KM. Tumor suppressor inactivation by double mitotic recombination at clustered breakpoint intervals. Nature Genet, submitted.
   This manuscript has been provisionally accepted as an article in Nature Genetics pending our responses to the reviewers and editor. Responses and revisions have been submitted and are currently under review. The appended manuscript is the revised version currently under consideration.
2. Cooper LJN, Shannon KM, Loken MR, Weaver M, Stephens K, Sievers EL. Evidence that juvenile myelomonocytic leukemia can arise from a pluripotential stem cell. Blood 96:2310-2313, 2000.

Task 1 (months 1-12): Obtain additional tumor samples and determine their *NF1* gene dosage by the gene dosage PCR assay; confirm by *NF1* FISH that tumors predicted to undergo LOH by UPD have two *NF1* alleles, while those predicted to result from LOH by deletion have one *NF1* allele; determine the frequency of UPD-LOH.

Leukemic tissues from 10 additional children with NF1 who also developed malignant myeloid disease were obtained. This was a significant accomplishment for these rare cases, which have an incidence in the United States of about 10/yr. To determine the zygosity of NF1, the tumors were analyzed by an NF1 gene dosage assay developed in this lab and by interphase FISH of cryopreserved bone marrow (Stephens et al., submitted). The frequency of UPD-LOH (later termed isodisomy) was 80% (n=10), with 20% of cases cause by deletion.

Task 2 (months 10-25): Map the extent of each uniparental disomy region; assay normal tissue for mosaicism for the UPD of the *NF1* region; write a manuscript addressing mechanisms of UPD-LOH.
The patterns of LOH at chromosome 17 loci were analyzed to gain insight into the mechanisms leading to allelic loss of *NF1* in primary leukemia cells of NF1 children. Our analyses showed that LOH occurred by two distinct mechanisms, each of which resulted in loss of the normal *NF1* allele. Eighty percent (n=10) of leukemias with LOH resulted from isodisomy (called UPD-LOH in the original application) for a >60 Mb chromosomal segment harboring a defective *NF1* allele. In at least 4 of these cases, we were able to prove unambiguously that the isodisomic segment (UPD) was interstitial to the chromosome 17q arm. Two cases resulted from interstitial deletion. Therefore, we found that isodisomy for NF1 and the majority of chromosome 17 is the predominant mechanism (80%), with 20% of cases due to 1-2 Mb interstitial deletion (Stephens et al., submitted).
Unexpectedly, both the centromeric and telomeric LOH breakpoints were clustered at the same marker intervals.

This is the first report of interstitial isodisomy at common breakpoints as a mechanism of LOH in any tumor. We propose that interstitial isodisomy arose by a double mitotic recombination event between non-sister chromatids during the S/G2 phase of the cell cycle of an ancestral cell. The clustering of the both LOH breakpoints suggests the existence of recombination-prone sequences in these regions of chromosome 17. While functional inactivation of neurofibromin is apparently sufficient for the myeloproliferative phenotype, these data suggest a putative role of modifying locus on chromosome 17 that may contribute to the development of leukemia. This locus may be low copy number repeat sequences that facilitate the homologous mitotic recombination events leading to LOH (Stephens et al., submitted).
Our analyses of an additional patient support the hypothesis that JMML can arise in a pluripotent hematopoietic cell We have also mapped the LOH region in different tissues from a child with juvenile monomyelocytic leukemia

(JMML), who later developed a T cell lymphoma. We demonstrated that the mechanism of LOH was by an interstitial deletion and that the LOH regions were identical in length in the B cells, lymph node, and sorted cells from the node (Cooper *et al.*, 2000). These data show that the malignant JMML and lymphoid cells shared a common loss of genetic material involving the NF1 gene, suggesting that the abnormal T lymphoid and myeloid populations were derived from a common cell.

Together, these data prove our original hypothesis that a novel chromosomal rearrangement in a precursor cell that results in somatic uniparental disomy (or interstitial isodisomy) of the NF1 region is a frequent event that may contribute to development of malignant myeloid disorders in NF1 patients. The results of our studies also identify new and important questions that should be addressed. How might this unusual mechanism of LOH contribute to leukemia in children with NF1? Are the LOH patterns similar simply because recombination is favored in certain regions or do they reflect the expression of loci or effects of mutagenic agents that may contribute to the development of malignant myeloid leukemias in children with NF1? Perhaps biallelic expression of a gene (or genes) on the q arm is essential for the clonal proliferation of neurofibromin-deficient hematopoietic cells. Therefore, LOH patterns at NF1 are restricted to either a 1-2 Mb interstitial deletion or a large isodisomic segment of the q arm. This would predict that different chromosome 17 LOH regions and mechanisms would be found in other NF1-associated tumors, for example, neurofibromas, malignant peripheral nerve sheath tumors, pheochromocytomas, pilocytic astrocytomas. To date, such analyses have not used a sufficient number of loci to test this prediction. We detected no correlations between extensive isodisomy or confined deletions and a parent of origin effect, leukemia type, or disease course. Thus, our data do not provide a simple explanation for the relative increase in the risk of leukemia in sons who inherit NF1 from their mothers(Miles *et al.*, 1997). No imprinted genes are known to map to human chromosome 17 nor on mouse chromosome 11, which carries all the syntenic sequences with the exception of a handful of loci that are scattered among other mouse chromosomes (Beechey *et al.*, 2000). Recently, noncontiguous loci showing LOH were observed in a kidney cell line treated with hydrogen peroxide, suggesting that oxidative damage can induce complex LOH patterns that are unrelated to tumor suppressor gene inactivation (Turker *et al.*, 1999). Whether oxidative damage increases the mitotic recombination rate or plays a role in development of the leukemias studied here is unknown.

Our results have several broad implications for NF1 and other human tumors. First, interstitial isodisomy may be a frequent but previously unrecognized mechanism in human cancers. The apparent clustering of both isodisomic and deletion breakpoints implies the presence of regions prone to mitotic recombination. Second, sequence analysis and tissue specificity of such putative hotspots would contribute significantly to the poorly understood mechanism of mitotic recombination in mammals. Third, the functional consequences of interstitial isodisomy versus interstitial deletion is basically mono-allelic versus or bi-allelic expression from a locus (loci), other than the tumor suppressor gene itself, which could significantly affect the efficacy of putative therapeutic agents.

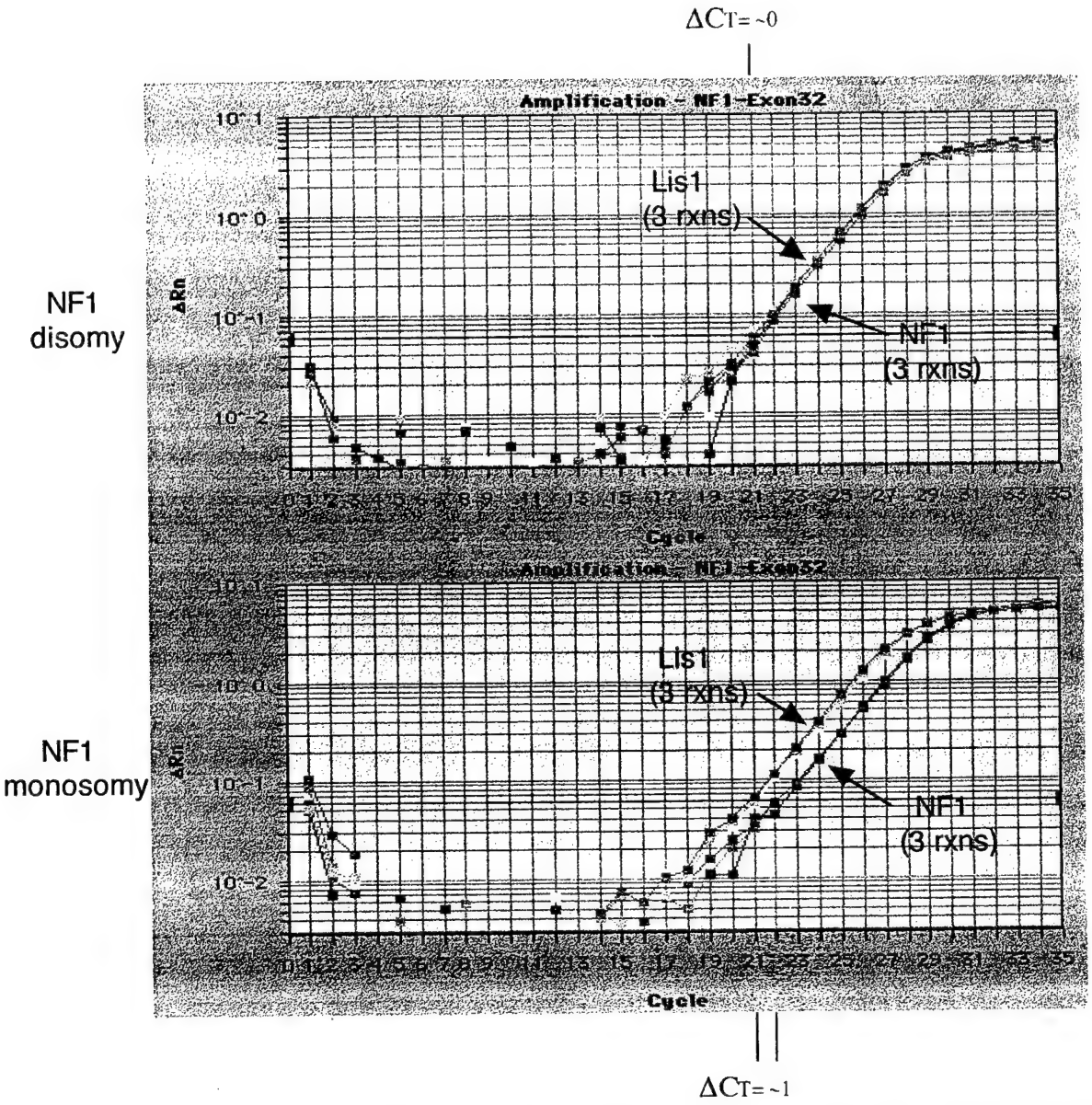

A. Disomic control sample:

Lis1 C_T - Ex32 C_T = 0

21 - 21 = 0

therefore: $\Delta C_T = 0$

B. Unknown sample:

Lis1C_T - Ex32 C_T: = 1

21 - 22 = 1

therefore: $\Delta C_T = 1$

C. Calculate the dosage value:

$$2^{-\Delta\Delta C_T} = 2^{-(1-0)} = 0.5$$

A dosage value of .40 -.60 is consistent with NF1 monosomy
A dosage value of .85- 1.10 is consistent with NF1 disomy

Figure *1-1* : Data output and sample comparative C_T calculation. The panels above show data output from the ABI SDS 7700. Each PCR reaction is run in triplicate and an average C_T is used for dosage calculations. The almost complete overlap of the amplification curves demonstrates the reproducibility of the reactions. Comparison of the amplification curves between *NF1* disomy and monosomy shows a shift of the *NF1* curve from left to right indicating the addtional cycle(s) required to reach the C_T threshold due to the difference in *NF1* copy number.

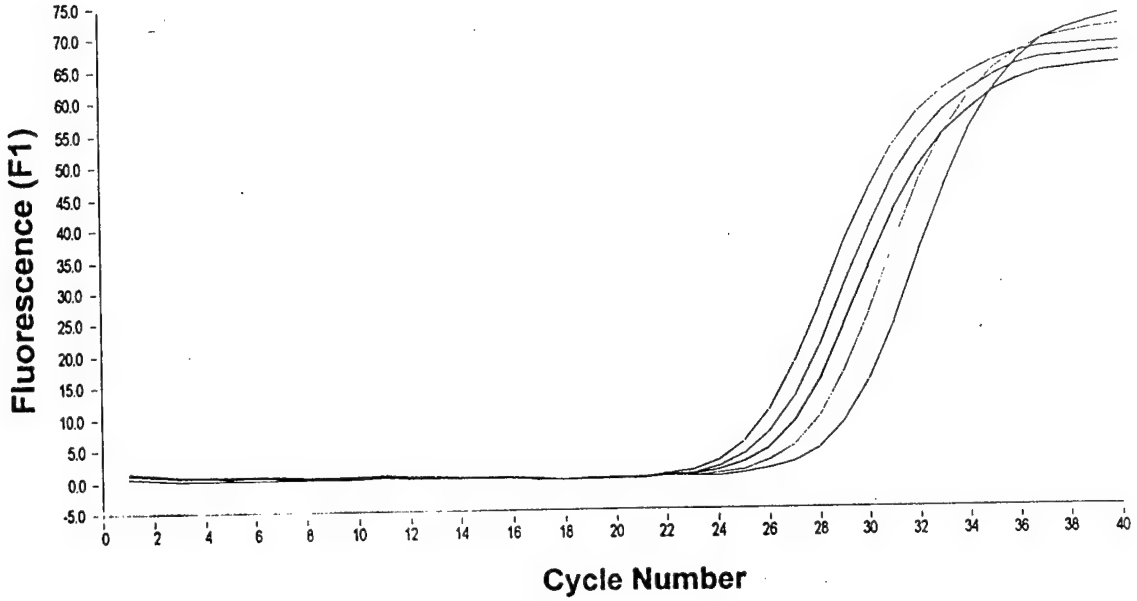

Figure 1-2

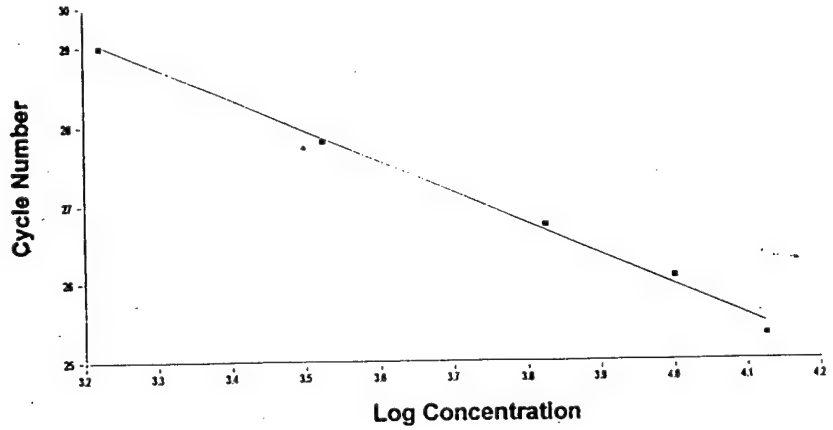

Figure 1-3

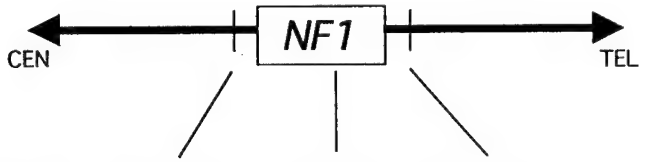

patient	FB12A2	Ex32	N25049
1	0.46	0.46	0.64
2	0.99	0.41	0.5
3	0.57	0.54	0.53
4	0.35	0.42	0.42
5	0.45	0.39	0.41
6	0.44	0.37	0.52
7	0.43	0.36	0.42

Figure 2-1. Status of the physical map of the NF1 deleted region in 1998 when grant application was submitted.

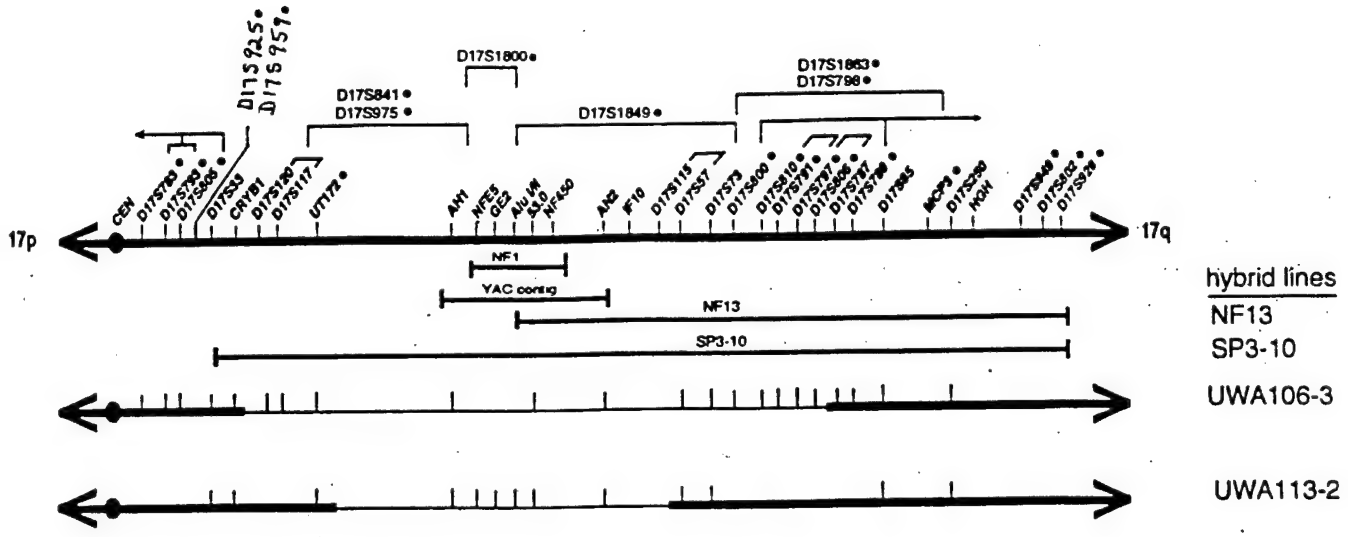

Figure 2-2. Physical contig of the *NF1* region (see next page). The thick black bar is a schematic of the chromosome 17q11.2 region with STS loci placed above the bar and genes and EST loci below. The BAC, PAC, and YAC clones comprising the contig are shown above; open elipses are aligned with the loci on the chromosome schematic and indicate a positive hit in the clone; sequenced BAC/PAC clones are indicated with an asterisk. Vertical bars at the ends of BACs represent termini that were sequenced and submitted to Genbank and converted to amplimers. Scale in Mb is at the top of the figure. The size and extent of microdeletions of NF1 patients are shown below the chromosome; boxes represent flanking repetitive sequences (NF1REP) where the breakpoints mapped.

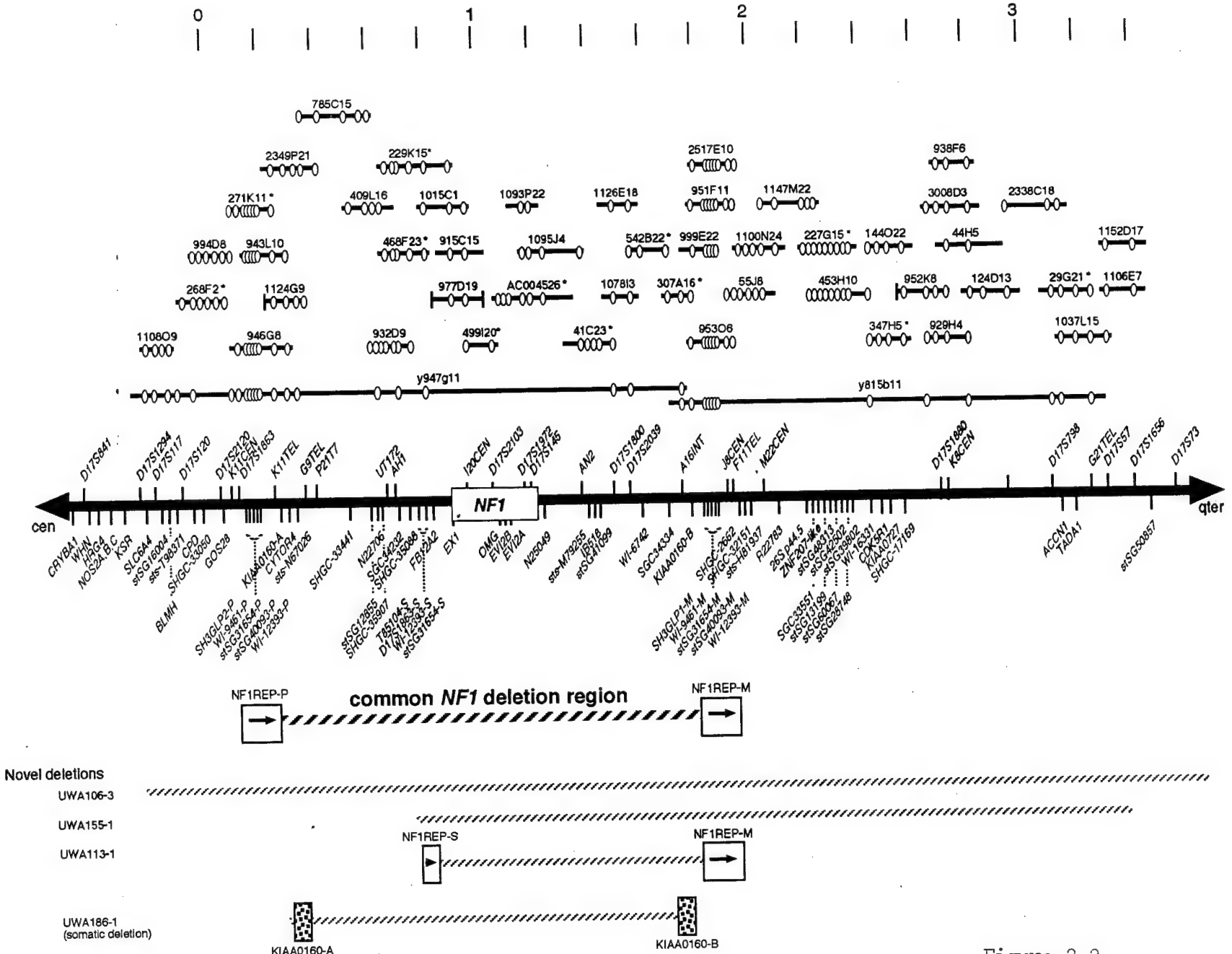
0
1
2
3
785C15
2349P21
229K15*
2517E10
938F6
271K11*
409L16
1015C1
1093P22
1126E18
951F11
1147M22
3008D3
2338C18
994D8
943L10
468F23*
915C15
1095J4
542B22*
999E22
1100N24
227G15*
144O22
44H5
1152D17
268F2*
1124G9
977D19
AC004526*
1078I3
307A16*
55J8
453H10
952K8
124D13
29G21*
1106E7
1108O9
946G8
932D9
499I20*
41C23*
953O6
347H5*
929H4
1037L15
y947g11
y815b11
D17S841
D17S1294
D17S117
D17S120
D17S2120
K111CEN
D17S1863
K111TEL
G9TEL
P2177
UT172
AH1
I20CEN
D17S2103
D17S1972
D17S145
AN2
D17S1800
D17S2039
A16INT
J8CEN
F11TEL
M22CEN
D17S1880
K8CEN
D17S738
G21TEL
D17S57
D17S1656
D17S73
NF1
cen
qter
CRYBA1
WHN
HBG4
NOS2A.B.C
KSR
SLC6A4
stSG16004
sts-T96371
CPD
SHGC-33050
GOS28
BLMH
KIAA0160-A
SH3GLP2-P
WI-9461-P
stSG31654-P
stSG40093-P
WI-12393-P
CYTOR4
sts-N67026
SHGC-33441
N22706
SGC34232
SHGC-35086
FB12A2
EX1
OMG
EVI2B
EVI2A
N25049
sts-M79255
JP518
stSG41089
WI-6742
SGC34334
KIAA0160-B
SHGC-2662
SHGC-33151
sts-H81937
R22783
2SS P44.5
ZNF207-like
stSG48313
stSG42502
stSG39802
WI-16331
CDK5R1
KIAA0727
SHGC-77169
ACCN1
TADA1
stSG50857
stSG12855
SHGC-35907
T85104-S
D17S1863-S
WI-12393-S
stSG31654-S
SH3GLP1-M
WI-9461-M
stSG31654-M
stSG40093-M
WI-12393-M
SGC33551
stSG13199
stSG40067
stSG26748
NF1REP-P
common NF1 deletion region
NF1REP-M
Novel deletions
UWA106-3
UWA155-1
UWA113-1
NF1REP-S
NF1REP-M
UWA186-1
(somatic deletion)
KIAA0160-A
KIAA0160-B

Figure 2-2

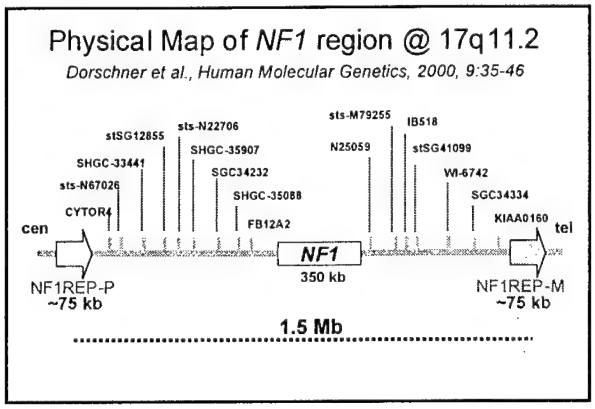

Figure 2-3: Physical Map of NF1 region Dotted line indicates deletion commonly found in NF1 microdeletion patients.

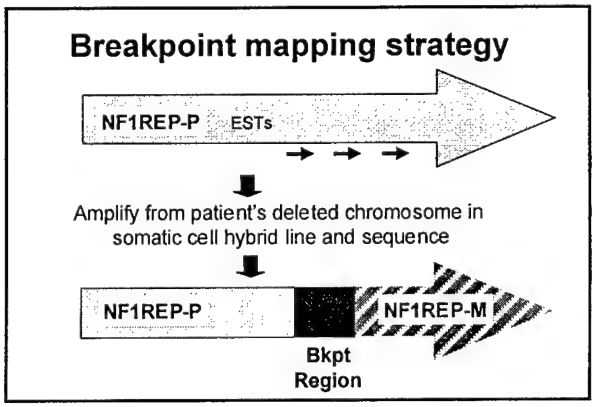

Figure 2-4: Breakpoint strategy

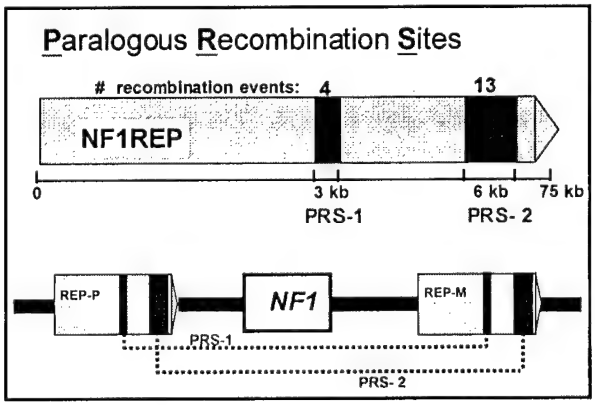

Figure 2-5: Parologous Recombination sites.

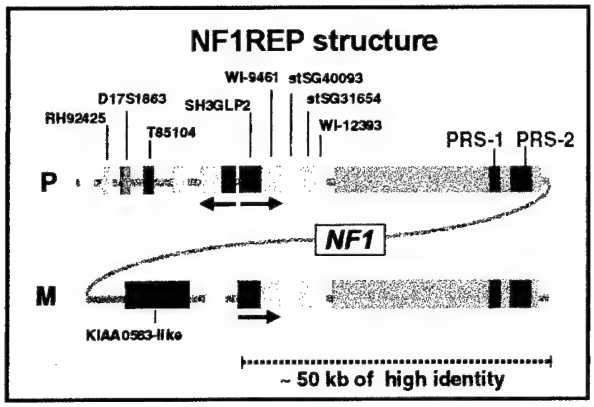

Figure 2-6: NF1 Structure

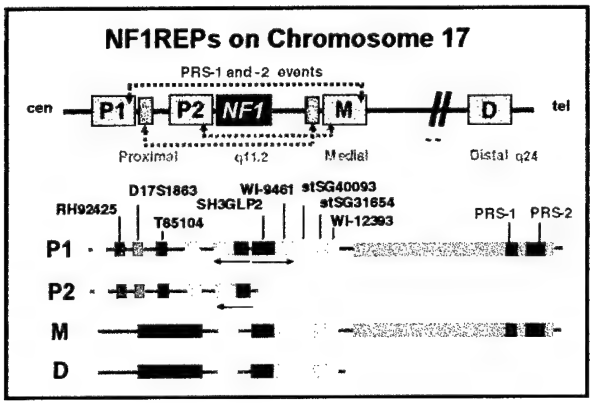

Figure 2-7

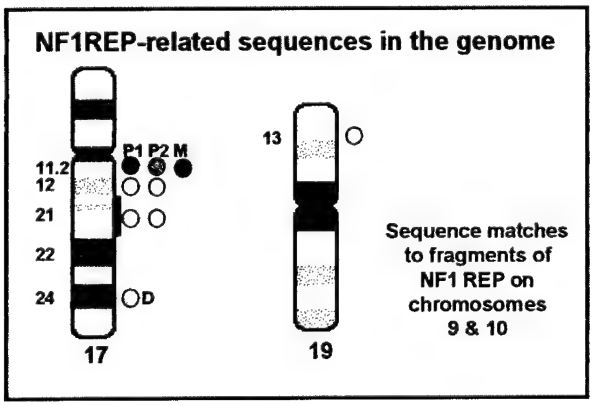

Figure 2-8

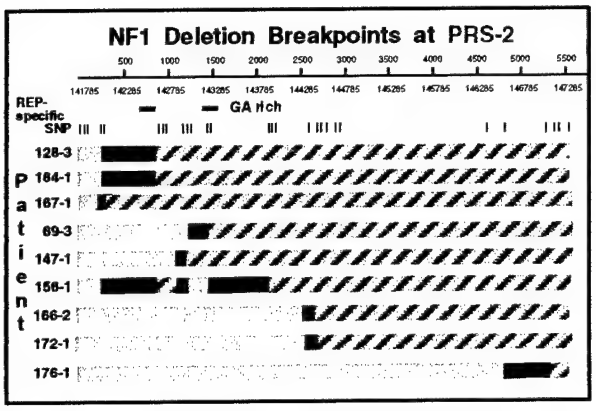
NF1 Deletion Breakpoints at PRS-2
500
1000
1500
2000
2500
3000
3500
4000
4500
5000
5500
141785
142285
142785
143285
143785
144285
144785
145285
145785
146285
146785
147285
REP-specific SNP
GA rich
Patient
128-3
184-1
167-1
69-3
147-1
156-1
166-2
172-1
176-1

Figure 2-5a

KEY RESEARCH ACCOMPLISHMENTS

In Germline NF1 Microdeletions

- Identifying the molecular mechanism of NF1 microdeletion as homologous recombination between ~75 kb paralogous repeats (termed NF1REPS).
- Identifying discrete recombination hotspots within the large NF1REPs
- Identifying a common 2kb recombination hotspot where about 50% of NF1 microdeletion breakpoints occur.
- Identifying the first REP-mediated rearrangement that deletes a tumor suppressor gene. This has broad implications for molecular mechanisms that cause neoplasia.
- Designing and developing PCR assays that detect the deletion junction breakpoints at the two recombination hotspots. This assay will facilitate identifying more deletion patients for research and may provide the basis for a clinical diagnostic test.
- Developing an automated fluorescent quantitative gene dosage assays for rapid identification of patients with NF1 microdeletions.
- Constructing a ~4 Mb physical map spanning the germline NF1 microdeletion.
- Identifying a total of 8 NF1REPs: 3 in NF1 gene region, 2 partial REPS at 17q12, 2 partial REPS at 17q21, 1 REP at 17q24, and 1 REP at 19p. These elements may additional mediate germline or somatic rearrangements.

In Somatic NF1 Rearrangements

- Identifying a novel mechanism of loss of constitutional heterozygosity at NF1 by double mitotic recombination at clustered breakpoint intervals. This mechanism results in interstitial isodisomy in the precursor cell of the malignant clone.
- Showing that this novel LOH mechanism is predominant in leukemias of children with NF1 that also develop malignant myeloid disorders
- Proving that the LOH breakpoints were clustered within specific marker intervals.
- Demonstrating that JMML can arise in a pluripotent hematopoietic cell.
- Identifying an NF1 patient mosaic for a REP-mediated microdeletion. This is the first evidence that such REP-mediated microdeletions can occur in somatic tissue.
- Showing that the mosaic patient had delayed onset of dermal neurofibromas, consistent with our hypothesis that the microdeletions potentiate neurofibromagenesis.

REPORTABLE OUTCOMES

- **Manuscripts**
  1. Dorschner MO, Sybert VP, Weaver M, Pletcher BA, Stephens K. 2000. NF1 microdeletion breakpoints are clustered at flanking repetitive sequences. Hum Mol Genet 9:35-46.
  2. Shen S, Battersby S, Weaver M, Clark E, Stephens K, Harmar AJ. 2000. Refined mapping of the human serotonin transporter (SLC6A4) gene within 17q11 adjacent to the CPD and NF1 genes. Eur J Hum Genet 8:75-78.
  3. Cooper LJN, Shannon KM, Loken MR, Weaver M, Stephens K, Sievers EL. 2000. Evidence that juvenile myelomonocytic leukemia can arise from a pluripotential stem cell. Blood 96:2310-2313.
  4. Stephens K, Weaver M, Leppig KA, Maruyama K, Emanuel PD, Davis EM, Espinosa III R, Le Beau MM, Shannon KM. Tumor suppressor inactivation by double mitotic recombination at clustered breakpoint intervals. Nature Genetics, submitted.
- **Manuscripts in preparation**
  5. López-Correa C, Dorschner MO, Brems H, Lázaro C, Clementi M, Upadhayaya M, Dooijes D, Moog U, Kehrer-Sawatzki H, Rutkowski JL, Fryns J-P, Marynen P, Stephens K, Legius E. A 2 kb meiotic recombination hotspot flanking NF1 microdeletions. In preparation.

6. Maruyama, M. Weaver, K.A. Leppig, R. Farber, A. Aylsworth, Michael Dorschner, J. Ortenberg, A. Rubenstein, L. Immken, E. Haan, C. Curry and K. Stephens. Ascertainment of NF1 microdeletion patients by quantitative PCR. In preparation.

- **Abstracts**
  1. Stephens K, Weaver M, Leppig K, Maruyama K, Side L, Davis EA, Espinosa III R, Le Beau M, Shannon K. 1998. A novel and frequent mechanism of loss of heterozygosity in malignant myeloid cells of NF1 children: Double mitotic recombination at common breakpoint intervals. Am J Hum Genet 63S:A39.
  2. Stephens K, Weaver M, Leppig K, Maruyama K, Side L, Davis EA, Espinosa III R, LeBeau M, Shannon K. 1998. A novel and frequent mechanism of loss of heterozygosity in malignant myeloid cells of NF1 children: Double mitotic recombination at common breakpoint intervals. National Neurofibromatosis Foundation International Consortium for the Molecular Biology of NF1 and NF2, Aspen, CO.
  3. Dorschner MO, Weaver MA, Sybert VP, Stephens KG. 1999. NF1 microdeletions are mediated by homologous recombination between duplicons. Am J Hum Genet 65S:151.
  4. Dorschner MO, Stephens K. 2000. NF1 gene loss by recombination at flanking hotspots. National Neurofibromatosis Foundation International Consortium for the Molecular Biology of NF1 and NF2, Aspen, CO, June, 2000.
  5. Livingston RJ, Stephens K. 2000. A hydropathic complementarity analysis of neurofibromin identifies two protein motifs in potential neurofibromin-interacting proteins. National Neurofibromatosis Foundation International Consortium for the Molecular Biology of NF1 and NF2, Aspen, CO, June, 2000.
  6. Dorschner MO, Leppig KA, Weaver M, Stephens K. 2000. Allelic losses due to recombination between paralogs can occur in somatic cells. Am J Hum Genet 67(Supp 2):23.
  7. Stephens K, Dorschner MO, Friedman CL, Trask BJ, Sybert VP. 2000. Recombination hotspots for NF1 microdeletions. Am J Hum Genet 67 (Supp 2):67.

- **Seminars and Invited Talks.**
  1. K. Stephens. "A novel and frequent mechanism of loss of heterozygosity in malignant myeloid cells of NF1 children: Double mitotic recombination at common breakpoint intervals". American Society of Human Genetics, October, 1998, Denver.
  2. K. Stephens. "Progress on NF1 research at the University of Washington". Washington Chapter, National Neurofibromatosis Foundation, February, 1998. Invited speaker.
  3. K. Stephens. "A novel and frequent mechanism of loss of heterozygosity in malignant nyeloid cells of NF1 children: Double mitotic recombination at common breakpoint intervals". National Neurofibromatosis Foundation Consortium, June, 1998, Aspen, CO.
  4. Washington Chapter, National Neurofibromatosis Foundation, Seattle, WA. 1998.
  5. M. Dorschner. "NF1 microdeletions are mediated by homologous recombination between duplicons." American Society of Human Genetics, October, 1999, San Francisco.
  6. K. Stephens. Medical Genetics Seminar, University of Washington. 1999. "Role of recombination between paralogous repeats in tumorigenesis".
  7. K. Stephens. Washington Chapter, National Neurofibromatosis Foundation, NF Medical Symposium & Annual Membership Meeting, "Different kinds of NF1 gene mutations and what they mean." 1999.
  8. K. Stephens. The British Columbia Neurofibromatosis Foundation, Vancouver, BC. "Other genes that affect the severity of NF1" February, 2000.
  9. M. Dorschner. National Neurofibromatosis Foundation International Consortium on Gene Cloning and Gene Function of NF1 and NF2, Aspen, CO, June, 2000.
  10. M. Dorschner. "Allelic losses due to recombination between paralogs can occur in somatic cells." American Society of Human Genetics, Philadelphia, October, 2000.

11. K. Stephens. American Society of Human Genetics, Philadelphia, October, 2000. "Recombination hotspots for NF1 microdeletions".

- **Invited participant at meetings.**
  K. Stephens, National Neurofibromatosis Foundation International Consortium on Gene Cloning and Gene Function of NF1 and NF2, Boston, 1999
- **Databases**
  We developed a database in FileMaker Pro to track all of the NF1 patients referred for this research study. Fields clinical history, referring physician, tissue available for study, etc.
  We developed a database in FreezerWorks to track the multiple vials of immortalized patient cells that are stored in a liquid nitrogen freezer.
- **Cell lines**
  We have established immortalized lymphoblastoid cell lines for approximately 20 patients and relatives. In addition, we constructed somatic cell hybrids carrying each of a patient's chromosome 17s for 5 cases.
- **Invention Disclosure**
  We have submitted an Invention Disclosure (Form ID-1) with the Office of Technology Transfer at the University of Washington. Title of invention: Diagnosis of neurofibromatosis type 1 microdeletion syndrome. Description: Describes the PCR primers for detection of the deletion junction fragment at site PRS-2. The purpose of this disclosure is to allow the University of Washington to review the putative invention and, if deemed appropriate, to secure intellectual property rights and to fulfill obligations the University may have to external sponsors of research.
- **Funding awarded and pending**
  1. We have been awarded a grant from the U.S. Army Medical Research and Materiel Command.
  Title: Genetic factors that affect tumorigenesis in NF1.
  Principal Investigator: Karen Stephens
  Dates: 10-29-00 to 10-28-03
  2. We have a pending application to the U.S. Army Medical Research and Materiel Command
  Title: QuEST: A New Approach to Molecular Staging of Tumors
  Principal Investigator: Karen Stephens
  Dates: 9/01 to 9/03

CONCLUSIONS

We have determined that very unusual rearrangements involving the NF1 gene occur in both germline and somatic tissues of certain patients. Germline microdeletions of 1.5 Mb are caused by recombination between repeated elements that flank the NF1 gene. Identification of these elements suggests that perhaps a subset of individuals are prone to developing NF1 microdeletion due to individual variation in size, number, or complexity of these repeats. Our data provide strong support for a co-deletion of NF1 and a novel gene that potentiates neurofibromagenesis (NPL) and narrow the chromosomal location of NPL to a 1 Mb interval. We describe the larger number and most detailed clinical description of NF1 deletion patients to date. These data suggest that NF1 microdeletion may be predictive for an early age at onset and large numbers of cutaneous neurofibromas. We have designed and developed PCR primers that detect the deletion junction fragment, these will most likely provide the basis for a diagnostic test for NF1 microdeletion syndrome. We have developed 3 automated PCR-based gene dosage assays to facilitate identification and mapping of NF1 microdeletions. In somatic tissues, we have identified a patient who is mosaic for an NF1 microdeletion. This proves for the first time that these rearrangements occur in somatic tissues and that somatic mosaicism may be more prevalent among NF1 patients than we might have predicted. We describe for the first time somatic rearrangements tumor cells that arise by double mitotic recombination with clustered breakpoints. These rearrangements result in interstitial isodisomy for a 60 Mb region of chromosome 17 and occurred in leukemic tumor cells of children with NF1 and myeloid dysplasia. Because both

the germline and somatic rearrangements involve not only the NF1 gene but many other genes, our data implicate other elements/loci that play an important role in sporadic cases of NF1 and in somatic loss of NF1 during leukemogenesis and possibly during other NF1-associated neoplasias. In addition, these results have direct implications for rationale design of putative therapies.

REFERENCES

Beechey, C. V., Cattanach, B. M., and Selley, R. L., 2000, World Wide Web Site - Mouse Imprinting Data and References (URL: http://www.mgu.har.mrc.ac.uk/imprinting/implink.html)., MRC Mammalian Genetics Unit, Harwell, Oxfordshire.

Cooper, L. J., Shannon, K. M., Loken, M. R., Weaver, M., Stephens, K., and Sievers, E. L. (2000) Evidence that juvenile myelomonocytic leukemia can arise from a pluripotential stem cell. Blood 96:2310-3.

Correa, C. L., Brems, H., Lazaro, C., Estivill, X., Clementi, M., Mason, S., Rutkowski, J. L., Marynen, P., and Legius, E. (1999) Molecular studies in 20 submicroscopic neurofibromatosis type 1 gene deletions. Hum Mutat 14:387-93.

Dorschner, M. O., Sybert, V. P., Weaver, M., Pletcher, B. A., and Stephens, K. (2000) NF1 microdeletion breakpoints are clustered at flanking repetitive sequences. Hum Mol Genet 9:35-46.

Friedman, J., and VM, R. (1999) Neurofibromatosis 1. Clinical and Epidemiologic Features. In: (F. JM, G. DH, M. M, and R. VM, eds.)*Neurofibromatosis. Phenotype, Natural History, and Pathogenesis*Third, The Johns Hopkins University Press, Baltimore, pp. 29-86.

Kayes, L. M., Burke, W., Riccardi, V. M., Bennett, R., Ehrlich, P., Rubenstein, A., and Stephens, K. (1994) Deletions spanning the neurofibromatosis 1 gene: identification and phenotype of five patients. Am J Hum Genet 54:424-36.

Kayes, L. M., Riccardi, V. M., Burke, W., Bennett, R. L., and Stephens, K. (1992) Large de novo DNA deletion in a patient with sporadic neurofibromatosis 1, mental retardation, and dysmorphism. J Med Genet 29:686-90.

Leppig, K., Kaplan, P., Viskochil, D., Weaver, M., Orterberg, J., and Stephens, K. (1997) Familial neurofibromatosis 1 gene deletions: cosegregation with distinctive facial features and early onset of cutaneous neurofibromas. Am J Med Genet 73:197-204.

Leppig, K. A., Viskochil, D., Neil, S., Rubenstein, A., Johnson, V. P., Zhu, X. L., Brothman, A. R., and Stephens, K. (1996) The detection of contiguous gene deletions at the neurofibromatosis 1 locus with fluorescence in situ hybridization. Cytogenet Cell Genet 72:95-8.

Miles, D., Freedman, M., Stephens, K., Pallavicini, M., Sievers, E., Weaver, M., Grunberger, T., Thompson, P., and Shannon, K. (1997) Patterns of hematopoietic lineage involvement in children with neurofibromatosis, type 1 and malignant myeloid disorders. Blood 88:4314-4320.

Mulvihill, J. J. (1994) Malignancy: epidemiologically associated cancers. In: (S. M. Huson, and R. A. C. Hughes, eds.)*The Neurofibromatoses: A pathogenetic and Clinical Overview*First, Chapman & Hall Medical, London, pp. 487.

Shannon, K. M., P, O. C., Martin, G. A., Paderanga, D., Olson, K., Dinndorf, P., and McCormick, F. (1994) Loss of the normal NF1 allele from the bone marrow of children with type 1 neurofibromatosis and malignant myeloid disorders [see comments]. N Engl J Med 330:597-601.

Shen, S., Battersby, S., Weaver, M., Clark, E., Stephens, K., and Harmar, A. J. (2000) Refined mapping of the human serotonin transporter (SLC6A4) gene within 17q11 adjacent to the CPD and NF1 genes. Eur J Hum Genet 8:75-8.

Turker, M. S., Gage, B. M., Rose, J. A., Elroy, D., Ponomareva, O. N., Stambrook, P. J., and Tischfield, J. A. (1999) A novel signature mutation for oxidative damage resembles a mutational pattern found commonly in human cancers. Cancer Res 59:1837-9.

APPENDICES

Abstracts:

Stephens K, Weaver M, Leppig K, Maruyama K, Side L, Davis EA, Espinosa III R, Le Beau M, Shannon K. 1998. Double mitotic recombination at common breakpoint intervals leading to interstitial isodisomy and LOH. Am J Hum Genet 63(4): A205.

Dorschner MO, Weaver M, Sybert VP and Stephens K. 1999. NF1 microdeletions are mediated by homologous recombination between duplicons. Am J Hum Genet 65(4): A151.

Stephens K, Weaver M, Leppig K, Maruyama K, Side L, Davis EA, Espinosa III, R, Le Beau M, and Shannon K. A novel and frequent mechanism of loss of heterozygosity in malignant myeloid cells of NF1 children: Double mitotic recombination at common breakpoint intervals. National Neurofibromatosis Foundation Consortium, June, 1998, Aspen, CO.

Manuscripts:

Dorschner MO, Sybert VP, Weaver M, Pletcher BA, Stephens K. 2000. NF1 microdeletion breakpoints are clustered at flanking repetitive sequences. Hum Mol Genet 9:35-46.

Shen S, Battersby S, Weaver M, Clark E, Stephens K, Harmar AJ. 2000. Refined mapping of the human serotonin transporter (SLC6A4) gene within 17q11 adjacent to the CPD and NF1 genes. Eur J Hum Genet 8:75-78.

Cooper LJN, Shannon KM, Loken MR, Weaver M, Stephens K, Sievers EL. 2000. Evidence that juvenile myelomonocytic leukemia can arise from a pluripotential stem cell. Blood 96:2310-2313.

Stephens K, Weaver M, Leppig KA, Maruyama K, Emanuel PD, Davis EM, Espinosa III R, Le Beau MM, Shannon KM. Tumor suppressor inactivation by double mitotic recombination at clustered breakpoint intervals. Nature Genetics, submitted.

PERSONNEL WHO RECEIVED PAY FROM THIS PROJECT

The following personnel at the University of Washington, Seattle, WA received pay during the 3 years of this project.

Karen G. Stephens, PhD, Principal Investigator
Virginia P. Sybert, MD, Co-Investigator
Michael O. Dorschner, PhD, Postdoctoral Fellow
Molly Weaver, BS, Research Technologist
Rosalynda Le, BS, Research Technologist
Sue Fredell, BS, Research Technologist
John Calhoun, Student Lab Helper

√ The following abstract is submitted for oral presentation or poster presentation

ABSTRACT

A novel and frequent mechanism of loss of heterozygosity in malignant myeloid cells of NF1 children: Double mitotic recombination at common breakpoint intervals

K Stephens[1], M Weaver[1], K Leppig[1], K Maruyama[1], L Side[3], EA Davis[2], R Espinosa III[2], M Le Beau[2], K Shannon[3]

[1]University of Washington, [2]University of Chicago, [3]University of California, San Francisco
[1]Depts Medicine and Laboratory Medicine, Mail Box 357720, University of Washington, Seattle, WA 98195
Ph 206-543-8285; Fax 206-685-4829, millie@u.washington.edu

Leukemic cells of NF1 children with malignant myeloid disorders commonly show loss of constitutional heterozygosity (LOH) at the NF1 gene and flanking loci. We have found that a novel mechanism of LOH is employed, which involves an apparent double mitotic recombination at common breakpoint intervals. Quantitative PCR and FISH analyses of leukemic cells revealed that, despite showing LOH at NF1, these cells harbor two NF1 alleles. NF1 LOH in conjunction with NF1 disomy was detected in 9 out of 11 cases analyzed. Six of these cases were further studied by genotypic analyses of loci spanning chromosome 17. In each of these 6 cases, a large interstitial region of the q arm of chromosome 17 showed LOH. The LOH breakpoints mapped to common intervals. The centromeric LOH breakpoint in 5 of 6 cases mapped centromeric to NF1 between D17S1878 and D17S975. The breakpoint of the remaining case mapped to an adjacent interval bounded by D17S1878 and D17S959. Similarly, 4 of the 6 cases had LOH breakpoints close to the telomere in intervals bounded by D17S928 and D17S1822/D17S1830. The other 2 cases had breakpoints within this region, but it is unclear if they map in the same interval due to lack of informative markers. Together, these data are consistent with a mechanism whereby the LOH region originated by a double mitotic recombination event in a hematopoietic progenitor cell that gave rise to the malignant clone. The high frequency of this rearrangement in leukemic cells of NF1 children implies that it either has biological significance, such as selecting for growth of the malignant clone, or is favored due to recombination-prone sequences in specific regions of chromosome 17.

205

Double mitotic recombination at common breakpoint intervals leading to interstitial isodisomy and LOH. *K. Stephens[1], M. Weaver[1], K. Leppig[1], M. Maruyama[1], L. Side[2], E. Davis[3], R. Espinoza III[2], M. Le Beau[2], K. Shannon[3].* 1) Univ of Washington, Seattle, WA; 2) Univ of Chicago, Chicago, IL; 3) Univ of California, San Francisco, CA.

Leukemic cells of children with neurofibromatosis 1 (NF1) who develop malignant myeloid disorders commonly show loss of constitutional heterozygosity (LOH) of the normal NF1 allele at 17q11.2 and cytogenetically normal chromosomes 17. Mapping the LOH region revealed that the predominant mechanism is interstitial isodisomy. FISH and quantitative PCR analyses of 11 cases, whose bone marrows had LOH at the NF1 locus, showed that in 8 cases the leukemic cells were disomic for NF1, while the remaining 3 cases were monosomic. In each of the 8 NF1 disomic cases, a large interstitial 17q segment had undergone LOH with breakpoints mapping to common intervals. The proximal LOH breakpoints mapped centromeric to NF1 between D17S1878 and D17S975, while the distal LOH breakpoints were subtelomeric and bounded by D17S928 and D17S1822/D17S1830. Together these data indicate that the leukemic cells were isodisomic for an ~50 Mb interstitial 17q segment which carried the mutated NF1 allele, thereby resulting in LOH and functional loss of NF1. Interstitial isodisomy most likely arose by a double mitotic recombination during the S/G2 cell cycle of a hematopoietic progenitor cell, which gave rise to the malignant clone. The high frequency and common recombination breakpoint intervals of these novel rearrangements imply that along with NF1, additional chromosome 17 loci play a role in development of malignant myeloid disorders in NF1 children, perhaps by favoring growth of the malignant clone. Because cases of maternal and paternal isodisomic regions were both observed, genomic imprinting is unlikely to be a factor. Bone marrow cells in the remaining 3 cases showed NF1 LOH, NF1 monosomy, and small LOH regions of 1-2 Mb spanning the NF1 locus, indicating that they arose by small interstitial deletions. These studies demonstrate that critical genetic loci and mechanisms underlying neoplasia may not be detected if LOH analyses are not performed in conjunction with physical mapping.

NF1 microdeletions are mediated by homologous recombination between duplicons

M. Dorschner, M. Weaver, V.P. Sybert, K. Stephens
Department of Medicine, University of Washington, Seattle, WA

Neurofibromatosis type 1 patients with a submicroscopic deletion spanning the NF1 gene are remarkable for an early age at onset of cutaneous neurofibromas, suggesting the co-deletion of a novel locus that potentiates neurofibromagenesis. Construction of a 3.5 Mb BAC/PAC contig at chromosome 17q11.2 and analysis of somatic cell hybrids from microdeletion patients showed that 14 of 17 cases had deletions of 1.5 Mb in length. The deletions encompassed the entire 350 kb NF1 gene, 3 additional genes, 1 pseudogene, and 13 ESTs. The critical region harboring the putative locus that exacerbates neurofibroma development was narrowed to 1 Mb by the identification of a smaller deletion in one of the 3 remaining patients. Of the 14 cases with 1.5 Mb deletions, both the proximal and distal breakpoints mapped within chromosomal regions of high homology, termed NF1 duplicons. These duplicons, with an estimated length of 15-100 kb, harbor at least 4 ESTs and an expressed SH3GL pseudogene. Therefore, homologous recombination between duplicons either in cis or in trans on sister chromatids is a predominant mechanism of NF1 microdeletion. Refined breakpoint mapping will facilitate identifying sequences within the duplicons that are susceptible to chromosome breakage and recombination. The number of NF1 duplicons in the genome is unknown, however, we have identified a third one at chromosome 17q24. These data suggest that NF1 duplicons may also play a role in germline or somatic rearrangements

NF1 gene loss by recombination at flanking hotspots

Michael O. Dorschner and Karen Stephens
Department of Medicine, University of Washington, Seattle, WA

NF1 gene loss occurs both in germline and somatic tissues. We found that breakpoints of 14/17 patients with 1.5 Mb germline NF1 microdeletions were clustered at NF1REPs, 120 kb paralogous regions flanking NF1. These data suggest the existence of recombinogenic elements that mediate NF1 deletion. Sequence analysis of the NF1REPs revealed a cluster of processed pseudogenes, a GC rich minisatellite, and no apparent functional genes. To map the deletion breakpoints, we identified single nucleotide and sequence length polymorphisms between the two NF1REPs, which share >95% identity. The breakpoints of unrelated patients were located within a 20 kb segment, which contains GA rich regions, a CpG island, and retroviral long terminal repeats (LTRs). These motifs could facilitate recombination by misalignment or by maintaining a recombination-proficient chromatin structure via methylation or active transcription. In addition to germline deletions, we hypothesize that recombination occurs at these sites in somatic tissues. This predicts that site-specific recombination is a molecular basis for NF1 gene loss in some cases of NF1 mosaicism, segmental NF1, and NF1-associated malignancies. An ongoing test of these predictions has identified an NF1 patient who is mosaic for an NF1 microdeletion. Additional NF1REPs have been identified in the genome by FISH at chromosome bands 17q21, 17q23, and 19p13. Therefore, recombination between NF1REPs may be an important mechanism for restructuring of the genome during tumorigenesis in NF1 affected and unaffected individuals.

National Neurofibromatosis Foundation International Consortium on
Gene Cloning and Gene Function of NF1 and NF2, Aspen, CO, June, 2000

A hydropathic complementarity analysis of neurofibromin identifies two protein motifs in potential neurofibromin-interacting proteins. Robert J. Livingston[1] and Karen Stephens[2], Departments of Pathology[1], Medicine[2], and Laboratory Medicine[2], University of Washington, Seattle, WA 98195-7720.

The phenomenon of hydropathic complementarity (HC) was used to characterize potential neurofibromin interacting proteins. HC is the observation behind the Molecular Recognition Theory (MRT) which explains the molecular evolution of receptor-ligand and enzyme-substrate pairs. HC is based on a novel property of the codon table, that amino acids encoded by codons and their reverse complements have opposing hydropathic properties. The MRT posits that when polypeptides are translated in frame from complementary nucleic acids, they form complementary, interacting structures. In this study, the reverse complement of the neurofibromin cDNA was translated and examined computationally for protein motifs in the PROSITE database. Two domains were identified in the reverse translated, "complementary" neurofibromin polypeptide: a P-loop type ATP/GTP binding site and two lipid binding sites. These results suggest these two domains might be present in neurofibromin-interacting proteins. Consistent with these results is neurofibromin's role as a negative regulator of ras•GTP and a critical step in ras activation is post translational modification by farnesylation. Ras binds GTP via the P-loop type ATP/GTP motif. The location of the ATP/GTP binding site in the "complementary" protein corresponds to the central rasGAP-related domain of neurofibromin, further supporting this analysis. Strengthening the argument for a lipid-neurofibromin interaction is the observation that the GTPase activating potential of neurofibromin is inhibited by arachidonic acid and other fatty acids. This analysis may provide insight into downstream neurofibromin effectors and assist in identifying new therapeutic targets for this disease.

National Neurofibromatosis Foundation International Consortium on Gene Cloning and Gene Function of NF1 and NF2, Aspen, CO, June, 2000

Abstract Preview

Allelic losses due to recombination between paralogs can occur in somatic cells. *M.O. Dorschner[1], K.A. Leppig[2], M. Weaver[1], K. Stephens[1].* 1) Division of Medical Genetics ; 2) Department of Pediatrics, University of Washington, Seattle, WA.

A germline recombination event between flanking paralogous DNA segments is a common mechanism underlying contiguous gene deletion/duplication disorders, such as Charcot-Marie-Tooth 1A and neurofibromatosis (NF1) microdeletion. The role of paralogs in genomic rearrangements is extended by our identification of an NF1 microdeletion in somatic tissues. FISH and somatic cell hybrid analyses identified a 1.3 Mb deletion encompassing NF1 and contiguous loci. This deletion was present in ~50% of the patients peripheral blood cells as determined by quantitative PCR. The centromeric and telomeric breakpoints mapped to ~26 kb paralogs with ~98% nucleotide identity. Therefore, the deletion arose by paralogous recombination early in embryogenesis. This mosaic microdeletion patient had hundreds of dermal neurofibromas on all body segments at 80 years of age. This is consistent with our hypothesis, originally based on analyses of germline NF1 microdeletions, that codeletion of NF1 and a nearby gene(s) potentiates neurofibromagenesis. However, unlike the germline deletion patients who develop dermal neurofibromas in childhood, this patient had no tumors until her mid-20s. Mosaicism appears to have ameliorated the phenotype by delaying the age at onset of dermal neurofibromas. This predicts that site-specific recombination is a molecular basis for some cases of NF1 mosaicism, and possibly segmental NF1 and NF1-associated malignancies. Our data have broad implications for human disease pathogenesis. If recombination between paralogs is common during mitosis in somatic cells and confers a growth advantage, the resulting allelic changes may modify a disease phenotype, contribute to intrafamilial variability, and/or play a role in genome restructuring during neoplasia.

Return to Abstract Submission Form

Abstract Preview

Recombination hotspots for NF1 microdeletions. *K. Stephens[1], C.L. Friedman[2], B.J. Trask[2], M.O. Dorschner[1].* 1) Dept of Medicine; 2) Dept of Molecular Biotechnology, University of Washington, Seattle, WA.

Patients with 1.5 Mb neurofibromatosis 1 (NF1) microdeletions are remarkable for an early age at onset and large numbers of dermal neurofibromas. The clustering of breakpoints in ~100 kb flanking paralogous DNA segments (NF1REPs) suggested that these deletions arose by homologous recombination. Breakpoint mapping of 11 patients revealed two recombination hotspots. The hotspots are 20 kb apart and each is 2-3 kb in length. At one of these hotspots, the majority of breakpoints fall at or within two GA-rich regions. This region has an upstream CpG island, several LINE elements and retroviral LTRs, but no transposons or open reading frames. Although the breakpoints could have occurred anywhere in the NF1REPs, which share >97% sequence identity, only specific sites were recombination-prone. We hypothesize that the GA-rich regions facilitate recombination via localized effects on DNA secondary structure. SNP analysis surrounding the breakpoints revealed chimerism indicating that the recombinant NF1REP consisted of piecemeal fragments of the two flanking parental NF1REPs. This supports a model of homologous recombination between NF1REPs followed by double strand break repair. The human genome contains at least 9 paralogs belonging to the NF1REP family of sequences. The two REPs that mediate NF1 microdeletions are in direct orientation and share ~50 kb of near identical sequence along with an additional ~30 kb that are shared with other family members but not with each other. FISH and BLAST analyses mapped a third NF1REP at the NF1 gene region (17q11.2) and 5 additional paralogs on chromosome 17 with two at band q12, two at q21 and one at q24. A ninth paralog is at chromosome 19p13. None of these are identical in structure but are mosaics of subrepeats resulting from regional-specific duplication events during evolution. NF1REP-mediated rearrangements may provide a model system for the identification of sequence motifs that predispose to mammalian homologous recombination.

Return to Abstract Submission Form

Human Molecular Genetics, 2000, Vol. 9, No. 1 35–46

ARTICLE

NF1 microdeletion breakpoints are clustered at flanking repetitive sequences

Michael O. Dorschner*, Virginia P. Sybert, Molly Weaver, Beth A. Pletcher[1] and Karen Stephens

Department of Medicine, University of Washington, 1959 NE Pacific Street, Room I-204, Medical Genetics Box 357720, Seattle, WA 98195, USA and [1]Department of Pediatrics, University of Medicine and Dentistry, New Jersey Medical School, Newark, NJ 07103, USA

Received 27 September 1999; Revised and Accepted 3 November 1999 DDBJ/EMBL/GenBank accession nos AF170177–AF170186

Neurofibromatosis type 1 patients with a submicroscopic deletion spanning the *NF1* tumor suppressor gene are remarkable for an early age at onset of cutaneous neurofibromas, suggesting the deletion of an additional locus that potentiates neurofibromagenesis. Construction of a 3.5 Mb BAC/PAC/YAC contig at chromosome 17q11.2 and analysis of somatic cell hybrids from microdeletion patients showed that 14 of 17 cases had deletions of 1.5 Mb in length. The deletions encompassed the entire 350 kb *NF1* gene, three additional genes, one pseudogene and 16 expressed sequence tags (ESTs). In these cases, both proximal and distal breakpoints mapped at chromosomal regions of high identity, termed NF1REPs. These REPs, or clusters of paralogous loci, are 15–100 kb and harbor at least four ESTs and an expressed SH3GL pseudogene. The remaining three patients had at least one breakpoint outside an NF1REP element; one had a smaller deletion thereby narrowing the critical region harboring the putative locus that exacerbates neurofibroma development to 1 Mb. These data show that the likely mechanism of *NF1* microdeletion is homologous recombination between NF1REPs on sister chromatids. *NF1* microdeletion is the first REP-mediated rearrangement identified that results in loss of a tumor suppressor gene. Therefore, in addition to the germline rearrangements reported here, NF1REP-mediated somatic recombination could be an important mechanism for the loss of heterozygosity at *NF1* in tumors of NF1 patients.

INTRODUCTION

Haploinsufficiency for neurofibromin is the likely molecular basis of neurofibromatosis type 1 (NF1), a common autosomal disorder that predisposes to the development of benign and malignant tumors. Genetic, biochemical and proliferative studies of cells from NF1-associated tumors are consistent with a tumor suppressor function for neurofibromin. Tumor suppressor activity is due, at least in part, to a ras-GTPase activating protein (ras-GAP) domain which accelerates the conversion of activated GTP-ras to inactivated GDP-ras (1). Evidence in human and mouse shows that neurofibromin-deficient tumor cells have increased activated ras and dysregulated proliferative properties (2,3), which may be mediated by the ras-dependent mitogen-activated protein kinase signaling pathway (4). Both benign and malignant tumors show homozygous inactivation of *NF1* resulting in lack of functional neurofibromin. Although *NF1* inactivation in a tumor progenitor cell can occur by numerous mechanisms, the identification of defined intragenic *NF1* mutations in primary tumor tissue argues that lack of neurofibromin is central to their development (5–7).

Over 70% of germline mutations of the *NF1* gene are intragenic and predict a premature truncation of neurofibromin (8). These mutations are distributed throughout the coding region. They are generally unique for a given patient or family, and are not predictive for any of the diverse clinical manifestations that can develop in this multisystemic disorder. Nearly all NF1 patients develop café-au-lait macules, axillary and inguinal freckling, multiple neurofibromas, and Lisch nodules, which are hamartomas of the iris of the eye. Other significant, but less common, manifestations of the disorder include learning disabilities, optic glioma, bony abnormalities (sphenoid bone dysplasia, pseudoarthrosis, scoliosis), increased risk of specific malignancies, and others (9,10). NF1 has been considered to be primarily a disorder of cells derived from the neural crest, which is supported by recent evidence consistent with neurofibromas arising by clonal proliferation of a neurofibromin-deficient Schwann cell (11).

Previously, we identified five patients that carried a deletion of one entire *NF1* allele. These patients were remarkable for an early age (<10 years) at onset of dermal neurofibromas, an increased number or heavy burden of neurofibromas relative to their age, and certain atypical facial features (12,13). The asso-

*To whom correspondence should be addressed. Tel: +1 206 685 9066; Fax: +1 206 685 4829; Email: mod@u.washington.edu

ciation of an *NF1* microdeletion with this phenotype was subsequently confirmed by us and other investigators (14–18). In addition, the identification of families segregating an *NF1* microdeletion demonstrated that the rearrangement was co-inherited with the remarkable facial and tumor features (17,19,20).

The molecular basis for precocious neurofibromagenesis in microdeletion patients is unknown. Previously, we estimated the microdeletions at 0.7–2 Mb, which, even accounting for the large 350 kb *NF1* gene, implies that many additional genes are deleted (13,14,19). Theoretically, early age at onset of neurofibromagenesis could be attributed to: (i) deletion of the *NF1* gene alone; (ii) co-deletion of *NF1* and one of the three genes of unknown function that are embedded in an *NF1* intron; (iii) co-deletion of *NF1* and a novel contiguous gene(s); or (iv) dysregulation of a gene at the deletion breakpoint. We consider it unlikely that neurofibromin haploinsufficiency alone could account for early onset of tumorigenesis. Over 70% of NF1 patients are heterozygous for a mutation that predicts premature truncation of neurofibromin, yet in a population-based study only ~14% of subjects developed dermal neurofibromas before 10 years of age (21,22). However, it is unknown whether neurofibroma development could be ameliorated in any of these patients due to possible residual activity from the mutant *NF1* allele. The role of a putative co-deleted locus has been difficult to assess because the number of deletion patients is small and information regarding number and age at onset of neurofibromas and deletion magnitude are not always evaluated or reported. Recently, however, we described 12 unrelated *NF1* microdeletion patients with early onset and/or high burden of neurofibromas with deletion breakpoints that clustered in the same centromeric and telomeric locus intervals (K. Maruyama, M. Weaver, K. Leppig, A.S. Aylsworth, M.O. Dorschner, R. Farber, J. Ortenberg, A. Rubenstein, L. Immken, C. Curry and K. Stephens, submitted for publication). Towards mapping and identifying a locus that potentiates neurofibromagenesis in NF1 patients, we constructed a 3.5 Mb physical map of the *NF1* region, precisely mapped the deletion, and examined deletion genotype with patient phenotype. We report that the breakpoints in the majority of patients are clustered at flanking genomic segments of paralogous sequence (sequence similarity due to duplication). These results have important implications regarding germline and somatic rearrangements involving *NF1*.

RESULTS

Construction of a 3.5 Mb contig

Recently, we determined that both the centromeric and telomeric breakpoints in 14 of 15 NF1 patients with submicroscopic deletions were clustered in two distinct marker intervals. Quantitative PCR and the analysis of somatic cell hybrid lines carrying deleted chromosome 17 of each patient mapped the centromeric breakpoints between marker loci *D17S2120* and *UT172* and the telomeric breakpoints between *D17S1800* and *D17S1880* (K. Maruyama *et al.*, submitted for publication) (Fig. 1). Although these data were suggestive of breakpoint clustering, the length of each interval was unknown. In addition, the number and unique order of other markers within each of these initial breakpoint intervals was unknown. To refine the

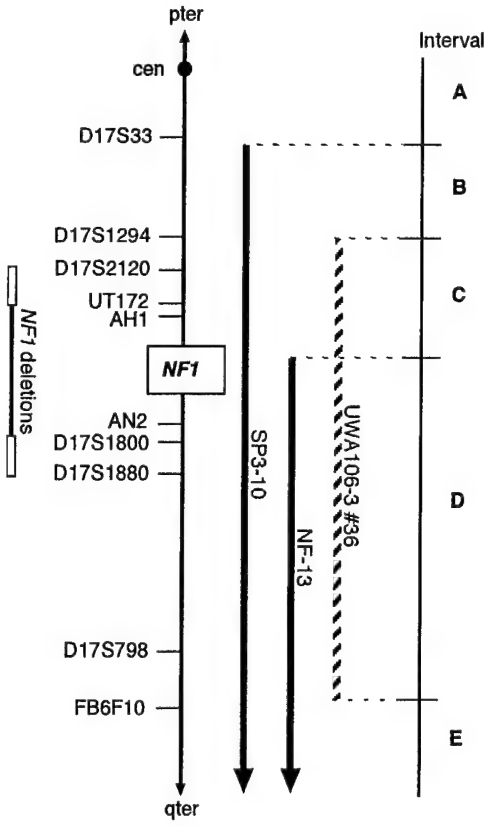

Figure 1. Hybrid mapping panel for the *NF1* region. The location of markers in the *NF1* region are depicted, along with the *NF1* deletion previously defined in patients, with open bars representing the breakpoint cluster regions (K. Maruyama *et al.*, submitted for publication). Loci were mapped to one of five intervals (A–E) on chromosome 17 by their presence or absence in human/rodent somatic cell hybrid lines. The hybrid line UWA106-3-#36 was constructed from *NF1* microdeletion patient UWA106-3 and carries a chromosome 17 deleted for the indicated segment (13). Line SP3-10 carries human chromosome segment 17q11.2 to qter (76) and NF13 carries a segment from *NF1* intron 27b to qter (77).

location of the deletion breakpoints, we sought to construct a physical map encompassing both breakpoint cluster regions. Initially, chromosome 17 loci reported to map at or near band q11.2 were gleaned from the literature and publicly available electronic databases and screened by PCR against a somatic cell hybrid mapping panel. This placed each locus into one of five possible chromosomal intervals (Fig. 1). Loci that mapped to intervals C and D were used to identify and construct a contig of novel and previously reported bacterial artificial chromosome (BAC) and P1-derived artificial chromosome (PAC) clones. Initial database searches identified five sequenced clones that served as a framework for contig construction. Two BACs, 468F23 and 41C23, were found to harbor *AH1* and *AN2*, respectively, which are end sequences of a previously described *NF1* yeast artificial chromosome (YAC) contig (23) (Fig. 2). A 297 kb sequence carrying a large portion of the *NF1* gene (GenBank accession no. AC004526), and clones 542B22 and 307A16, were identified from database searches. Together, the three clones 499I20, AC004526 and 41C23 comprise a 476 kb contiguous sequence spanning from intron 1 of the *NF1* gene to *D17S1800* (Fig. 2). The remainder of the contig was assembled by screening a BAC library with

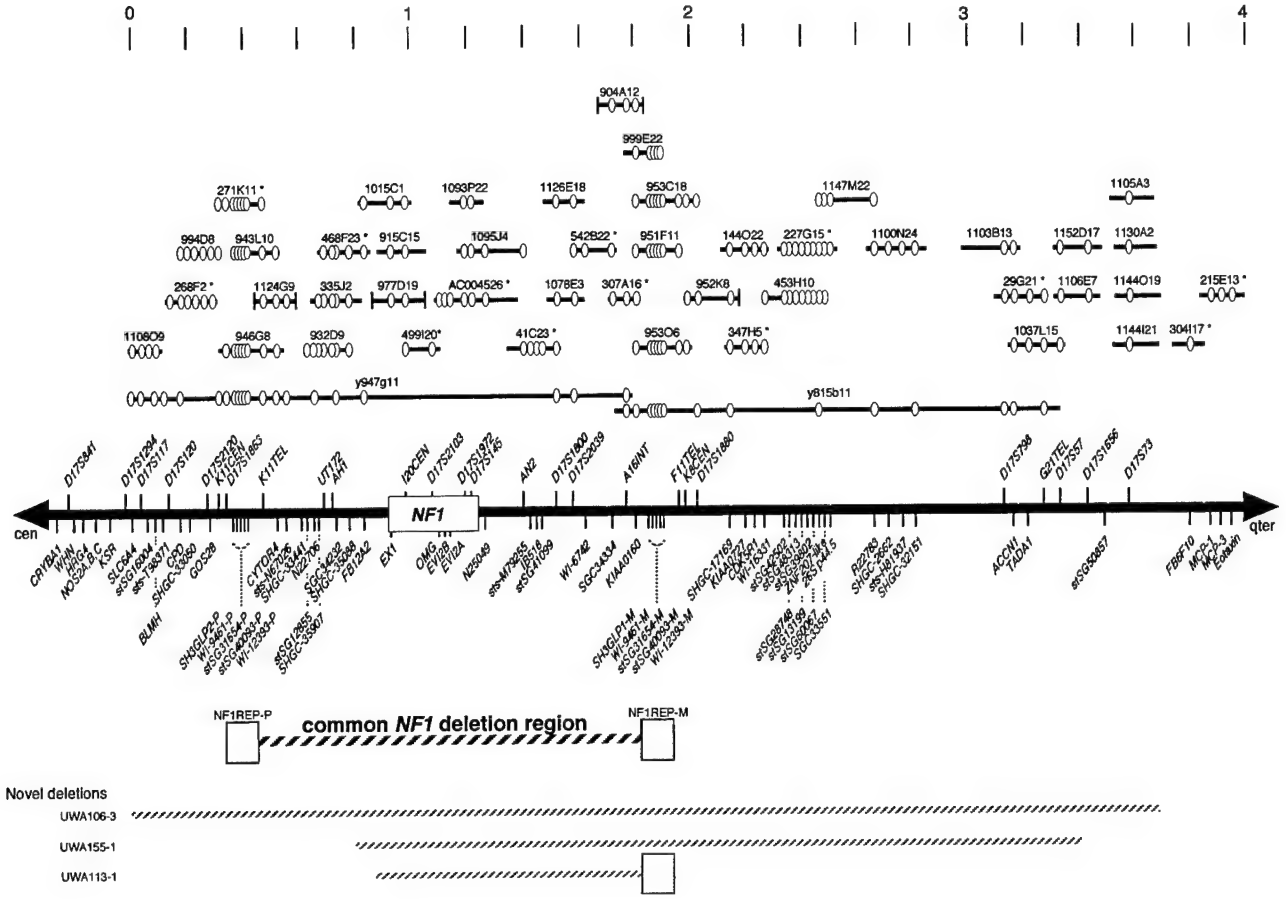

Figure 2. Physical contig of the *NF1* region. The thick black bar is a schematic of the chromosome 17q11.2 region with STS loci placed above the bar and genes and EST loci below. The BAC, PAC and YAC clones comprising the contig are shown above; open elipses are aligned with the loci on the chromosome schematic and indicate a positive hit in the clone; sequenced BAC/PAC clones are indicated with an asterisk. Vertical bars at the ends of BACs represent insert termini that were sequenced and submitted to GenBank, but not converted to amplimers. The scale in Mb is at the top of the figure. The size and extent of microdeletions of NF1 patients are shown below the chromosome. The common *NF1* deletion region was identified in 14 of 17 unrelated patients; whereas three patients had novel deletions as shown. The open boxes represent flanking repetitive sequences (NF1REP) where the majority of breakpoints mapped.

selected loci that mapped in intervals C and D (Figs 1 and 2) and by utilizing newly released chromosome 17 sequences from the Whitehead Institute for Biomedical Research/MIT Center for Genome Research (http://www-genome.wi.mit.edu/). The clones comprising the BACs are listed in Table 1.

The contig consisted of 39 BAC/PAC and two YAC clones (Fig. 2, Table 1). The new marker *A16INT* linked together the two YACs y947g11 and y815b11 (http://www-genome.wi.mit.edu/), creating a YAC contig of the region. In addition, loci prominent for their previous use in genetic mapping and loss of constitutional heterozygosity (LOH) analyses were mapped precisely. *UT172*, previously estimated to be 1.5 Mb centromeric of *NF1* (24), is only ~250 kb distant within BAC 468F23. *D17S117* and *D17S120* are located ~1 Mb centromeric of *NF1*; the latter marker actually lies within an intron of the carboxypeptidase D (*CPD*) gene. *D17S798* is located ~1.8 Mb telomeric of *NF1*.

Fine mapping of the *NF1* microdeletion breakpoints

Over 10 loci were placed precisely in each of the breakpoint cluster regions (Fig. 1), thereby facilitating fine mapping of the breakpoints of all 17 microdeletion patients. Fourteen microdeletion patients had proximal breakpoints in the locus interval of *SH3GLP2* to *CYTOR4* (*SHGC-37343*) and distal breakpoints in the interval between *SH3GLP1* and *D17S1880* (Fig. 2). The remaining three deletion cases had at least one novel breakpoint (Fig. 2). Patient UWA113-1 had a novel centromeric breakpoint between *FB12A2* and exon 1 of the *NF1* gene. Both breakpoints of patient UWA155-1 were novel and located between the intervals defined by *SHGC35088–FB12A2* and *D17S1656–stSG50857*. Patient UWA106-3, who had the largest deletion in our cohort (13), also had two unique breakpoints. The telomeric breakpoint mapped in the interval of *D17S73* to *FB6F10* and the centromeric breakpoint was mapped previously between *D17S1294* and *SCL6A4* during construction of a physical contig of the latter gene that encodes the serotonin transporter (25).

The contig provided more precise estimates of the physical lengths of both the region and the patient deletions. Because YACs 947g11 and 815b11, each estimated at 1.7 Mb (http://www-genome.wi.mit.edu/), are completely contained within the deletion of UWA106-3, this patient's deletion is approximated at 3.5 Mb. YAC 947g11 spans from *SLC6A4* to *A16INT*

Table 1. BAC/PAC clones from 17q11.2

Clone source	Clone name	GenBank accession no.	Size (kb)
hRPK	1108 O 9		
hRPK	268 F 2	AC006050	163
hRPK	994 D 8		
hRPK	946 G 8		
hRPK	271 K 11	AC005562	199
hRPK	943 L 10		
hRPK	1124 G 9		
hRPK	932 D 9		
hCIT	335 J 2		
hCIT	468 F 23	AC004666	120
hRPK	1015 C 1		
hRPK	915 C 15		
hRPK	997 D 19		
hCIT	499 I 20	AC004222	119
		AC004526[a]	297
hRPK	1093 P 22		
hRPK	1095 J 4		
hCIT	41 C 23	AC003101	208
hRPK	1078 I 13		
hRPK	1126 E 16		
hCIT	542 B 22	AC004523	131
hCIT	307 A 16	AC003041	78
hRPK	904 A 12		
hRPK	999 E 22		
hRPK	953 O 6		
hRPK	951 F 11		
hRPK	953 C 18		
hRPC	144 O 22		
hRPK	952 K 8		
hCIT	347 H 5	AC002119	109
hCIT	453 H 10		
hRPK	227 G 15	AC005899	184
hRPK	1147 M 22		
hRPK	1100 N 24		
hRPK	1103 B 13		
hRPC	29 G 21	AC003687	141
hRPK	1037 L 15		
hRPK	1106 E 7		
hRPK	1152 D 17		
hRPK	1014 I 16		
hRPK	1144 I 21		
hRPK	1130 A 2		
hRPK	1105 A 3		
hCIT	304 I 17	AC004147	139
hRPK	215 E 13	AC005549	147

hRPK, clones from RPCI-11 Human Male BAC library; hCIT, clones from CITB Caltech Human BAC library; hRPC, clones from RPCI Human PAC library.

[a]Contiguous sequence of two overlapping BAC clones.

and overlaps 815b11, which extends to just beyond *D17S798*. The known lengths of sequenced BACs and the average length of 185 kb for non-sequenced BACs derived from the RPC1-11 library were subtracted from the YAC lengths to give the estimated scale in Figure 2. The length of the common *NF1* microdeletion was estimated at 1.5 Mb.

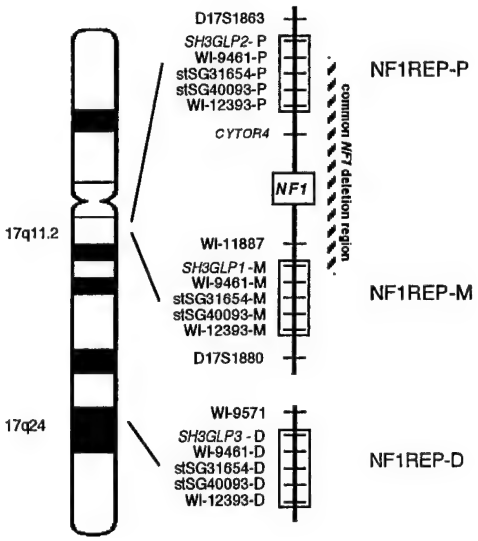

Figure 3. NF1REP domains on chromosome 17. The locations of the three NF1REP regions, designated -P, -M and -D (for proximal, medial and distal) are shown along with the five loci they are known to contain. In addition, the closest unique marker flanking each REP is indicated. The cross-hatched bar represents the 1.5 Mb region commonly deleted in *NF1* microdeletion patients.

NF1 microdeletion breakpoints cluster at repetitive sequences

Fine mapping of the region led to the discovery of two *SH3GL* expressed pseudogenes, *SH3GLP2* and *SH3GLP1*, that mapped near the breakpoints of the common *NF1* deletions (Fig. 2). Because low copy repeats are known to flank deletions/duplications responsible for some contiguous gene syndromes (26), a search for additional multicopy transcripts was initiated. A third expressed pseudogene, *SH3GLP3*, was reported to map distally at 17q24 (27). BLAST analyses of the *SH3GL* pseudogenes identified BACs 271K11 and 147L13, which carried *SH3GLP2* and *SH3GLP3*, respectively. The sequence-tagged site (STS)/expressed sequence tag (EST) content of the BAC clones was obtained (http://www-genome.wi.mit.edu/) and BLAST analyses identified their locations within each clone. This revealed that two ESTs, *WI-12393* and *WI-9461*, were present in both BACs and located near each respective *SH3GL* pseudogene. Systematic BLAST analyses of loci reportedly mapping near *NF1* in publicly available genome databases revealed that *stSG40093* and *stSG31654* were not only in BAC 271K11 centromeric to *NF1*, but were also harbored by BAC 147L13 at chromosome 17q24 (http://www.ncbi.nlm.nih.gov/genemap98). Together these analyses identified two clusters of five transcripts for which the order and relative distance between markers was conserved. These clusters of paralogous loci were designated as NF1REP, using the suffixes -P and -D to distinguish the proximal repeat at 17q11.2 from the distal repeat at 17q24 (Figs 2 and 3).

To determine whether the unsequenced region surrounding *SH3GLP1* comprised an additional NF1REP, PCR primers for

Table 2. Physical features of subjects with *NF1* microdeletions

Patient ID[a]	Cutaneous neurofibromas[b]		Ht[c] (%)	Macrocephaly (cm)	Facial features	Intelligence[d]	Hands/feet	Heart[e]	Other tumors	
	Age (years)	Number							Type, number	Age (years)
Patients with deletion breakpoints at NF1REP-P and NF1REP-M										
69-3	8	Many	5	– (54.5)	Hypertelorism	IQ 59	'Normal'		Plexiform neurofibroma, 2	10
119-1	22	TNTC	50	+	Hypertelorism	IQ 80s, 'dull normal'	NI	–		
123-3	5	Many	Normal	+	Hypertelorism, ptosis	LD	25–50%	ASD	Plexiform neurofibroma, 1 Neurofibrosarcoma, 1	5 9
128-3	7 29	Several TNTC	3	– (55)	Ptosis, downslanting palpebral fissures	Normal	10–25%	–		
147-3	6	Numerous	40	–	Hypertelorism, ptosis, coarse, downslanting palpebral fissures	Significant delays	NI	–		
156-1	31	TNTC	NI	NI	'Dysmorphic'	Mild MR with severe LD	NI	–	Optic glioma	
160-1	11 35	Several TNTC	<3	NI	'Noonan-like', coarse	LD, special education	NI	–	Plexiform neurofibroma, 1	7
166-1	39	TNTC	NI	NI	Telecanthus, downslanting palpebral fissures	'Dull'	'Large'	–		
166-2	7 19	Several TNTC	90	– (56.5)	Hypertelorism, downslanting palpebral fissures	Special education	>97%	–		
166-3	4	None	NI	– (49)	Downslanting palpebral fissures, 'unusual face'	'Normal', speech impediment	97%	–		
166-4	5 6	None 9	90	– (48.5)	Downslanting palpebral fissures	'Normal', speech problems	97%	–		
167-1	4 7	7 20	NI	NI	Ptosis, broad neck	Mild development delay	NI	ASD, PS		
169-1	18	Present	NI	+	Coarse, hypertelorism, downslanting palpebral fissures	'Dull normal', LD	'Large'	Dilated aortic valve replaced	f	
172-1	Childhood 35	None TNTC	NI	NI	'Dysmorphic'	Severe LD	'Large'	–	Optic gioma, 1 Plexiform neurofibroma, 2	
176-1	13	NI	10	–	Webbed neck, 'Noonan'	WISC-III, mild/ borderline MR	97%	–	Plexiform neurofibroma, 2	
183-1	12	10	25–50	NI	Hypertelorism, ptosis, broad nose	Borderline development delay	50%	PS	Plexiform neurofibrma, 1	1
184-1	5	TNTC	NI	NI	Telecanthus, coarse face	IQ 71 full-scale, 81 verbal, 66 performance	97%	–		
Patients with at least one unique *NF1* deletion breakpoint										
106-3	18	TNTC	Normal	+ (61.5)	Coarse	IQ 46	'Large'	–	Plexiform neurofibroma, 1 Spinal neurofibromas, TNTC	3 25
11311	8 15	TNTC TNTC	10	+ (59)	Coarse, hypertelorism	IQ 88 LD	>97%	–	–	
15511	27	TNTC	NI	+ (59.5)	Coarse, ptosis	Moderate MR	>97% hands, 75% feet	–	Spinal neurofibroma, 1 Neurofibrosarcoma, 1[g]	Sym 27 28

[a]The UWA- prefix for patient identifiers is not shown. All patients are unrelated, with the exception of four members of family UWA166.
[b]TNTC, too numerous to count.
[c]Height in percentile; NI, no information available.
[d]LD, learning disabilities; MR, mental retardation.
[e]ASD, atrial septal defect; PS, pulmonic stenosis.
[f]Patient's mother and sister with NF1, presumably due to the same *NF1* microdeletion, had retroperitoneal fibrosarcoma with metastases (age ~30) and cerebellar medulloblastoma (age 16), respectively.
[g]Spinal neurofibroma was symptomatic at age 27; patient inherited *NF1* from his father who died of malignant central nervous system tumor in fifth decade.

WI-9461, *stSG31654*, *stSG40093* and *WI-12393* were used to amplify these loci from BACs overlapping the *SH3GLP1* locus. BAC clones 953C18, 951F11 and 95306 were positive for each of the transcripts; 999E22 was positive for all but the *WI-12393* locus. This medially positioned repeat cluster was designated NF1REP-M (Fig. 3). These results demonstrated that chromosome 17 carries at least three clusters of paralogous loci: *WI-9461*, *stSG31654*, *stSG40093* and *WI-12393*, each in association with a specific *SH3GL* pseudogene (Fig. 3). The absence of *WI-12393* from BAC 999E22 and preliminary sequence analysis (M. Dorschner, unpublished data) strongly suggests that NF1REP-P and -M are direct repeats of 15–100 kb in length. The repetitive sequences may extend further beyond *WI-12393*. The breakpoints of the patients carrying the common *NF1* microdeletion lie within, or adjacent to, NF1REP regions. The centromeric breakpoints were between *SH3GLP2* and *CYTOR4*, whereas the telomeric breakpoints occurred between *SH3GLP1* and *K8CEN*. Finer mapping of the breakpoints will require the development of REP-specific primers or Southern blot analyses that identify junction fragments. The size and orientation of NF1REP-D is unknown.

Several lines of evidence confirmed that, despite carrying sequences with a high degree of identity, BACs spanning NF1REP-P and -M were localized unambiguously. First, the primers for amplification of *SH3GLP1* and *SH3GLP2* were locus specific, exploiting base differences in the 5′ region of the transcripts (27). BACs 943L10 and 946G8 were the only clones that possessed *SH3GLP2*, whereas clones 953C18, 951F11, 999E22 and 95306 carried only *SH3GLP1*. In addition, these BACs harbored the expected unique loci based on our deletion analysis. BAC 943L10 was positive for *D17S1863* and *CYTOR4*, whereas BACs spanning the medial REP contained *KIAA0160* or *D17S1880*.

Mouse orthologs for all of the genes located in interval B (Fig. 1), *SLC6A4*, *CPD*, *CDK5R1* and the chemokine cluster, have been mapped to the same region of mouse chromosome 11 that carries the *NF1* ortholog. It appears that synteny has been conserved between human and mouse for the region from *CRYBA1* to at least the chemokine cluster.

NF1 deletion genotype/phenotype and parental origin of deletion

The physical features of the 13 unrelated *NF1* microdeletion patients and the four members of family UWA166 are summarized in Table 2. There were no obvious differences detected between the features present in those individuals with the common *NF1* deletion and the three with deletions of different lengths. No single feature was present or absent consistently within either group. The location of the putative gene that potentiates neurofibromagenesis was narrowed to an interval of 1 Mb between *FB12A2* and *SH3GLP1*, as defined by the deletion of patient UWA113-1 (Fig. 2). This critical region is known to harbor four genes, two pseudogenes, and seven ESTs (Fig. 2, Table 3).

A preference for *de novo* microdeletion of the maternally derived chromosome was observed. Among the eight cases with documented *de novo* microdeletions, six were derived from the maternal homolog (UWA patients 113-1, 119-1, 147-3, 167-1, 183-1, 184-1) and two from the paternal homolog (UWA106-3, UWA123-3) (13,19, data not shown). Three families inherited *NF1* microdeletions. Family UWA166 includes the affected mother UWA166-1 and her three affected children UWA166-2, -3 and -4 (19), patient UWA169-1 inherited NF1 from his affected mother (19,28), and UWA155-1 inherited NF1 from his affected father.

DISCUSSION

NF1REP elements

Three NF1REPs were mapped to chromosome 17. NF1REP-P and -M flank the *NF1* locus at 17q11.2 and are separated by ~1.5 Mb of DNA. The third, NF1REP-D, is located at 17q24. Each REP is composed of at least five transcripts/ESTs including an *SH3GL* pseudogene, *WI-9461*, *stSG31654*, *stSG40093* and *WI-12393* (Fig. 3). In a search for proteins containing SH3 (src homology region 3) domains, three functional genes were identified from a fetal brain cDNA library, *SH3GL1*, *SH3GL2* and *SH3GL3*. These genes map at chromosomes 19p13.3, 9p22 and 15q24, respectively (27), and function in signal transduction, cytoskeleton and aggregation of huntingtin (29–31). In addition, three expressed *SH3GL* pseudogenes were identified that mapped by FISH to chromosome 17 (Fig. 3) (27). It will be important to characterize the expression of the other paralogous loci, *WI-9461*, *stSG31654*, *stSG40093* and *WI-12393*, at each of the NF1REPs. Although these loci were originally isolated as ESTs expressed in multiple tissues (Unigene: www.ncbi.nlm.nih.gov/UniGene/index.html), it is unclear whether each paralogous locus in NF1REP-P, -M and -D is expressed and whether they represent pseudogenes, functional loci or residual gene fragments.

NF1REP-mediated recombination

We propose that a high degree of homology between NF1REP-P and -M facilitates homologous recombination during meiosis or mitosis resulting in the deletion of intervening sequences. Consistent with this hypothesis, pseudogenes *SH3GLP1* and *-2* are 97.8% identical, whereas *SH3GLP3* shares only 90% identity with either of these (27). Further analysis of the identity between NF1REP-P and -M will require completing the sequence of the NF1REP-M domain; partial sequence analysis shows >98% identity (M. Dorschner, unpublished data). Recombination between the direct repeats NF1REP-P and -M could give rise to *NF1* microdeletions by either unequal recombination between sister chromatids or intrachromosomal recombination via a fold-back loop and excision. Distinguishing between these mechanisms will require further analyses to determine whether NF1REP-mediated recombination is associated with a meiotic crossover event. The apparent preference for *de novo NF1* microdeletion of the maternally derived chromosomes may provide a clue. Other REP-mediated rearrangements show a sex-dependent mechanism with maternally derived deletions resulting from excision of an intrachromatidal loop (32). Although in other cases, microdeletions mediated by flanking REP domains appear to arise by both mechanisms (33–35). If unequal meiotic recombination between sister chromatids underlies *NF1* microdeletion, it would predict the formation of a reciprocal duplication derivative. Whether a 1.5 Mb *NF1* duplication product would be stable is unknown; it may quickly undergo recombination and

Table 3. Genes and ESTs involved in *NF1* microdeletions

Gene/EST	Description	GenBank accession no.	Unigene cluster
SLC6A4	Serotonin transporter	L05568	553
stSG16004		R96721	155925
BLMH	Bleomycin hydrolase	X92106	78943
sts-T98371		T98371	15036
CPD	Carboxypeptidase D	U65090	5057
SHGC-33050		G29398	
GOS28	Golgi SNAP receptor complex member 1	AF073926	8868
SH3GLP2-P	SH3-domain GRB2-like 1 pseudogene	X99660	
WI-9461-P		G07297	183294
stSG31654-P		AA910341	191479
stSG40093-P		AI378068	124418
WI-12393-P	Moderately similar to KIAA0563 protein	G20446	14232
CYTOR4	Cytokine related receptor protein 4	G30528	119410
sts-N67026	Weakly similar to AD7C-NTP	N67026	206654
SHGC-33441		T70563	
stSG12855		H56424	221463
N22706		N22706	43234
SHGC-35907		D19648	94891
SHGC-34232	Weakly similar to IP4/PIP3 binding protein	G28215	28802
SHGC-35088		H79008	
FB12A2		T02847	
NF1	Neurofibromin	M89914	93207
OMG	Oligodendrocyte myelin glycoprotein	M63623	194772
EVI2A	Ecotropic viral integration site	M55267	41846
EVI2B	Ecotropic viral integration site	M60830	5509
AK3-p1	Adenylate kinase pseudogene	X60674	
N25049	Expressed only in olfactory epithelium	N25049	183219
sts-M79255		M79255	
IB518	Weakly similar to KIAA0665 protein	T03582	3454
stSG-41099		H29300	7985
WI-6742		R44280	8179
SHGC-34334		D19683	30670
KIAA0160		D63881	170329
SH3GLP1-M	SH3-domain GRB2-like 1 pseudogene	X99658	
WI-9461-M		G07297	183294
stSG31654-M		AA910341	191479
stSG40093-M		AI378068	124418
WI-12393-M	Moderately similar to KIAA0563 protein	G20446	14232
SHGC-17169		G19390	192761
KIAA0727	Similar to unconventional myosins	AB018270	39871
CDK5R1	CDK5 regulatory subunit 1/p35	X80343	2869
WI-16331		G20991	120762
stSG42502		H86705	40488
stSG28748		AA860832	
stSG48313		AA279265	97128
stSG13199		H75373	
stSG39802		AA084612	125286
stSG60067		AI017068	131740
ZNF207-like	Zinc finger transcription factor	AF046001	62112
SGC33551	*Homo sapiens* clone 23685 mRNA sequence	AF052093	9800
p44.5/ PMSD11	Macropain 26S proteosome subunit	AB003102	90744
R22783		R22783	
SHGC-2662	Weak similarity to ubiquitin-like protein 8	D11824	109701
sts-H81937	Moderate similarity to serine/threonine kinase	H81937	37528
SHGC-32151	Weak similarity to RAS gene family	AA199845	14202
ACCN1	Sodium channel (hBNaCl), degenerin	U57352	6517
TADA1	Maid-like gene	N37022	3447
stSG50857		AA400117	125747

Genes and ESTs in bold are within the 1.5 Mb commonly deleted NF1 region.

Table 4. Contiguous gene rearrangements involving low copy repeats

Disorder	Location	Rearrangement		REP size (kb)	Transcripts in REP	Reference
		Type	Size (kb)			
NF1	17q11.2	Deletion	1500	15–100	*SH3GLP, WI-9461, stSG31654, stSG40093, WI-12393*	This paper
VCFS/DGS CES	22q11	Deletion Duplication	2000/1500	200	*GGT, GGT-rel, BCRL, V7-rel, POM121-like*	45,48
Williams' syndrome	7q11.23	Deletion	2000	>30	*GTF2I, IB1445*	47
HNPP CMT1A	17p11.2	Deletion Duplication	1500	24	*COX10*	43
Smith–Magenis	17p11.2	Deletion	5000	200	*TRE, KER, SRP, CLP*	44
PWS/AS	15q11–13	Deletion	4000	50–200	*SGC32610, SHGC15126, SHGC17218, A006B10, MN7, A008B26, HERC2*	46,49
NPHP1 (nephronopthisis type 1)	2q12–13	Deletion	250	100	*D2S1735, D2S2087*	53

'revert' to a deletion (36). Non-mosaic trisomy 17 has not been reported in a live born, and partial 17p or 17q trisomy is rare and even mosaic cases are uncommon (37), suggesting that many such rearrangements are lethal.

Patterns of REP domains and chromosomal rearrangements

About 10 years ago it became clear that intragenic, or relatively small, deletions, duplications and inversions of the human genome could be mediated by homologous recombination between tandem genes, or other nearby repetitive sequences. Such rearrangements have been well described for the steroid sulfatase, α-globin, Factor VIII, LDL receptor and other genes (reviewed in refs 36,38). Recently, however, the breakpoints of large contiguous gene deletions and duplications from 1–5 Mb in length were mapped to flanking repetitive sequences of high identity. Such low copy repetitive elements have been designated as REPs, duplicons or paralogous regions (39,40). There is compelling evidence that homologous recombination between REPs is the molecular basis for a number of disorders (Table 4) (reviewed in refs 26,38). The precedence was established for the neuropathies Charcot–Marie–Tooth type 1A (CMT1A) and hereditary neuropathy with liability to pressure palsies (HNPP). Unequal recombination between flanking REPs during meiosis I results in duplication (CMT1A) or deletion (HNPP) of a 1.5 Mb segment of chromosome 17p11.2 (41,42). The two 24 kb CMT1A-REPs have 98.7% identity with an internal 557 bp recombination hotspot where 21 of 23 breakpoints occurred (43).

Although the characterization of REPs flanking large contiguous gene rearrangements is in its infancy, variability in REP length, number, complexity and orientation is apparent. REP length varies considerably (Table 4) and may correlate directly with the size of the intervening deletion/duplication. This suggests that recombination between distant REPs may require longer tracts of identity for efficient pairing (26). Although a single CMT1A-REP lies on each side of the CMT1A/HNPP rearrangement, the number of REPs and the apparent preference for recombination between specific REPs can vary considerably. Three Smith-Magenis syndrome (SMS)-REPs are found in the 17p11.2 region, yet nearly all SMS deletions are due to crossover events between the proximal and distal REPs (44). The identification of eight REPs at 22q11 suggests that recombination between specific REP pairs may account for different rearrangements underlying multiple congenital anomaly disorders that map to this chromosomal region, such as velocardiofacial syndrome/DiGeorge syndrome (VCFS/DGS) and cat eye syndrome (CES) (45). REP domains may be very complex repeats that include multiple subrepeats, which can be in tandem or interspersed, inverted or direct in orientation (46–48). REPs may even be dispersed among chromosomes; FISH experiments suggest that copies of the Prader-Willi syndrome/Angelman syndrome (PWS/AS) REP may be at 15q24 and 16p11 (49). The apparent preference for REP domains to occur near the centromere of chromosomes (Table 4) (26) is consistent with reports of a strong bias for these regions to acquire paralogous segments. This phenomenon is referred to as pericentromeric plasticity and presumably accounts for the varied *NF1*-related fragments that are scattered among the centromeric regions of seven different autosomes (50; reviewed in ref. 39). Homologous recombination events and the resulting chromosomal rearrangements are also dependent on the orientation of the repetitive sequences involved. For example, recombination between direct CMT1A-REPs results in deletion and duplication via unequal crossing-over between chromatids (reviewed in ref. 51), whereas recombination between indirect duplicons can result in either deletions or inversions (52–54).

Unique pathological aspects of NF1REP-mediated recombination

Several aspects of *NF1* microdeletions are unique among REP-mediated contiguous gene rearrangements in the human genome. For other disorders, REP-mediated rearrangements commonly account for a large fraction of analyzed cases. For example, >98% of CMT1A cases are caused by a duplication that results in partial trisomy of the 17p11.2 region that includes the *PMP22* locus, whereas <2% are due to missense mutations in the *PMP22* gene itself (55). In AS, large maternal deletions account for 70% of cases, uniparental disomy and imprinting mutations for an additional 5%, and inactivating mutations in *UBE3A* for another 5% (56). In marked contrast, only 2–13% of NF1 cases result from *NF1* microdeletions (16,18,57,58), whereas >70% result from intragenic mutations that predict premature truncation of neurofibromin (8). Under-

Table 5. New BAC-end derived loci

Locus	Forward primer (5′→3′)	Reverse primer (5′→3′)	Size (bp)	GenBank accession no.
F2-CEN	GCTGGAAGCCACATTTGTCTG	GCACACAAATTCTCTTGGGA	77	AC006050
F2-TEL	TCCCCTTGCAGCATTGCTAT	CAGACACTTCTCCCCTCTACCCT	150	AC006050
K11-CEN	ACACTGCTGCTCTTCACCATTG	CCACCCATGAGCAAGTTCG	150	AC005562
K11-TEL	AGGTGTGAGCCACTGTGCACT	GGCTCCCCTAGGAAGCTCC	200	AC005562
I20-CEN	CGAACTCCTGACCTCGTGATC	ACCTGGTGTCTAGAGCTGATG	788	AC004222
F11-TEL	TGAGACTGATTGTAGCAGAAGTC	ACCTGTGGCTGTTGAACACTTG	325	AF170177
K8-CEN	GCTCCATGTTCCATGCTATGAG	TCTTCTCCACTCATTCCTTTGTC	363	AF170179
G21-TEL	TTAGTTAGAGCCCACCCCTCC	CCATAGGTGTGCTGGCCAC	155	AC003687
A16-INT	GGCCTCCAACTTGGTAGTCTG	GTCTGCAAATGAGCTGACAAGCT	320	AC004523

standing why microdeletion is not the prevalent mutational mechanism may reveal important parameters that affect the efficiency of REP-mediated rearrangements. Perhaps the size and sequence identity of NF1REP-P and -M are comparatively less than those of other genomic disorders, thereby reducing the probability of *NF1–REP* pairing. Or, polymorphism in the number and orientation of, or identity between, NF1REPs may result in a haplotype that is recombination-prone. A precedent for an inversion polymorphism mediated by flanking repetitive repeats has been established (54).

Our data suggest that *NF1* microdeletion may also predispose patients to the development of malignant tumors. This hypothesis is supported by our observation that 2 of the 17 (11%) unrelated microdeletion patients had a neurofibrosarcoma (Table 2, UWA124-3 and UWA155-1). This clearly is greater than the expected occurrence of 1.4–3.5% in NF1 patients (21,59), more so given the young age of the microdeletion patients. In addition, first degree affected relatives of two microdeletion patients died of malignancies (Table 2, UWA155-1 and UWA169-1). Further studies are needed to confirm this hypothesis and to determine whether this effect is mediated by the same putative gene that causes early onset of benign neurofibromas. Two lines of evidence suggest that the increased burden of cutaneous neurofibromas in deletion patients would be an unlikely cause of an apparent increased frequency of malignancy. First, cutaneous neurofibromas do not undergo malignant transformation; in cases where neurofibrosarcomas are associated with a neurofibroma it is either a plexiform neurofibroma or a neurofibroma involving a large nerve or nerve plexus (60). Second, the malignancies of the affected first degree relatives of our patients were central nervous system and fibrosarcoma, not neurofibrosarcoma (Table 2).

NF1REP-P and -M-mediated deletion in early embryogenesis may be an underlying mechanism of somatic mosaicism of *NF1*. It has been proposed that somatic mosaicism may be common among NF1 patients and could explain, for example, cases of a mildly affected parent with a severely affected child (61,62). Patients with somatic mosaicism for an *NF1* deletion have been described (16,57,63–65). Because breakpoints were not mapped in these cases, it is not known whether these deletions involved the entire *NF1* gene and/or contiguous genes. The frequency of somatic mosaicism for an *NF1* deletion was estimated at 1.5% (16,57). However, this may be underestimated significantly due to the low detection rate of the methods employed.

This is the first report of a REP-mediated rearrangement resulting in the loss of a tumor suppressor gene. Therefore, in addition to the germline rearrangements reported here, NF1REP-mediated somatic recombination could be an important mechanism for the LOH at *NF1* in tumors of NF1 patients (5,7,66,67). This hypothesis is consistent with our recent analysis of LOH at *NF1* in primary leukemic cells of children affected with NF1 that developed malignant myeloid disorders (K. Stephens, M. Weaver, K. Leppig, K. Maruyama, E.D. Davis, R. Espinosa III, M.H. Freedman, P. Emanuel, L. Side, M.M. LeBeau and K. Shannon, unpublished data). LOH in 2 of 20 tumors arose by an interstitial deletion of a 1–2 Mb segment comparable with the germline deletions described here. Additional informative polymorphisms are needed to determine whether the deletion breakpoints are at NF1REP-P and -M. Other examples of clustered neoplasia-related rearrangements could also result from a REP-mediated recombination mechanism. For example, the interstitial 20q deletion in polycythemia vera and myeloid malignancies (54) and the i(17q)-associated hematologic malignancies (68).

The precocious neurofibromagenesis and severe tumor burden of patients with *NF1* microdeletions is consistent with our hypothesis that deletion of a gene or regulatory sequence, in conjunction with neurofibromin haploinsufficiency, potentiates development of neurofibromas. All of the deletion patients showed either childhood onset and/or large numbers of cutaneous neurofibromas (Fig. 2, Table 2), with the exception of UWA166-3 who is only 4 years old. Patient UWA113-1 has the smallest deletion of ~1 Mb, thereby establishing a critical interval between *FB12A2* and *SH3GLP1* as the location of the putative tumor-promoting gene (Fig. 2). These data excluded the strong candidate gene kinase suppressor of ras (*KSR*) (69). Currently, the critical region is known to harbor four genes, *NF1*, *OMG*, *EVI2A* and *EVI2B*, two pseudogenes and seven ESTs (Fig. 2, Table 3). The products of these genes are not strong candidates for potentiating neurofibromagenesis. *OMG*, *EVI2A* and *EVI2B* are genes of unknown function located entirely within intron 27b of the *NF1* gene, but they are transcribed from the opposite direction. *OMG* encodes a glycoprotein, OMgp, which is expressed only in the central nervous system in neurons and oligodendrocytes, and is displayed in central nervous system myelin (70,71). Although growth suppression of NIH3T3 fibroblasts overexpressing OMgp suggests that it plays a role in cell proliferation (72), its lack of expression in the peripheral nervous system makes it a poor candidate. *EVI2A* and *-B* genes are more widely expressed and

predict a putative transmembrane protein of unknown function (73); it is not known whether they are expressed in Schwann cells, which appear to be the progenitor cells of neurofibromas (11). *EVI2A* and *-B* are human orthologs of mouse loci where retroviral integration causes myeloid leukemia. Further investigation, however, revealed that it was inactivation of *NF1*, not the *EVI2* genes, that caused the leukemia (74). The identification of patients deleted for *OMG*, *EVI2A*, *EVI2B* or a segment of *NF1* along with flanking sequences would be a direct test of a role for these genes in the early onset of neurofibromas. Assuming exclusion of *NF1* and the embedded genes, the critical region is reduced to ~700 kb in length. The seven ESTs that we mapped to this region, and the sequence-ready contig, will provide the basis for identifying and characterizing the putative tumor-modifying gene.

MATERIALS AND METHODS

Subjects

Patients described previously include UWA106-3 (12,13); UWA69-3, UWA119-1, UWA123-3 and UWA128-3 (13); UWA166-2 and UWA169-1 (19); UWA147-3, UWA156-1, UWA160-1, UWA167-1, UWA172-1 and UWA176–1 (K. Maruyama *et al.*, submitted for publication). Table 2 includes clinical findings from these reports and more recent clinical evaluations. This study was approved by the Institutional Review Boards of the University of Washington and Children's Hospital and Regional Medical Center (Seattle, WA). Immortalized cell lines and human/rodent somatic cell hybrid lines carrying a single human chromosome 17 were constructed as described previously (13).

BAC library screening

Marker loci were amplified in the presence of [^{32}P]dCTP as described previously (http://www.sanger.ac.uk). A cocktail of probes, 1×10^6–10^7 c.p.m./ml hybridization solution each, was used to screen the RPCI-11 human BAC library, segment 4 (BACPAC Resources, Buffalo, NY; http://bacpac.med.buffalo.edu) by hybridization. Membranes were prehybridized in 25 ml of hybridization buffer (75) at 65°C for 1 h, hybridized overnight, and washed four to six times at increasing stringency, with a final wash of 0.2× SSC/0.1% SDS for 45 min. Following autoradiography for 1–2 days at –70°C with intensifying screens, positive clone addresses were determined and obtained from BACPAC resources. BAC DNA was isolated from 3 ml overnight cultures using the Qiagen Spin miniprep plasmid kit (Qiagen, Chatsworth, CA) according to the manufacturer's directions.

STSs, ESTs and generation of new markers

Loci were amplified either as described in the database entry or using a program with an initial denaturation of 94°C for 2 min, followed by 35 cycles of 94°C for 15 s, 59°C for 15 s, and 72°C for 60 s, and a final extension of 8 min. Primers for the amplification of *D17S117* and *D17S120* were designed from partial sequence analysis of plasmid clones. *D17S117* was amplified with primers 5′-AGGATGGACTAGGATTCTTAGTG-3′ and 5′-GCTGTCAATCACCAAAGTCGAG-3′ for *D17S117*. *D17S210* were amplified with primers 5′-CTCGAAGGTAGGATAGTGACAG-3′ and 5′-GATAGTTTGAGCTCAGGAATGTG-3′.

New markers were developed from the ends of BAC clone inserts. DNA was extracted from 300 ml of overnight culture from selected BAC clones using the Qiagen MIDI prep plasmid kit. BAC end termini were sequenced using 0.8–1.0 µg of purified BAC DNA, T7 or SP6 primers, and BigDye terminator chemistry (Applied Biosystems, Foster City, CA). Nucleotide sequences were analyzed with Sequencher 3.0 (Gene Codes, Ann Arbor, MI) and primers were designed (Table 5).

ACKNOWLEDGEMENTS

We thank the NF1 patients and their families for their continued cooperation. This research was supported by the Department of the Army, US Army Medical Research and Material Command grant NF960043 awarded to K.S.

REFERENCES

1. Martin, G.A., Viskochil, D., Bollag, G., McCabe, P.C., Crosier, W.J., Haubruck, H., Conroy, L., Clark, R., O'Connell, P., Cawthon, R.M. *et al.* (1990) The GAP-related domain of the neurofibromatosis type 1 gene product interacts with ras p21. *Cell*, **63**, 843–849.
2. Feldkamp, M.M., Angelov, L. and Guha, A. (1999) Neurofibromatosis type 1 peripheral nerve tumors: aberrant activation of the Ras pathway. *Surg. Neurol.*, **51**, 211–218.
3. Bollag, G., Clapp, D.W., Shih, S., Adler, F., Zhang, Y.Y., Thompson, P., Lange, B.J., Freedman, M.H., McCormick, F., Jacks, T. and Shannon, K. (1996) Loss of NF1 results in activation of the Ras signaling pathway and leads to aberrant growth in haematopoietic cells. *Nature Genet.*, **12**, 144–148.
4. Zhang, Y.Y., Vik, T.A., Ryder, J.W., Srour, E.F., Jacks, T., Shannon, K. and Clapp, D.W. (1998) Nf1 regulates hematopoietic progenitor cell growth and ras signaling in response to multiple cytokines. *J. Exp. Med.*, **187**, 1893–1902.
5. Sawada, S., Florell, S., Purandare, S.M., Ota, M., Stephens, K. and Viskochil, D. (1996) Identification of NF1 mutations in both alleles of a dermal neurofibroma. *Nature Genet.*, **14**, 110–112.
6. Serra, E., Puig, S., Otero, D., Gaona, A., Kruyer, H., Ars, E., Estivill, X. and Lazaro, C. (1997) Confirmation of a double-hit model for the NF1 gene in benign neurofibromas. *Am. J. Hum. Genet.*, **61**, 512–519.
7. Side, L., Taylor, B., Cayouette, M., Conner, E., Thomspon, P., Luce, M. and Shannon, K. (1997) Homozygous inactivation of the NF1 gene in bone marrow cells from children with neurofibromatosis type 1 and malignant myeloid disorders. *N. Engl. J. Med.*, **336**, 1713–1720.
8. Park, V.M. and Pivnick, E.K. (1998) Neurofibromatosis type 1 (NF1): a protein truncation assay yielding identification of mutations in 73% of patients. *J. Med. Genet.*, **35**, 813–820.
9. Riccardi, V.M. (1993) Molecular biology of the neurofibromatoses. *Semin. Dermatol.*, **12**, 266–273.
10. Gutmann, D.H., Aylsworth, A., Carey, J.C., Korf, B., Marks, J., Pyeritz, R.E., Rubenstein, A. and Viskochil, D. (1997) The diagnostic evaluation and multidisciplinary management of neurofibromatosis 1 and neurofibromatosis 2. *JAMA*, **278**, 51–57.
11. Kluwe, L., Friedrich, R. and Mautner, V.F. (1999) Loss of NF1 allele in Schwann cells but not in fibroblasts derived from an NF1-associated neurofibroma. *Genes Chromosomes Cancer*, **24**, 283–285.
12. Kayes, L.M., Riccardi, V.M., Burke, W., Bennett, R.L. and Stephens, K. (1992) Large *de novo* DNA deletion in a patient with sporadic neurofibromatosis 1, mental retardation, and dysmorphism. *J. Med. Genet.*, **29**, 686–690.
13. Kayes, L.M., Burke, W., Riccardi, V.M., Bennett, R., Ehrlich, P., Rubenstein, A. and Stephens, K. (1994) Deletions spanning the neurofibromatosis 1 gene: identification and phenotype of five patients. *Am. J. Hum. Genet.*, **54**, 424–436.
14. Leppig, K.A., Viskochil, D., Neil, S., Rubenstein, A., Johnson, V.P., Zhu, X.L., Brothman, A.R. and Stephens, K. (1996) The detection of contiguous

gene deletions at the neurofibromatosis 1 locus with fluorescence *in situ* hybridization. *Cytogenet. Cell Genet.*, **72**, 95–98.
15. Wu, B.-L., Austin, M., Schneider, G., Boles, R. and Korf, B. (1995) Deletion of the entire NF1 gene detected by FISH: four deletion patients associated with severe manifestations. *Am. J. Med. Genet.*, **59**, 528–535.
16. Ainsworth, P.J., Chakraborty, P.K. and Weksberg, R. (1997) Example of somatic mosaicism in a series of *de novo* neurofibromatosis type 1 cases due to a maternally derived deletion. *Hum. Mutat.*, **9**, 452–457.
17. Cnossen, M.H., van der Est, M.N., Breuning, H., van Asperen, C.J., Breslau-Siderius, E.J., van der Ploeg, A.T., de Goede-Bolder, A., van den Ouweland, A.M.W., Halley, D.J.J. and Niermeijer, M.F. (1997) Deletions spanning the neurofibromatosis type 1 gene: implications for genotype-phenotype correlations in neurofibromatosis type 1? *Hum. Mutat.*, **9**, 458–464.
18. Valero, M.C., Pascual Castroviejo, I., Velasco, E., Moreno, F. and Hernández Chico, C. (1997) Identification of *de novo* deletions at the NF1 gene: no preferential paternal origin and phenotypic analysis of patients. *Hum. Genet.*, **99**, 720–726.
19. Leppig, K., Kaplan, P., Viskochil, D., Weaver, M., Orterberg, J. and Stephens, K. (1997) Familial neurofibromatosis 1 gene deletions: cosegregation with distinctive facial features and early onset of cutaneous neurofibromas. *Am. J. Med. Genet.*, **73**, 197–204.
20. Wu, B.L., Schneider, G.H. and Korf, B.R. (1997) Deletion of the entire NF1 gene causing distinct manifestations in a family. *Am. J. Med. Genet.*, **69**, 98–101.
21. Huson, S., Harper, P. and Compston, D. (1988) Von Recklinghausen neurofibromatosis: a clinical and population study in south-east Wales. *Brain*, **111**, 1355–1381.
22. Huson, S.M. (1994) Neurofibromatosis 1: a clinical and genetic overview. In Huson, S.M. and Hughes, R.A.C. (eds), *The Neurofibromatoses: A Pathogenetic and Clinical Overview*, 1st edn. Chapman and Hall Medical, London, UK, pp. 160–203
23. Marchuk, D.A., Tavakkol, R., Wallace, M.R., Brownstein, B.H., Taillon Miller, P., Fong, C.T., Legius, E., Andersen, L.B., Glover, T.W. and Collins, F.S. (1992) A yeast artificial chromosome contig encompassing the type 1 neurofibromatosis gene. *Genomics* **13**, 672–680.
24. Shannon, K.M., O'Connell, P., Martin, G.A., Paderanga, D., Olson, K., Dinndorf, P. and McCormick, F. (1994) Loss of the normal NF1 allele from the bone marrow of children with type 1 neurofibromatosis and malignant myeloid disorders. *N. Engl. J. Med.*, **330**, 597–601.
25. Shen, S., Battersby, S., Weaver, M., Clark, E., Stephens, K. and Harmar, A.J. (1999) Refined mapping of the human serotonin transporter (SLC6A4) gene within 17q11 adjacent to the CPD and NF1 genes. *Eur. J. Hum. Genet.*, in press.
26. Lupski, J.R. (1998) Genomic disorders: structural features of the genome can lead to DNA rearrangements and human disease traits. *Trends Genet.*, **14**, 417–422.
27. Giachino, C., Lantelme, E., Lanzetti, L., Saccone, S., Bella Valle, G. and Migone, N. (1997) A novel SH3-containing human gene family preferentially expressed in the central nervous system. *Genomics*, **41**, 427–434.
28. Kaplan, P. and Rosenblatt, B. (1985) A distinctive facial appearance in neurofibromatosis von Recklinghausen. *Am. J. Med. Genet.*, **21**, 463–470.
29. Mayer, B.J. and Gupta, R. (1998) Functions of SH2 and SH3 domains. *Curr. Top. Microbiol. Immunol.*, **228**, 1–22.
30. Sittler, A., Walter, S., Wedemeyer, N., Hasenbank, R., Scherzinger, E., Eickhoff, H., Bates, G.P., Lehrach, H. and Wanker, E.E. (1998) SH3GL3 associates with the huntingtin exon 1 protein and promotes the formation of polygln-containing protein aggregates. *Mol. Cell*, **2**, 427–436.
31. So, C.W., Caldas, C., Liu, M.M., Chen, S.J., Huang, Q.H., Gu, L.J., Sham, M.H., Wiedemann, L.M. and Chan, L.C. (1997) EEN encodes for a member of a new family of proteins containing an Src homology 3 domain and is the third gene located on chromosome 19p13 that fuses to MLL in human leukemia. *Proc. Natl Acad. Sci. USA*, **94**, 2563–2568.
32. Lopes, J., Ravise, N., Vandenberghe, A., Palau, F., Ionasescu, V., Mayer, M., Levy, N., Wood, N., Tachi, N., Bouche, P. *et al.* (1998) Fine mapping of *de novo* CMT1A and HNPP rearrangements within CMT1A-REPs evidences two distinct sex-dependent mechanisms and candidate sequences involved in recombination. *Hum. Mol. Genet.*, **7**, 141–148.
33. Dutly, F. and Schinzel, A. (1996) Unequal interchromosomal rearrangements may result in elastin gene deletions causing the Williams-Beuren syndrome. *Hum. Mol. Genet.*, **5**, 1893–1898.
34. Carrozzo, R., Rossi, E., Christian, S.L., Kittikamron, K., Livieri, C., Corrias, A., Pucci, L., Fois, A., Simi, P., Bosio, L. *et al.* (1997) Inter- and intrachromosomal rearrangements are both involved in the origin of 15q11–q13 deletions in Prader–Willi syndrome. *Am. J. Hum. Genet.*, **61**, 228–231.
35. Baumer, A., Dutly, F., Balmer, D., Riegel, M., Tukel, T., Krajewska-Walasek, M. and Schinzel, A.A. (1998) High level of unequal meiotic crossovers at the origin of the 22q11. 2 and 7q11.23 deletions. *Hum. Mol. Genet.*, **7**, 887–894.
36. Cooper, D.N., Krawczak, M. and Antonarakis, S.E. (1995) The nature and mechanisms of human gene mutation. In Scriver, C.R., Beaudet, A.L., Sly, W.S. and Valle, D. (eds), *The Metabolic and Molecular Bases of Inherited Disease*, 7th edn, McGraw-Hill, New York, NY, Vol. 1, pp. 259–292.
37. Lenzini, E., Leszl, A., Artifoni, L., Casellato, R., Tenconi, R. and Baccichetti, C. (1988) Partial duplication of 17 long arm. *Ann. Genet.*, **31**, 175–180.
38. Mazzarella, R. and Schlessinger, D. (1998) Pathological consequences of sequence duplications in the human genome. *Genome Res.*, **8**, 1007–1021.
39. Eichler, E.E. (1998) Masquerading repeats: paralogous pitfalls of the human genome. *Genome Res.*, **8**, 758–762.
40. Reiter, L.T., Murakami, T., Koeuth, T., Pentao, L., Muzny, D.M., Gibbs, R.A. and Lupski, J.R. (1996) A recombination hotspot responsible for two inherited peripheral neuropathies is located near a *mariner* transposon-like element. *Nature Genet.*, **12**, 288–297.
41. Reiter, L.T., Hastings, P.J., Nelis, E., De Jonghe, P., Van Broeckhoven, C. and Lupski, J.R. (1998) Human meiotic recombination products revealed by sequencing a hotspot for homologous strand exchange in multiple HNPP deletion patients. *Am. J. Hum. Genet.*, **62**, 1023–1033.
42. Chance, P.F., Abbas, N., Lensch, M.W., Pentao, L., Toa, B.B., Patel, P.I. and Lupski, J.R. (1994) Two autosomal dominant neuropathies result from reciprocal DNA duplication/deletion of a region on chromosome 17. *Hum. Mol. Genet.*, **3**, 223–228.
43. Reiter, L.T., Murakami, T., Koeuth, T., Gibbs, R.A. and Lupski, J.R. (1997) The human COX10 gene is disrupted during homologous recombination between the 24 kb proximal and distal CMT1A-REPs. *Hum. Mol. Genet.*, **6**, 1595–1603.
44. Chen, K.-S., Manian, P., Koeuth, T., Potocki, L., Zhao, Q., Chinault, A.C., Lee, C.C. and Lupski, J.R. (1997) Homologous recombination of a flanking repeat gene cluster is a mechanism for a common contiguous gene deletion syndrome. *Nature Genet.*, **17**, 154–163.
45. Edelmann, L., Pandita, R.K., Spiteri, E., Funke, B., Goldberg, R., Palanisamy, N., Chaganti, R.S., Magenis, E., Shprintzen, R.J. and Morrow, B.E. (1999) A common molecular basis for rearrangement disorders on chromosome 22q11. *Hum. Mol. Genet.*, **8**, 1157–1167.
46. Amos-Landgraf, J.M., Ji, Y., Gottlieb, W., Depinet, T., Wandstrat, A.E., Cassidy, S.B., Driscoll, D.J., Rogan, P.K., Schwartz, S. and Nicholls, R.D. (1999) Chromosome breakage in the Prader–Willi and Angelman syndromes involves recombination between large, transcribed repeats at proximal and distal breakpoints. *Am. J. Hum. Genet.*, **65**, 370–386.
47. Perez Jurado, L.A., Peoples, R., Kaplan, P., Hamel, B.C. and Francke, U. (1996) Molecular definition of the chromosome 7 deletion in Williams syndrome and parent-of-origin effects on growth. *Am. J. Hum. Genet.*, **59**, 781–792.
48. Edelmann, L., Pandita, R.K. and Morrow, B.E. (1999) Low-copy repeats mediate the common 3-Mb deletion in patients with velo-cardio-facial syndrome. *Am. J. Hum. Genet.*, **64**, 1076–1086.
49. Christian, S.L., Fantes, J.A., Mewborn, S.K., Huang, B. and Ledbetter, D.H. (1999) Large genomic duplicons map to sites of instability in the Prader–Willi/Angelman syndrome chromosome region (15q11–q13). *Hum. Mol. Genet.*, **8**, 1025–1037.
50. Regnier, V., Meddeb, M., Lecointre, G., Richard, F., Duverger, A., Nguyen, V.C., Dutrillaux, B., Bernheim, A. and Danglot, G. (1997) Emergence and scattering of multiple neurofibromatosis (NF1)-related sequences during hominoid evolution suggest a process of pericentromeric interchromosomal transposition. *Hum. Mol. Genet.*, **6**, 9–16.
51. Lupski, J.R. (1999) Charcot–Marie–Tooth polyneuropathy: duplication, gene dosage, and genetic heterogeneity. *Pediatr. Res.*, **45**, 159–165.
52. Konrad, M., Saunier, S., Heidet, L., Silbermann, F., Benessy, F., Calado, J., Le Paslier, D., Broyer, M., Gubler, M.C. and Antignac, C. (1996) Large homozygous deletions of the 2q13 region are a major cause of juvenile nephronophthisis. *Hum. Mol. Genet.*, **5**, 367–371.
53. Nothwang, H.G., Stubanus, M., Adolphs, J., Hanusch, H., Vossmerbaumer, U., Denich, D., Kubler, M., Mincheva, A., Lichter, P. and Hildebrandt, F. (1998) Construction of a gene map of the nephronophthisis type 1 (NPHP1) region on human chromosome 2q12–q13. *Genomics*, **47**, 276–285.

54. Small, K., Iber, J. and Warren, S.T. (1997) Emerin deletion reveals a common X-chromosome inversion mediated by inverted repeats. *Nature Genet.*, **16**, 96–99.
55. Bird, T. (1999) Charcot–Marie–Tooth type 1. GeneClinics web site (http://www.geneclinics.org). Accessed 15 August.
56. Moncla, A., Malzac, P., Livet, M.O., Voelckel, M.A., Mancini, J., Delaroziere, J.C., Philip, N. and Mattei, J.F. (1999) Angelman syndrome resulting from UBE3A mutations in 14 patients from eight families: clinical manifestations and genetic counselling. *J. Med. Genet.*, **36**, 554–560.
57. Rasmussen, S.A., Colman, S.D., Ho, V.T., Abernathy, C.R., Arn, P.H., Weiss, L., Schwartz, C., Saul, R.A. and Wallace, M.R. (1998) Constitutional and mosaic large NF1 gene deletions in neurofibromatosis type 1. *J. Med. Genet.*, **35**, 468–471.
58. Upadhyaya, M., Ruggieri, M., Maynard, J., Osborn, M., Hartog, C., Mudd, S., Penttinen, M., Cordeiro, I., Ponder, M., Ponder, B.A. *et al.* (1998) Gross deletions of the neurofibromatosis type 1 (NF1) gene are predominantly of maternal origin and commonly associated with a learning disability, dysmorphic features and developmental delay. *Hum. Genet.*, **102**, 591–597.
59. Riccardi, V.M. and Powell, P.P. (1989) Neurofibrosarcoma as a complication of von Recklinghausen neurofibromatosis. *Neurofibromatosis*, **2**, 152–165.
60. Woodruff, J.M. (1999) Pathology of tumors of the peripheral nerve sheath in type 1 neurofibromatosis. *Am. J. Med. Genet. (Semin. Med. Genet.)*, **89**, 23–30.
61. Riccardi, V.M. (1993) Genotype, malleotype, phenotype, and randomness: lessons from neurofibromatosis-1 (NF-1). *Am. J. Hum. Genet.*, **53**, 301–304.
62. Zlotogora, J. (1993) Mutations in von Recklinghausen neurofibromatosis: an hypothesis. *Am. J. Med. Genet.*, **46**, 182–184.
63. Colman, S.D., Rasmussen, S.A., Ho, V.T., Abernathy, C.R. and Wallace, M.R. (1996) Somatic mosaicism in a patient with neurofibromatosis type 1. *Am. J. Hum. Genet.*, **58**, 484–490.
64. Tonsgard, J.H., Yelavarthi, K.K., Cushner, S., Short, M.P. and Lindgren, V. (1997) Do NF1 gene deletions result in a characteristic phenotype? *Am. J. Med. Genet.*, **73**, 80–86.
65. Wu, B.L., Boles, R.G., Yaari, H., Weremowicz, S., Schneider, G.H. and Korf, B.R. (1997) Somatic mosaicism for deletion of the entire NF1 gene identified by FISH. *Hum. Genet.*, **99**, 209–213.
66. Xu, W., Mulligan, L.M., Ponder, M.A., Liu, L., Smith, B.A., Mathew, C.G. and Ponder, B.A. (1992) Loss of NF1 alleles in phaeochromocytomas from patients with type I neurofibromatosis. *Genes Chromosomes Cancer*, **4**, 337–342.
67. Lothe, R.A., Slettan, A., Saeter, G., Brogger, A., Borresen, A.L. and Nesland, J.M. (1995) Alterations at chromosome 17 loci in peripheral nerve sheath tumors. *J. Neuropathol. Exp. Neurol.*, **54**, 65–73.
68. Fioretos, T., Strombeck, B., Sandberg, T., Johansson, B., Billstrom, R., Borg, A., Nilsson, P.G., Van Den Berghe, H., Hagemeijer, A., Mitelman, F. and Hoglund, M. (1999) Isochromosome 17q in blast crisis of chronic myeloid leukemia and in other hematologic malignancies is the result of clustered breakpoints in 17p11 and is not associated with coding TP53 mutations. *Blood*, **94**, 225–232.
69. Cacace, A.M., Michaud, N.R., Therrien, M., Mathes, K., Copeland, T., Rubin, G.M. and Morrison, D.K. (1999) Identification of constitutive and ras-inducible phosphorylation sites of KSR: implications for 14-3-3 binding, mitogen-activated protein kinase binding, and KSR overexpression. *Mol. Cell Biol.*, **19**, 229–240.
70. Habib, A.A., Marton, L.S., Allwardt, B., Gulcher, J.R., Mikol, D.D., Hognason, T., Chattopadhyay, N. and Stefansson, K. (1998) Expression of the oligodendrocyte-myelin glycoprotein by neurons in the mouse central nervous system. *J. Neurochem.*, **70**, 1704–1711.
71. Mikol, D.D. and Stefansson, K. (1988) A phosphatidylinositol-linked peanut agglutinin-binding glycoprotein in central nervous system myelin and on oligodendrocytes. *J. Cell Biol.*, **106**, 1273–1279.
72. Habib, A.A., Gulcher, J.R., Hognason, T., Zheng, L. and Stefansson, K. (1998) The OMgp gene, a second growth suppressor within the NF1 gene. *Oncogene* **16**, 1525–1531.
73. Cawthon, R.M., Andersen, L.B., Buchberg, A.M., Xu, G.F., O'Connell, P., Viskochil, D., Weiss, R.B., Wallace, M.R., Marchuk, D.A., Culver, M. *et al.* (1991) cDNA sequence and genomic structure of EV12B, a gene lying within an intron of the neurofibromatosis type 1 gene. *Genomics*, **9**, 446–460.
74. Largaespada, D.A., Shaughnessy Jr, J.D., Jenkins, N.A. and Copeland, N.G. (1995) Retroviral integration at the Evi-2 locus in BXH-2 myeloid leukemia cell lines disrupts Nf1 expression without changes in steady-state Ras-GTP levels. *J. Virol.*, **69**, 5095–5102.
75. Church, G.M. and Gilbert, W. (1984) Genomic sequencing. *Proc. Natl Acad. Sci. USA*, **81**, 1991–1995.
76. van Tuinen, P., Rich, D.C., Summers, K.M. and Ledbetter, D.H. (1987) Regional mapping panel for human chromosome 17: application to neurofibromatosis type 1. *Genomics*, **1**, 374–381.
77. Ledbetter, D.H., Rich, D.C., O'Connell. P., Leppert, M. and Carey, J.C. (1989) Precise localization of NF1 to 17q11.2 by balanced translocation. *Am. J. Hum. Genet.*, **44**, 20–24.

European Journal of Human Genetics (2000) 8, 75–78

www.nature.com/ejhg

Refined mapping of the human serotonin transporter (*SLC6A4*) gene within 17q11 adjacent to the *CPD* and *NF1* genes

Sanbing Shen[1], Sharon Battersby[1], Molly Weaver[2], Elma Clark[1], Karen Stephens[2,3] and Anthony J Harmar[1]

[1]*MRC Brain Metabolism Unit, University Department of Neuroscience, Edinburgh, Scotland; Departments of* [2]*Medicine and* [3]*Laboratory Medicine, University of Washington, Seattle, WA 98195, USA*

The *SLC6A4* gene encodes the serotonin transporter, the target of an important class of antidepressant drugs (serotonin selective reuptake inhibitors). Polymorphisms in the *SLC6A4* gene have been reported to be associated with susceptibility to depression and other psychiatric disorders. We have constructed a 1 Mb YAC and PAC contig which harbours both the *SLC6A4* and the carboxypeptidase D (*CPD*) genes. The order of loci within the contig was cen–D17S975–D17S1549–24R–D17S1294–*SLC6A4*–28L–(*CPD*, D17S2009, D17S2004)–D17S2120–ter. Both genes were deleted in one of 17 neurofibromatosis type 1 (NF1) patients carrying submicroscopic *NF1* contiguous gene deletions. *European Journal of Human Genetics* (2000) **8**, 75–78.

Keywords: serotonin transporter; *CPD*; *NF1*; YAC contig

Introduction

The actions of the neurotransmitter serotonin (5-HT) are terminated by reuptake via a Na^+-dependent serotonin transporter (SERT) encoded by the *SLC6A4* gene. The SERT is the target for an important class of antidepressant drugs (the serotonin selective reuptake inhibitors) and also of certain drugs of abuse including 3,4-Methylenedioxymethamphetamine (MDMA or 'ecstasy'). Polymorphisms in the *SLC6A4* gene have been reported to be associated with depression and other psychiatric disorders and to influence personality traits (reviewed by Lesch[1]). To facilitate studies of the molecular basis of these associations, we have constructed a map of a 1 Mb region encompassing the human *SLC6A4* and *CPD* genes. We have evaluated the contribution of these genes to the phenotype observed in patients with *NF1* contiguous gene deletions.

Materials and methods

Construction and analyses of physical contig

Positive clones were identified by hybridisation of [α-^{32}P]dCTP-labelled SLC6A4 cDNA to the RPC-1 PAC library and YAC libraries from ICRF (35D8, 132C6 and 49A9) and CEPH (704F1, 782E2 and 765D1). Yeast DNA was prepared by combined methods of Schedl *et al*[2] and Bellis *et al*.[3] Pulsed-field gel electrophoresis was performed in 0.5 × TBE buffer at 6 V/cm for 24 h at 14°C with 60 s switch time and gels were blotted overnight onto Appligene Positive Membrane. Filters were sequentially hybridized with: (i) a 854 bp Pst I fragment of *SLC6A4* cDNA (bp 785–1639, GenBank accession no. L05568); (ii) a 2.3 kb Eco RI–Pvu II fragment of pBR322; (iii) 28L, a 3.2 kb Not I – Eco RI fragment of PAC 50G6, about 40 kb 5' of the *SLC6A4* gene adjacent to the T7 promoter sequence from the vector pCYPAC2N; (iv) 24R, a 8.4 kb Not I – Hind III fragment of PAC 50G6, about 15 kb 3' of the *SLC6A4* coding sequence adjacent to the SP6 promoter sequence of the vector. YACs were sized by hybridisation to pBR322 plasmid DNA, using the endogenous yeast chromosomes as size references. PCR was performed for 30 or 35 cycles with primers listed in Table 1.

Patient and somatic cell hybrid lines

Patient UWA106-3 is hemizygous for a microdeletion of about 1–1.5 Mb that spans the entire *NF1* gene.[4] The human/rodent somatic hybrid cell lines UWA106-3-#36 and UWA106-3-#41 harbour, respectively, the deleted and non-deleted chromosomes 17 from this patient.[4] Fluorescence *in*

Correspondence: Dr Sanbing Shen, MRC Brain Metabolism Unit, University Department of Neuroscience, 1 George Square, Edinburgh, EH8 9JZ, Scotland, UK. Tel: +44 131 537 6527; Fax: +44 131 537 6110; E-mail: Sanbing.Shen@ed.ac.uk
Received 19 April 1999; revised 5 July 1999; accepted 6 August 1999

situ hybridisation (FISH) was carried out with biotin-11-dATP-labelled 50G6 PAC DNA.[5]

Results

Characterisation of the *SLC6A4* gene and PAC clones

Long-range PCR of human genomic DNA with six pairs of primers indicated that the *SLC6A4* gene spanned approximately 40 kb (Table 1). One PAC (50G6) contained the entire coding sequence of the *SLC6A4* gene. Southern blot analysis of NotI digested 50G6 DNA revealed a 40 kb fragment that hybridised to end clone 28L, a 55 kb fragment that hybridised to end clone 24R, and a 16 kb fragment from the PAC vector (data not shown). We concluded that 50G6 contains the entire *SLC6A4* gene flanked by about 40 kb of 5' sequence and about 15 kb of 3' sequence.

Construction of *SLC6A4* contig

The contig depicted in Figure 1 was assembled by analysis of 6 YACs and the PAC 50G6 for the presence of 6 STS markers and for the PAC end clones 24R and 28L. Five of the six YACs harboured the entire *SLC6A4* gene, whereas 704F1 lacked the 5' untranslated region and first exon. These data oriented the 3' end of the *SLC6A4* gene towards the chromosome 17 centromere. D17S1294 mapped < 15 kb centromeric to the 3' end of the *SLC6A4* gene, since it was present in 704F1 but not in 49A9. All clones carried the 10 repeat allele of *SLC6A4* intron 2 polymorphism;[6] YAC clones from ICRF library carried the short allele of the promoter polymorphism,[7] while those from the CEPH library carried the long allele.

Carboxypeptidase D gene maps telomeric to *SLC6A4*

A 163 kb genomic sequence from human chromosome 17 (GenBank AC006050) encodes the entire *CPD* gene, with D17S2004 and D17S2009 within the predicted 3' untranslated region. The presence of the *CPD* gene in YACs 35D8, 765D1 and 49A9 was confirmed using both forward primers of D17S2009 and D17S2004 and with two pairs of primers (cpd6740F/cpd6858R, and cpd1065F/cpd1768R: Table 1) from *CPD* cDNA. We concluded that the *CPD* gene lies telomeric to the *SLC6A4* gene within the contig.

Hemizygotic deletion of the *SLC6A4* and *CPD* genes in a NF1 patient

Our YAC contig does not contain the *NF1* gene, since none of the YAC clones yielded products with PCR primer pairs from exons 1, 27a and 49.2 of the gene.[8] However, because the deletion in UWA106-3 included loci predicted to map nearer the centromere than *SLC6A4* , we subjected metaphase chromosomes prepared from immortalised lymphoblasts of this patient to FISH using 50G6 as the probe. Only one hybridisation signal was observed, confirming the hemizygosity of the SLC6A4 locus (Figure 2a). PCR of DNA from rodent/human somatic hybrid cell lines carrying either the deleted or non-deleted chromosomes 17 of UWA106-3 indicated that the deletion encompassed the *CPD* and *SLC6A4* genes and D17S2120 but not D17S1294 or D17S1549 (Figure 2b). Therefore, the centromeric breakpoint of the deletion in this patient lies in a < 15 kb region between exon 14 of the *SLC6A4* gene and D17S1294 (arrow head, Figure 1b). Neither the *SLC6A4* nor the *CPD* gene was deleted in 16 additional *NF1* microdeletion patients[4] examined.

Discussion

We report here the construction of a 1 Mb contig encompassing the *SLC6A4* and *CPD* genes and eight marker loci. Our results confirm the localisation of *SLC6A4*[9,10] and *CPD*[11] to chromosome 17q11.2–17q12. The *SLC6A4* and *CPD* genes were deleted in 1/17 *NF1* microdeletion patients tested, but our data suggest that the majority of such patients will not be haploinsufficient for SERT and *CPD*. The identification of eight marker loci flanking the *SLC6A4* and *CPD* genes will facilitate future studies of their role in susceptibility to developmental and psychiatric disorders. This contig will also provide a centromeric anchor for chromosomal walking towards the *NF1* gene, which may lead to the discovery of other genes contiguous to *NF1*. Functional analysis of these

Table 1 PCR primers for *SLC6A4* and *CPD* genes

Forward primers (5'–3')		*Reverse primers (5'–3')*		*Product*	*Size*
31013	CACCTAACCCCTAATGTCCCTACT	31014	GGACTGAGCTGGACAACCAC	SLC6A4 5-HTTLPR	458/502 bp
1AP(F)	GCGTCTAGGTGGCACCAGAATC	1AP(R)	TCGCGCTTGTGTTCCCAGCTAC	SLC6A4 Exon 1a	545 bp
43084	CCTGCGAGGAGGCGAGGAGG	43085	AACTCCTCTCGGTGACTAATCG	SLC6A4 Exon 1–Intron 1a	10 kb
44771	CTAGTGACTGACATTGCCTGG	44772	TGTCCAGTCTATCTGCACATG	SLC6A4 Exon 1b	824 bp
43088	GCCTGGCGTTGCCGCTCTGAATGC	43089	TAGCAGCAGCAGTGAGCAGTTACC	SLC6A4 Intron 1a–Exon 2	3.5 kb
26373	ACTAACCAGCAGGATGGAGACG	26374	TAGAGTGCCGTGTGTCATCTCC	SLC6A4 Exon 2	199 bp
18564	GTCAGTATCACAGGCTGCGAG	18565	TGTTCCTAGTCTTACGCCAGTG	SLC6A4 Intron 2 VNTR	249/266/299 bp
E2F	ACTAACCAGCAGGATGGAGACG	2B	TTAGACCGGTGGATCTGCAG	SLC6A4 Exons 2–5	5 kb
54073	TGGCAAGGTGAGGAAGGCTCTGG	54074	CCACCTCAGACACATCTTCATTCC	SLC6A4 Exons 5–8	4 kb
5A	ATGAAGATGTGTCTGAGGTGG	5B	ACAGCGACTGCTTCGATCAG	SLC6A4 Exons 8–11	3.8 kb
6A	TACGTGGTGAAGCTGCTGGA	P3	GAGGAGGAGGTTGTGGAGAAGCC	SLC6A4 Exons 11–14	>12 kb
26375	AGTTCTGATGAGGCACGC	26376	TTCATCACCTCCATCCACATCC	SLC6A4 Exon 14	223 bp
60703	ATCACATTAGAACTGTCTTGTTGC	60704	AGGTATTCTATGAGGTTCAACAGC	CPD 1065F + CPD 1768R	2.7 kb
60705	TTATGTAGTTCAGTAAGATGTGCC	60706	GCAAGTATTCTTCAACTGGATAGG	CPD 6740F + CPD 6858R	118 bp

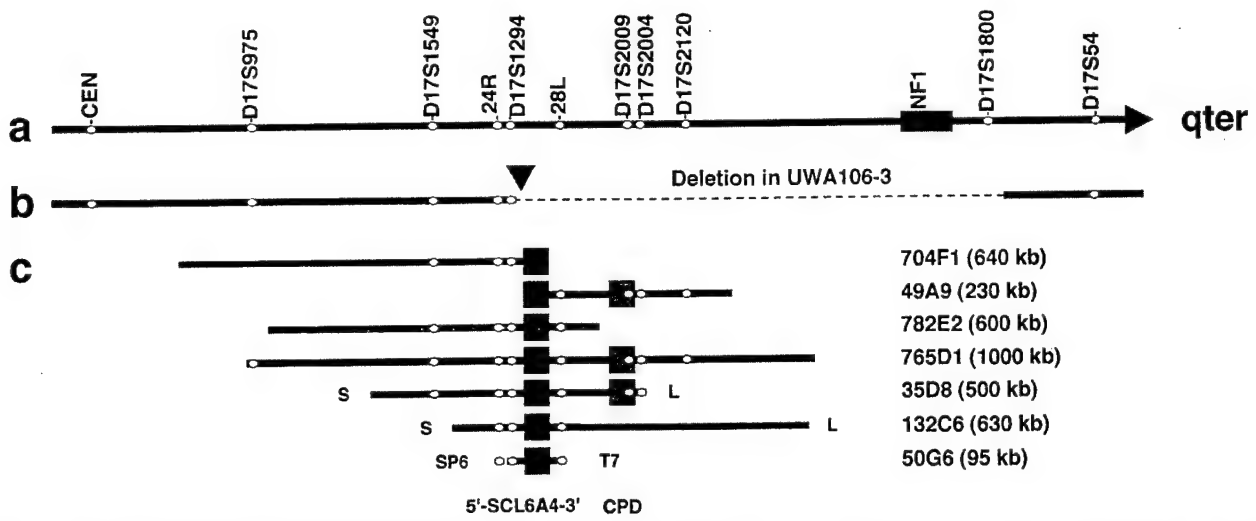

Figure 1 Mapping of the SLC6A4 and CPD genes to 17q11 in a YAC/PAC contig. **a** Physical map of the region between 17cen and D17S54; **b** the extent of the deletion (– – –) in the patient UWA106-3; **c** positions of the SLC6A4 (■) and CPD ▨ genes, STS markers and other probes (circles) in 6 YACs and one PAC (50G6) clone. Putative regions of chimaerism in YACs 704F1 and 132C6 are shaded. The orientations of the long (L) and short (S) YAC vector arms are indicated where known. Orientation of the insert in PAC 50G6 is shown relative to the SP6 and T7 promoters of the vector.

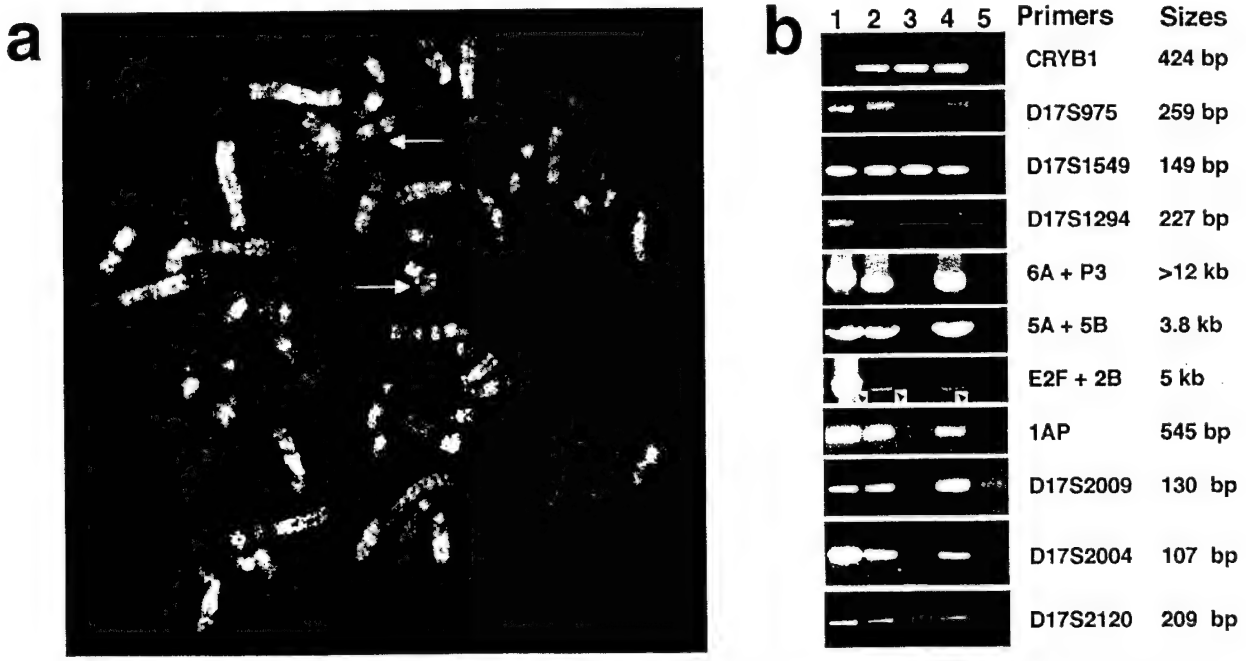

Figure 2 **a** Hemizygosity of the SLC6A4 in patient UWA106-3. Metaphase chromosome preparations from lymphoblasts of UWA106-3 were hybridised with 50G6 DNA. The two chromosomes 17 are arrowed: only one of them hybridised to the SLC6A4 probe; **b** Localisation by PCR of the centromeric breakpoint of the deletion in patient UWA106-3. DNA templates were as follows: (lane 1) YAC 765D1; (lane 2) genomic DNA from patient UWA106-3; (lane 3) cell line UWA106-3-#36 carrying the deleted chromosome 17; (lane 4) cell line UWA106-3-#41 carrying the non-deleted chromosome 17; (line 5) the Chinese hamster RJK cell line. The primers (see Table 1 and the Genome Database [http://gdbwww.gdb.org]) and sizes of PCR products are indicated. The specific PCR product of the E2F/2B primer pair is arrowed.

genes should play a role in the understanding of neurofibromatosis as well as other developmental/psychiatric disorders.

Acknowledgements

We thank Eli Lilly and Company Ltd for financial support.

References

1 Lesch KP: Molecular biology, pharmacology and genetics of the serotonin transporter: psychobiological and clinical implications. In: Baumgarten HG, Göthert M eds. *Serotoninergic Neurons and 5-HT Receptors in the CNS*, vol 129, *Handbook of Experimental Pharmacology*. Springer-Verlag: Berlin and Heidelberg, 1997, pp 671–705.

2 Schedl A, Montoliu L, Kelsey G, Schutz G: A yeast artificial chromosome covering the tyrosinase gene confers copy number-dependent expression in transgenic mice. *Nature* 1993; **362**: 258–261.

3 Bellis M, Pages M, Roizes G: A simple and rapid method for preparing yeast chromosomes for pulsed field gel electrophoresis. *Nucleic Acids Res* 1987; **15**: 6749.

4 Kayes LM, Burke W, Riccardi VM *et al*: Deletions spanning the neurofibromatosis 1 gene: identification and phenotype of five patients. *Am J Hum Genet* 1994; **54**: 424–436.

5 Edelhoff S, Ayer DE, Zervos AS *et al*: Mapping of two genes encoding members of a distinct subfamily of MAX interacting proteins: MAD to human chromosome 2 and mouse chromosome 6, and MXI1 to human chromosome 10 and mouse chromosome 19. *Oncogene* 1994; **9**: 665–668.

6 Ogilvie AD, Battersby S, Bubb VJ *et al*: A polymorphism of the serotonin transporter gene is associated with susceptibility to major affective disorder. *Lancet* 1996; **347**: 731–733.

7 Heils A, Teufel A, Petri S *et al*: Allelic variation of human serotonin transporter gene expression. *J Neurochem* 1996; **66**: 2621–2624.

8 Li Y, O'Connell P, Breidenbach HH *et al*: Genomic organization of the neurofibromatosis 1 gene (*NF1*). *Genomics* 1995; **25**: 9–18.

9 Gelernter J, Pakstis AJ, Kidd KK: Linkage mapping of serotonin transporter protein gene SLC6A4 on chromosome 17. *Hum Genet* 1995; **95**: 677–680.

10 Ramamoorthy S, Bauman AL, Moore KR *et al*: Antidepressant- and cocaine-sensitive human serotonin transporter: molecular cloning, expression, and chromosomal localization. *Proc Natl Acad Sci USA* 1993; **90**: 2542–2546.

11 Riley DA, Tan F, Miletich DJ, Skidgel RA: Chromosomal localization of the genes for human carboxypeptidase D (*CPD*) and the active 50-kilodalton subunit of human carboxypeptidase N (*CPN1*). *Genomics* 1998; **50**: 105–108.

Evidence that juvenile myelomonocytic leukemia can arise from a pluripotential stem cell

Laurence J. N. Cooper, Kevin M. Shannon, Michael R. Loken, Molly Weaver, Karen Stephens, and Eric L. Sievers

Children with neurofibromatosis type 1 (NF1) carry germline mutations in one allele of the *NF1* gene and are predisposed to myeloid malignancies, particularly juvenile myelomonocytic leukemia (JMML). Disruption of the remaining *NF1* allele can be found in malignant cells. Flow cytometric cell sorting techniques to isolate the malignant cell populations and molecular genetic methods to assay for somatic loss of the normal *NF1* allele were used to study an unusual child with NF1 and JMML who subsequently had T-cell lymphoma. The data show that malignant JMML and lymphoma cells share a common loss of genetic material involving the normal *NF1* gene and approximately 50 Mb of flanking sequence, suggesting that the abnormal T-lymphoid and myeloid populations were derived from a common precursor cell. These data support the hypothesis that JMML can arise in a pluripotent hematopoietic cell. (Blood. 2000;96:2310-2313)

Introduction

Juvenile myelomonocytic leukemia (JMML) is a relentless myeloproliferative disorder of children characterized by the monoclonal overproduction of myeloid cells.[1,2] Up to 14% of cases occur in children with neurofibromatosis type 1 (NF1),[3,4] an autosomal dominant disorder caused by germline inactivation of one allele of the *NF1* gene on chromosome 17. JMML can involve more than the myeloid lineage[5] because a malignant clonal expansion of erythroid cells has been inferred by cytogenetic,[6] X chromosome inactivation[7] and microsatellite polymorphic marker studies,[8] and a JMML patient has been reported whose disease evolved to pre-B–cell acute lymphoblastic leukemia (ALL).[9] Here we describe a boy with NF1 who was brought for treatment for JMML and in whom a T-cell lymphoma later developed. Molecular genetic and flow cytometric analyses provided strong evidence that both malignant clones derived from a common precursor with pluripotent potential, suggesting that JMML is a stem cell disorder.

Study design

Case report

A 3½-year-old boy with NF1 inherited through the maternal lineage was brought for treatment for JMML. Physical examination showed numerous café au lait spots and enlarged tonsils but an absence of hepatosplenomegaly. His white blood cell count was 96 700/μL, with 4% circulating myelocytes/metamyelocytes, a hemoglobin level of 10.1 g/dL, and a platelet count of 218 000/μL. The bone marrow showed an overwhelming myeloid predominance with less than 5% blasts and a normal karyotype, 46,XY. His peripheral blood myeloid cells formed colony-forming unit granulocyte-macrophage colonies in methylcellulose cultures without exogenous growth factors.

During the next 4 months leukocytosis persisted and was complicated by a worsening anemia and thrombocytopenia with an enlarging spleen, failure to thrive, and airway obstruction caused by hypertrophied tonsils. There was no response to isotretinoin administered at 100-200 mg/m^2 per day. Adenotonsillectomy and splenectomy were performed, and histopathologic examination of the adenoids and tonsils revealed a dense infiltration with myeloperoxidase-positive cells. Similarly, the enlarged spleen showed expansion of the red pulp by immature myeloid cells. New, diffuse adenopathy and hepatomegaly developed 6 weeks later. A lymph node biopsy revealed a T-cell expansion consistent with lymphoma. He received combination high-dose chemotherapy, but respiratory distress, anasarca, and renal failure ensued, which led to his death 8 months after the diagnosis of JMML.

Flow cytometry

Monoclonal antibodies were obtained from Becton Dickinson Immunocytometry Systems (San Jose, CA), DAKO (Carpinteria, CA), and Pharmingen (San Diego, CA). Flow cytometric analysis of the lymphomatous node and bone marrow aspirate was performed as previously described.[1] Using a FACS Vantage (Becton Dickinson), viable cells from an enlarged lymph node were separated into CD4$^+$surface CD3$^-$ (CD4$^+$sCD3$^-$) lymphoma cells, and CD4$^+$sCD3$^+$ (phenotypically normal T cells) populations and viable bone marrow cells were purified as bright CD45$^+$ with bright CD5$^+$ (phenotypically normal T lymphocytes), bright CD45 with intermediate side scatter (monocytes), and intermediate CD45 with high side scatter (maturing granulocytes) populations. The cells were lysed immediately with DNA preparation buffer (Gentra Systems, Minneapolis, MN) and were snap-frozen in liquid nitrogen.

DNA extraction and analysis for loss of constitutional heterozygosity

DNA was isolated from unfractionated and sorted blood, bone marrow, spleen, and lymph node populations as described.[11] To screen for loss of

From the Departments of Pediatrics, Medicine, and Laboratory Medicine, University of Washington, and Hematologics, Inc, Seattle WA; and the Department of Pediatrics, University of California, San Francisco, CA.

Submitted December 30, 1999; accepted May 25, 2000.

Supported by grants from the National Institutes of Health (CA72614 to K.M.S.; P30 HD28834 to the University of Washington Child Health Resource Center), the United States Army Medical Research and Material Command (NF960048 to K.S.), the National Cancer Institute (CA09351), and the Leukemia and Lymphoma Society of America.

Reprints: Laurence J. N. Cooper, Clinical Research Division, Fred Hutchinson Cancer Research Center, 1100 Fairview Avenue North, D3-100, Seattle, WA 98109-4417; e-mail: lcooper@fhcrc.org.

The publication costs of this article were defrayed in part by page charge payment. Therefore, and solely to indicate this fact, this article is hereby marked "advertisement" in accordance with 18 U.S.C. section 1734.

heterozygosity (LOH) at *NF1*, 4 intragenic polymorphisms were assayed: EVI-20,[12] an Alu repeat,[13] a dinucleotide repeat,[14] and a complex repeat.[15] The extent of the chromosome 17 LOH region was determined by assay of polymorphic loci UT172[12] and by 9 loci defined in the Genome Database (http://gdbwww.gdb.org/) by their identification numbers—D17S926 (GDB, 199252), D17S805 (GDB, 188452), D17S1294 (GDB, 686175), D17S1800 (GDB, 607032), D17S250 (GDB, 177030), D17S836 (GDB, 1218969), D17S1806 (GDB, 607848), D17S1830 (GDB, 1218973), and D17S928 (GDB, 1218974). Each locus was assayed using the polymerase chain reaction (PCR) to amplify DNA segments that contained a variable number of short nucleotide repeats. Thermocycle parameters and procedures for genotyping each locus have been described.[12,15] Radiolabeled PCR products were resolved by electrophoresis. Loss and retention of heterozygosity was determined by comparing the alleles detected in the blood of both parents with the allele(s) detected in the patient's tissues.

Results and discussion

LOH for *NF1* served as a marker of somatic inactivation of the normal allele in various hematopoietic compartments and cells showing LOH at *NF1* are likely to be derived from a common precursor cell. Similarly, X chromosome inactivation has been used to demonstrate the clonality of mononuclear cells in girls with JMML.[7] To test whether the lymphoid and myeloid cells shared a common LOH of *NF1* in this patient, subpopulations of normal and aberrant cells were identified and purified using flow cytometry and subjected to genetic analysis.

Cells from the enlarged lymph node showed 2 populations by forward and side scatter displays (Figure 1). The population of small cells revealed a mixture of phenotypically normal B, T, and natural killer lymphoid cells. The large lymphoma cells (red), which comprised 40% of viable cells, were consistent with T-cell lymphoma. Using surface (s) staining for CD4 and CD3, the T cells were sorted into an abnormal and a phenotypically normal population defined as $CD4^+sCD3^-$ and $CD4^+sCD3^+$, respectively. Cells with this abnormal phenotype could not be identified in the bone marrow (lower limit of detection less than 0.5%). Bone marrow was also used to purify aberrant myeloblasts expressing CD7 and normal T lymphocytes ($CD4^+sCD3^+$), as well as monocytoid forms and maturing neutrophils.

Loss of the normal *NF1* allele inherited from his father was detected in the patient's blood and bone marrow specimens obtained at the initial diagnosis of JMML (Figure 2A, lanes 3 and 4, respectively). A similar loss of the normal paternal *NF1* allele was identified in the lymph node and in bone marrow cells obtained with the onset of diffuse adenopathy (lanes 5 and 7, respectively), in maturing monocyte and neutrophil fractions purified from the bone marrow (lanes 8 and 9, respectively), and in the immunophenotypically aberrant $CD4^+sCD3^-$ subpopulation of cells purified from the lymphomatous lymph node (lane 11). Unfractionated spleen cells (lane 6) showed a marked reduction in the signal derived from the paternal allele, a result that is consistent with an admixture of $NF1^{-/-}$ and $NF1^{+/-}$ cells. In contrast, the intensities of the mutant maternal and normal paternal alleles were similar in the phenotypically normal $CD4^+CD3^+$ T cells isolated from the lymph node (lane 10) and from the phenotypically normal $CD5^+$ T cells purified from bone marrow (data not shown), suggesting that these cells were not involved in the malignant process.

To further investigate whether JMML and lymphoma cells derived from a common progenitor, loci spanning the length of chromosome 17 were assayed for LOH. Although multiple loci showed LOH in JMML cells and lymphomatous lymph node cells ($CD4^+sCD3^-$), representative data for the D17S805 locus, which retained heterozygosity, and D17S1294, which lost heterozygosity, are shown in Figure 2B. The loci that lost heterozygosity were identical and spanned the long arm of the chromosome, a large region greater than 50 Mb in length (Figure 2B). In contrast, the normal $CD4^+sCD3^+$ T cells from the lymph node retained heterozygosity at all chromosome 17 loci tested. These data strongly implicate a single genetic event that resulted in loss of the normal paternal *NF1* allele in a progenitor cell that gave rise to both the myeloid leukemia and the lymphoma clones.

The most likely genetic mechanism of LOH in this case is a recombination between D17S805 and D17S1294 of a maternal and a paternal chromatid during the S/G2 phase of the cell cycle of an ancestral cell. All possible recombinants would have 2 apparently normal chromosome 17 homologs, which is consistent with the results of the 2 independent cytogenetic normal analyses of bone marrow from our patient. One recombinant would carry the unaltered *NF1* maternal chromosome and a paternal chromosome in which the 17q arm with the $NF1^+$ allele had been replaced with

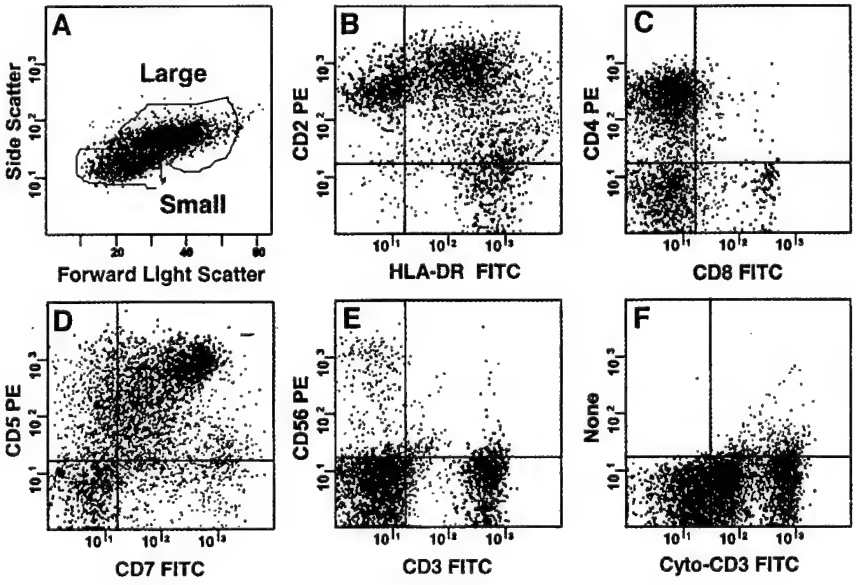

Figure 1. Multidimensional flow cytometric analysis of lymph node cells. Two populations could be defined based on forward and side light scatter (A). The larger T-cell lymphoma population (red) expressed CD2 and HLA-DR (B), CD4 without CD8 (C), and CD5 and CD7 (D). It did not express CD3 or CD56 on the surface (E), but it had CD3 in the cytoplasm (F) and were $CD5^{dim}$, $CD7^{dim}$, $CD10^{dim}$, $CD1a^-$, TdT^-, $CD13^-$, and $CD34^-$ and did not express B lymphoid markers (data not shown). Small cells in the lymph node contained normal B (green, 20%) and T (blue, 24%) lymphocytes and natural killer cells (gray, 7%).

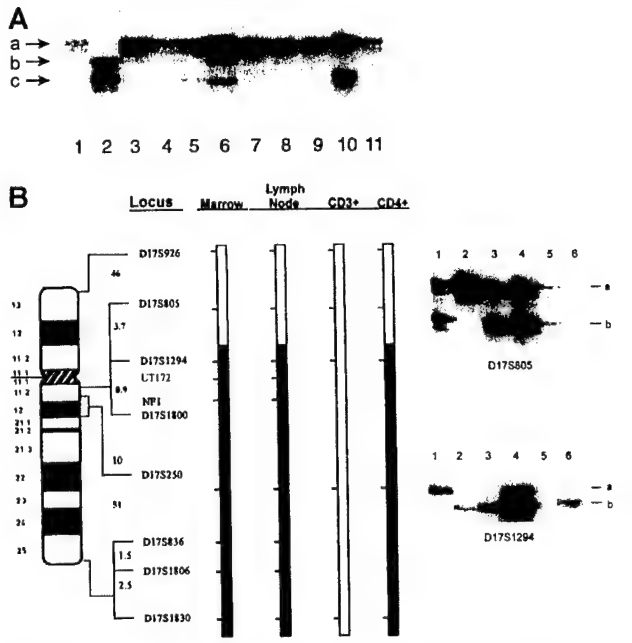

Figure 2. Analysis of tissue from the patient and of blood from his parents for LOH at *NF1*. (A) DNA samples were amplified using oligonucleotides corresponding to the intragenic marker EVI-20. DNA obtained from the mother with NF1 (*NF1*$^{\pm}$, lane 1) and the unaffected father (*NF1*$^{+/+}$, lane 2). Patient peripheral blood (lane 3) and unfractionated bone marrow (lane 4) were obtained at the time of initial presentation and diagnosis of JMML. Lymph node (lane 5), spleen (lane 6), unfractionated marrow (lane 7), maturing marrow monocytes (lane 8), and marrow-derived neutrophils (lane 9) and the lymph node subpopulations—CD4$^+$sCD3$^+$ (lane 10) and CD4$^+$sCD3$^-$ (lane 11)—were obtained at the time of the diagnosis of lymphoma. Different alleles are designated in size order, beginning with the letter a. (B) Identical chromosome 17 loci showed LOH in both primary leukemic and lymphoma cells. Bars represent a schematic of the patient's paternally derived chromosome 17 in bone marrow, lymph node, sCD3$^+$ (phenotypically normal CD4$^+$ T cells), and CD4$^+$sCD3$^-$ (abnormal lymphoma) cells, designated as CD4$^+$. The heterozygosity status of informative loci is indicated by the shaded bar for loci that lost heterozygosity or the open bar for loci that retained heterozygosity. Interlocus genetic distances in centiMorgans (cM) are indicated to the left of each interval as estimated from a chromosome 17 sex-averaged map (http://www.marshmed.org/genetics/). Data illustrating the retention of heterozygosity at the D17S805 locus and the loss of heterozygosity at the D17S1294 locus are shown to the right. DNA samples are as follows: lane 1, patient's unaffected father; lane 2, patient's mother affected with NF1; lane 3, patient's unfractionated bone marrow; lane 4, patient's lymph node; lane 5, CD3$^+$ cells from the lymph node; lane 6, CD4$^+$ cells from the lymph node; positive and negative controls are not shown. For each locus, 2 alleles, designated simply as a and b, are segregating in this family. Differences in band intensity are caused by differences in the amount of DNA loaded per lane.

the corresponding maternal 17q region carrying the *NF1* allele. This putative progenitor cell would carry 2 maternal *NF1* alleles, 2 maternal alleles for the additional approximately 500 genes in the LOH region, and a single maternal and paternal allele for the remaining chromosome 17 loci. Therefore, the progenitor cell showed maternal isodisomy for nearly all loci at chromosome 17q. Isodisomy resulting from a single mitotic recombination is a common mechanism of LOH in other tumor types.[17,18]

Although *NF1* allele loss was generally restricted to the myeloid compartment in previous studies of NF1-associated leukemia, it has been reported in B-lineage lymphoid cells, such as an Epstein-Barr virus (EBV)-transformed lymphoblastoid cell line derived from a child with JMML.[6] Additional evidence that the stem cell giving rise to JMML has pluripotent potential comes from a patient with JMML, whose disease evolved to B-cell acute lymphocytic leukemia.[9] Our data extend these reports by demonstrating clonal proliferation of malignant T-lymphoid lineage cells in a patient with JMML.

If the normal *NF1* gene is inactivated in a pluripotent hematopoietic stem cell, it is unclear why children with NF1 are strongly predisposed to JMML but not to lymphoid malignancies. This observation is not restricted to humans; the adoptive transfer of murine *Nf1*-deficient fetal liver cells consistently induces a JMML-like myeloproliferative disorder without lymphoid abnormalities.[19] Together, the human and murine data suggest that loss of *NF1* (or *Nf1*) confers a proliferative advantage that is predominately expressed in the myeloid lineage. As suggested by a previous report[20] showing polyclonality in the T-lymphoid lineage in a child with JMML, the emergence of a T-cell lymphoma may require the development of cooperating genetic mutations that are distinct from *NF1* inactivation.

NF1 encodes neurofibromin,[21] and genetic and biochemical studies have shown that *NF1* functions as a tumor suppressor gene in immature myeloid cells by negatively regulating Ras.[22] Inactivation of *NF1* is associated with the constitutive activation of Ras signaling resulting in hyperactivation in response to stem cell factor, IL-3, and granulocyte-macrophage colony-stimulating factor (GM-CSF).[19,23-25] These data raise the possibility that the myeloproliferative phenotype seen in JMML is caused by deregulated Ras signaling in response to GM-CSF and other myeloid growth factors. Presumably, additional mutations within the aberrant *NF1*$^{-/-}$ clone of our patient resulted in the outgrowth of a malignant T-lymphoid precursor clinically manifested as a T-cell lymphoma.

In conclusion, analysis of this unusual patient provides insights into the clonal origins of JMML and the proliferation of *NF1*-deficient hematopoietic cells, and our data support the hypothesis that at least some cases of JMML originate in a pluripotent hematopoietic stem cell.

Acknowledgment

We thank Beverley Tork-Storb for performing the CFU-GM cultures.

References

1. Arico M, Biondi A, Pui C-H. Juvenile myelomonocytic leukemia. Blood. 1997;90:479-488.
2. Emanuel PD, Shannon KM, Castleberry RP. Juvenile myelomonocytic leukemia: molecular understanding and prospects for therapy. Mol Med Today. 1996;2:468-475.
3. Niemeyer CM. Chronic myelomonocytic leukemia in childhood: a retrospective analysis of 110 cases. Blood. 1997;89:3534-3543.
4. Stiller CA, Chessells JM, Fitchett M. Neurofibromatosis and childhood leukemia/lymphoma: a population-based UKCCSG study. Br J Cancer. 1994;70: 969-972.
5. Miles DK, Freedman MH, Stephens K, et al. Genetic analysis and patterns of hematopoietic lineage involvement in children with neurofibromatosis type 1 and malignant myeloid disorders. Blood. 1996;88:4314-4320.
6. Amenomori T, Tomonaga M, Yoshida Y, et al. Cytogenic evidence for partially committed myeloid progenitor cell origin of chronic myelomonocytic leukaemia and juvenile chronic myeloid leukaemia: both granulocyte-macrophage precursors and erythroid precursors carry identical marker chromosome. Br J Haematol. 1986;64:539-546.
7. Busque L, Gilliland DG, Prchal JT, et al. Clonality in juvenile chronic myelogenous leukemia. Blood. 1995;85:21-30.
8. Papayannopoulou T, Nakamoto B, Anagnou NP, Chui D, Dow L, Sanders J. Expression of embryonic globins by erythroid cells in juvenile chronic myelocytic leukemia. Blood. 1991;77: 2569-2576.
9. Lau R, Shannon KM, Freedman MH. Lymphoid blast crisis of B-lineage phenotype with monosomy 7 in a patient with JCML. Leukemia. 1994; 8:903-908.

10. Loken MR, Wells DA. Immunofluorescence of cell surface markers. In: Omerod M, ed. Flow Cytometry—A Practical Approach. 2nd ed. Oxford: Oxford University Press; 1994.
11. Shannon KM, Turhan AG, Chang SSY, et al. Familial bone marrow monosomy 7: evidence that the predisposing locus is not on the long arm of chromosome 7. J Clin Invest. 1989;84:984-989.
12. Shannon KM, O'Connell P, Martin GA, et al. Loss of the normal NF1 allele from the bone marrow of children with type 1 neurofibromatosis and malignant myeloid disorders. N Engl J Med. 1994;330: 597-601.
13. Xu G, Nelson L, O'Connell P, White R. An Alu polymorphism intragenic to the neurofibromatosis, type 1 gene. Nucleic Acids Res. 1991;19:3764.
14. Lazaro C, Gaona A, Xu G, Weiss R, Estivill X. A highly informative CA/GT repeat polymorphism in intron 38 of the human neurofibromatosis type 1 (NF1) gene. Hum Genet. 1993;92:429-430.
15. Andersen LB, Tarle SA, Marchuk DA, Legius E, Collins FS. A compound nucleotide repeat in the neurofibromatosis (NF1) gene. Hum Mol Genet. 1993;2:1083.
16. Leppig KA, Kaplan P, Viskochil D, Weaver M, Ortenberg J, Stephens K. Familial neurofibromatosis 1 gene deletions: cosegregation with distinctive facial features and early onset of cutaneous neurofibromas. Am J Med Genet. 1997;73:197-204.
17. Tischfield JA. Loss of heterozygosity or: how I learned to stop worrying and love mitotic recombination. Am J Hum Genet. 1997;61:995-999.
18. Cavenee WK, Dryja TP, Phillips RA, et al. Expression of recessive alleles by chromosomal mechanisms in retinoblastoma. Nature. 1983;305:779-784.
19. Largaespada DA, Brannan CI, Jenkins NA, Copeland NG. *Nf1* deficiency causes Ras-mediated granulocyte-macrophage colony stimulating factor hypersensitivity and chronic myeloid leukemia. Nature Genet. 1996;12:137-143.
20. Flotho C, Valcamonica S, Mach-Pascual S, et al. *RAS* mutations and clonality analysis in children with juvenile myelomonocytic leukemia (JMML). Leukemia 1999;13;32-37.
21. Boguski MS, McCormick F. Proteins regulating Ras and its relatives. Nature. 1993;366:643-654.
22. O'Marcaigh AS, Shannon KM. Role of the NF1 gene in leukomenesis and myeloid growth control. J Pediatr Hematol Oncol. 1997;19:551-554.
23. Zhang Y, Vik, TA, Ryder, JW, et al. Nf1 regulates hematopoietic progenitor cell growth and Ras signaling in response to multiple cytokines. J Exp Med. 1998;187:1893-1902.
24. Emanuel PD, Bates LJ, Castleberry RP, Gualtieri RJ, Zuckerman KS. Selective hypersensitivity to granulocyte-macrophage colony stimulating factor by juvenile chronic myeloid leukemia hematopoietic progenitors. Blood. 1991;77:925-929.
25. Bollag G, Clapp DW, Shih S, et al. Loss of *NF1* results in activation of the Ras signaling pathway and leads to aberrant growth in murine and human hematopoietic cells. Nature Genet. 1996;12: 144-148.

Tumor Suppressor Inactivation by Double Mitotic Recombination at Clustered Breakpoint Intervals

Karen Stephens[1,2,3], Molly Weaver[1], Kathleen A. Leppig[4], Kyoko Maruyama[1], Peter D. Emanuel[5], Elizabeth M. Davis[6], Rafael Espinosa III[6], Michelle M. Le Beau[6], Kevin M. Shannon[7]

Departments of Medicine[1], Laboratory Medicine[2], Pathology[3], Pediatrics[4], University of Washington, Seattle, Washington 98195-7720

[4]Division of Hematology Oncology, Hospital for Sick Children, Toronto, Ontario, M5G1X8 Canada

[5]Division of Hematology/Oncology, Department of Medicine, University of Alabama at Birmingham, Birmingham, Alabama 35294-3300

[6]Department of Medicine, Section of Hematology/Oncology, University of Chicago, Chicago, Illinois 60637-1470

[7]Department of Pediatrics, University of California, San Francisco, California 94143-0519.

Communicating author:
Karen Stephens, PhD
University of Washington
Medical Genetics 357720
Seattle, WA 98195
Phone: 206-543-8285
FAX: 206-685-4829
millie@u.washington.edu

ABSTRACT

Homozygous inactivation of tumor suppressor genes is a fundamental mechanism of tumorigenesis that is frequently associated with loss of heterozygosity (LOH). Here we show that somatic inactivation at the *NF1* tumor suppressor gene is commonly associated with isodisomy of a 60 Mb interstitial segment of the long arm of chromosome 17 in myeloid leukemias from neurofibromatosis 1 patients. Unexpectedly, both the centromeric and telomeric LOH breakpoints were clustered at specific locus intervals. In these cases, the malignant precursor cell developed LOH by a novel mechanism whereby interstitial isodisomy occurred by homologous recombination at two putative mitotic recombination hotspots during the S/G2 phase of the cell cycle. LOH at interstitial chromosomal loci, which occurs frequently in human tumors, is commonly assumed to arise by deletion with ill-defined LOH breakpoints. Interstitial isodisomy with clustered breakpoints may be a common, but previously unrecognized, mechanism of LOH in human cancer. If so, this would have significant implications for mechanisms of tumorigenesis and for identifying mitotic recombination-prone sites in the genome.

INTRODUCTION

Homozygous inactivation of tumor suppressor genes is a fundamental mechanism of tumorigenesis. It occurs by either sequential somatic inactivation of both alleles or by a somatic mutation in the single normal homolog in individuals who inherit a germline mutation in one allele. Somatic inactivation is frequently associated with loss of heterozygosity (LOH) at the tumor suppressor locus and at multiple flanking loci[1,2]. Defining the minimum chromosomal region showing LOH in a collection of tumors has provided a powerful strategy for mapping and cloning tumor suppressor genes. The discovery of *RB1* was followed by extensive investigations showing that gene inactivation in retinoblastoma tumors involves any one of a number of mechanisms, for example, methylation, intragenic point mutation, deletion of a gene, a chromosome arm, or even loss of an entire chromosome[2-4]. Remarkably little is known, however, about the mechanisms that underlie LOH at most tumor suppressor loci and the potential involvement of linked genes that might cooperate in tumorigenesis has received limited attention.

Inactivating mutations in the *NF1* tumor suppressor gene at chromosome band 17q11.2 cause the autosomal dominant disorder neurofibromatosis type 1 (NF1), which affects about 1 in 4000 persons[5]. While virtually all affected individuals demonstrate multiple benign neurofibromas, only a small percentage develop other NF1-associated neoplasms such as optic glioma, pheochromocytoma, malignant myeloid leukemia or malignant peripheral nerve sheath tumor[6,7]. LOH at the *NF1* locus has been reported in neurofibromas, in a variety of NF1-associated malignancies, and in tumors from heterozygous *Nf1* mice[8-11]. Tumors that arise in individuals with familial NF1 invariably show LOH at the allele inherited from their unaffected parent, consistent with homozygous inactivation of *NF1*. Somatic intragenic *NF1* mutations have been identified in a few primary tumors[12,13], thereby providing compelling evidence that functional inactivation of *NF1* is central to tumorigenesis. Genetic and biochemical studies performed to date support a model whereby the tumor suppressor function of *NF1* is mediated by the ability of it's protein product, neurofibromin, to negatively regulate ras (reviewed in ref. 14). Neurofibromin is a GTPase activating protein (GAP) for members of the $p21^{ras}$ (Ras) family, which negatively regulate ras output by accelerating the conversion of active ras•GTP to inactive ras•GDP.

In the present study, we sought to determine whether LOH at the *NF1* locus in leukemic cells from children with NF1 was associated with a somatic deletion and whether it was comparable to those reported in patients with germline *NF1* contiguous gene deletions. Patients with germline 1.5 Mb microdeletions are remarkable for minor facial anomalies along with both an early age at onset and increased numbers of cutaneous neurofibromas[14-19]. These, and additional genetic studies, support a hypothesis whereby the co-deletion of *NF1* and a nearby putative neurofibroma-potentiating locus (*NPL*) causes an early age at onset and a heavy burden of neurofibromas. Recently, we found that in >80% of cases, the germline *NF1* microdeletion breakpoints clustered at flanking 75-100 kb elements of high sequence identity termed NF1REP[19]. These data strongly implicated a deletion mechanism involving NF1REP-mediated homologous recombination, which was subsequently shown to result from meiotic recombination primarily during female gametogenesis[20]. For this study, we hypothesized that somatic NF1REP-mediated deletion could be the mechanism of LOH in NF1-related myeloid leukemias and that hemizygosity at the putative *NPL* locus could contribute to development of the myeloid tumor. Instead, we found that the leukemic cells from multiple cases showed interstitial isodisomy for a large

segment of chromosome 17 that consistently harbored the inactivated *NF1* allele. The clustering of the LOH breakpoints at small centromeric and telomeric marker intervals is unprecedented and has broad implications for the pathogenesis of human tumors.

RESULTS

Delineation of a large region of LOH in an *NF1*-associated leukemia

In a previous study, genetic analysis of bone marrows from children with NF1 revealed LOH at *NF1* in the $CD34^+$ subpopulation of immature myeloid cells. Lymphoblasts immortalized by Epstein-Barr virus, however, typically retained *NF1* heterozygosity[21]. A single exception was found in a 9-month-old boy with sporadic NF1 and an unusual myeloproliferative disorder whose bone marrow and immortalized lymphoblastoid cells both showed loss of the maternal *NF1* allele[21]. Therefore, this malignant clone was derived from a progenitor cell capable of producing both myeloid and lymphoid cells. The retained *NF1* paternal allele carried a *de novo* R1276X mutation that encoded a truncated protein lacking the GAP domain[12,21]. To determine if the bone marrow cells of this patient showed LOH at loci flanking *NF1*, a series of chromosome 17 polymorphic loci were analyzed. LOH of maternally-derived alleles was detected at multiple loci spanning nearly the entire q arm from D17S33 in band q11.2 to D17S928 in band q25, an estimated 60 Mb (patient 1, Figures 1 and 2).

LOH is the result of interstitial isodisomy in patient 1

Cytogenetic analyses of bone marrow and immortalized lymphoblastoid cells from the malignant clone of patient 1 revealed a karyotype of 46,XY with no detectable chromosomal abnormalities. These results suggested that the 60 Mb LOH region was not deleted, but present in two copies. To address this possibility, we performed fluorescent *in situ* hybridization (FISH) on the lymphoblastoid cells with probe P1-12, a P1 bacteriophage genomic clone containing a large segment of *NF1* intron 27b[16]. Hybridization signals were detected on both chromosome 17 homologs (Figure 3a). Together, these data suggest that a large interstitial segment of the maternal chromosome had been replaced with the homologous paternally-derived segment carrying the *NF1* R1276X allele. The cells were homozygous not only for the *NF1* R1276X allele, but for all paternal alleles and sequences in the isodisomic region (Figures 1 and 2). Because interstitial isodisomy was unexpected, it was important to verify that the D17S928 locus, which retained heterozygosity, had not translocated elsewhere in the genome of the malignant cells. A BAC clone near 17qter containing D17S928 was isolated and used as a probe for FISH analysis. Hybridization signals were observed at the q terminus of both chromosome 17 homologs in the patient's tumor and in normal controls consistent with interstitial isodisomy (Figure 3b).

LOH is frequently associated with isodisomy in NF1-associated leukemias

Leukemia specimens showing LOH at *NF1* were identified from nine additional NF1 patients and analyzed by a quantitative *NF1* gene dosage PCR assay. Because this assay was originally validated for copy number determination in normal leukocytes, initial experiments using DNA from the tumor of patient 1 and DNA from normal tissue of his parents were performed. Each of these sample gave *NF1* gene dosage values ranging from 0.91 - 1.08 (Table 1). These values are consistent with disomy at *NF1* in the patient's tumor, as indicated by cytogenetic and FISH analyses, and in his parents constitutional DNA. Because these data suggested that the assay may be valid for zygosity analysis of leukemic cells,

9 additional NF1-related leukemias were assayed. Seven out of nine tumors had *NF1* dosage values consistent with disomy and two had values indicating monosomy (Table 1).

Cryopreserved bone marrow specimens, available from 5 of the 10 patients, were analyzed by FISH to corroborate the *NF1* dosage assay results. The cells were hybridized with a chromosome 17 centromere-specific probe (Cep®17) and with two *NF1* probes (P1-9 and P1-12). The probe P263P1 from a region of chromosome 5, not involved in leukemic rearrangements in these patients, was co-hybridized with each *NF1* probe to control for the increased number of cells with one or no signals that can be seen in cryopreserved bone marrow cells. Because the results for *NF1* probes P1-9 and P1-12 were comparable, only the P1-12 data are shown in Figure 3d. The complete distribution of signals for the four probes is available at website. These experiments provided physical confirmation that the leukemias of patients 3-6 contained two *NF1* alleles. Although the percentage of cells with two signals for the P1-12 probe was lower in patient 6 (76%) than for patients 3-5, two signals were noted in 95% of cells with the other *NF1* probe, P1-9. The bone marrow of patient 10 revealed monosomy for *NF1* showing two signals in 67% and one signal in 29% of cells. Two chromosomes 17 were detected by the centromere-specific probe, consistent with an interstitial deletion as predicted by the *NF1* dosage assay (Table 1). As a further control, cryopreserved bone marrow cells from four children with NF1 and malignant myeloid leukemias that did not show LOH, and from a non-NF1 patient with acute myeloid leukemia in complete remission were analyzed by FISH. Together the gene dosage and FISH data demonstrate that LOH at *NF1* is usually associated with isodisomy in NF1-related myeloid leukemias.

To confirm that the cells being examined represented the malignant clone, a chromosome 7-specific probe (Cep®7) was hybridized to bone marrow cells of patient 3, who had monosomy 7 and was disomic at *NF1* as measured by both the gene dosage assay and FISH (Table 1 and Figure 3d). As expected, FISH revealed one copy of chromosome 7 in cells that had two signals with the *NF1* probes (Table 2; Figure 3c,d).

Clustering and parental origin of chromosome 17 LOH breakpoints

To delineate the LOH region in the leukemias, multiple polymorphic loci on chromosome 17 were analyzed. Each of the eight leukemias with isodisomy at *NF1* showed a large region of LOH that spanned a 70 cM segment of the q arm (Figure 2). Among these cases, both the proximal and distal LOH breakpoints were clustered at marker intervals. In all eight leukemias, the centromeric breakpoints mapped to a 3 cM interval between D17S959 and D17S975. In some leukemias, informative markers mapped the breakpoint to a narrower interval, as in patient 5 where the breakpoint lies between D17S1878 and D17S975. These two markers are very tightly linked; no crossovers occurred between these markers in 186 meioses (http://www.marshmed.org/genetics/). The distal breakpoints of four of the eight leukemias (patients no. 1-3, and 6) clustered between D17S1822/D17S1830 and D17S928, an interval of 9.6 cM (Figure 2). Therefore, these patients had interstitial isodisomy at loci along a 70 cM (or ~60Mb) segment. We could not determine if the large isodisomic segment in the remaining four patients was interstitial. Each of these cases were isodisomic at D17S1822/D17S1830, but not informative at another qter locus.

In contrast to these eight cases, the region of LOH was much less extensive in the leukemias of patients 9 and 10, which were monosomic at *NF1* as shown by dosage analysis and FISH. The centromeric breakpoints in these cases mapped to the interval between D17S1294 and *NF1* intron 38, while the telomeric breakpoints localized between D17S1800 and D17S250. These data are consistent with an interstitial 1-2 Mb deletion in these leukemic clones.

Leukemic cells of patients 1-3, and 8 had lost maternal alleles and were isodisomic for paternally-derived alleles, whereas the cells of patients 4-7 had lost paternally alleles and were isodisomic for maternally-derived alleles of a comparable chromosomal segment (Figure 2). In each patient with familial NF1, the isodisomic segment was derived from the affected parent. The bone marrows of patients 1 and 10, who were *de novo* cases of NF1 in their families, showed loss of the maternal *NF1* allele (Table 1, Figure 2). These data infer that patients 1 and 10 carried a germline *de novo* mutation of the paternal *NF1* allele and underwent somatic loss of the normal maternal *NF1* allele, which is consistent with the reported parental predispositions for *NF1* germline mutations[19,22,23]. Neither isodisomy nor microdeletion involving either maternally- or paternally-derived sequences were specific to any one type of leukemia (Table 1, Figure 2). In addition, no obvious differences in disease course were detected.

DISCUSSION

Mechanisms of LOH at *NF1* in leukemic cells

Detailed analysis of myeloid malignancies from 10 children with NF1 revealed two distinct patterns of LOH (Figure 4a). In two cases, interstitial microdeletions of 1-2 Mb were identified that resulted in *NF1* monosomy. Surprisingly, the more common mechanism underlying LOH in the eight remaining cases involved isodisomy for about 60 Mb of 17q. We were able to confirm the interstitial nature of these large isodisomic segments in four cases where D17S928 was informative. In addition FISH verified that this 17q subterminal locus had not translocated elsewhere in the genome.

We propose that interstitial isodisomy occurred by a double mitotic recombination event between homologous non-sister chromatids during the S/G2 phase of the cell cycle of an ancestral cell (Figure 4b). One of four possible segregants would have interstitial isodisomy with homozygous inactivation of *NF1*. Tumors with the genotypes of any of the other three possible segregants were not detected, presumably because homozygous inactivation of *NF1* is essential for outgrowth of the leukemic clone[24,25]. The low frequency of double mitotic recombination events, estimated at about 10^{-10} in normal lymphocytes[26], initially makes such a mechanism seem implausible. However, a rare somatic genetic event may be detected frequently if it confers a strong proliferative advantage upon the malignant clone.

Other mechanisms that could give rise to 17q interstitial isodisomy are less likely. A double homologous recombination during G1 could occur, but would have the additional requirement for chromosome duplication. Two sequential single recombination events in different precursor cells are also possible, but would imply that each independent event conferred a proliferative advantage. A gene conversion-like event of a 60 Mb segment would be unprecedented as the converted segments reported in humans are several kb in length[27-29].

Less complex mechanisms could explain the LOH regions observed in the other leukemias. Lack of informative polymorphic markers near 17qter in leukemias of patients 4,5,7, and 8 precluded determining whether the isodisomic regions are interstitial. In these cases, if LOH extends throughout the q arm it presumably arose by a single homologous recombination event between non-sister chromatids during S/G2. The leukemias of patients 9 and 10, which showed LOH restricted to a 1-2 Mb region and *NF1* monosomy, had interstitial deletions. The locations of these deletions resemble those that occur in patients with germline *NF1* contiguous gene deletions[19].

Interstitial isodisomy

LOH in tumor tissue can occur by diverse mechanisms. As detailed in Table 3, tumors that undergo homozygous inactivation of a tumor suppressor gene can either retain or lose constitutional heterozygosity at the tumor suppressor and at neighboring loci. Promoter methylation leading to transcriptional silencing is the paradigm for somatic inactivation with retained heterozygosity[30,31]. In cases where constitutional heterozygosity is lost, the tumor can be either monosomic or disomic at a single locus or at multiple contiguous loci (reviewed in ref. 2-4). LOH resulting in monosomy is due to the physical loss of DNA sequences, while LOH resulting in isodisomy involves the "replacement" of the normal tumor suppressor allele with the mutated homolog. LOH and isodisomy of an entire chromosome occurs if loss by nondisjunction is followed by chromosomal gain (or vice versa)[32,33]. LOH and partial isodisomy for a chromosome arm results from a single mitotic recombination between homologs; all loci between the site of recombination and the telomere are homozygous. This is a common mechanism that accounts for the majority of LOH events in retinoblastomas and in normal human somatic cell lines[34 35,36]. This mechanism also accounts for the 20% of Beckwith-Wiedemann syndrome cases that are mosaic for 11p paternal isodisomy; interestingly, the degree of mosaicism correlates with organ enlargement[37,38].

Examples of LOH occurring at interstitial chromosomal loci are rife in the literature (for example ref. [34,39-44]. However, unambiguous evidence that the involved loci are isodisomic rather than monosomic (deleted) is lacking. In these cases the LOH breakpoints are either not clustered but are unique in each tumor or are poorly defined due to insufficient marker analysis. An extensive review of LOH studies in many tumor types revealed only a single report of two retinoblastomas with interstitial LOH where densitometry of Southern blots demonstrated disomy at the relevant loci[35]. These tumors had different LOH breakpoints. The occurrence of interstitial isodisomy in retinoblastomas reappears in the literature in a particularly intriguing study that screened 74 retinoblastomas with LOH at *RB1* with polymorphic markers across the region[36]. This study found that LOH occurred by nondisjunction (55%), by a single mitotic recombination event (39%), and by apparent triple recombination events leading to interstitial isodisomy (5%, n=4). From these latter cases the authors suggested that negative interference may occur in mitotic recombination. However, these results could also be due to the imprecision of the genetic map. Each apparent recombination event occurred between markers $\leq$3 cM apart and in some instances between markers for which the order could not be resolved with odds > 1,000:1 (ref. 44). The chromosome 13 map was constructed with priority given to marker density rather than marker resolution; only 186 meioses were sampled[45]. This sample size is too small for accurate estimates of meiotic map distances for small recombination fractions. This is demonstrated most elegantly in a comparison of the sex-averaged meiotic map and the DNA sequence of chromosome 21. Under the assumption that the DNA sequence contig is correct, 20% (13/64) of markers are incorrectly ordered on the genetic map; these markers mapped at small recombination fractions of 4 cM or less from their flanking markers[46].

Clustering of LOH breakpoints

Although each of the breakpoint marker intervals represent only about 5-8% of the genetic length of chromosome 17 (Figure 2), their precise physical length awaits the completion of the chromosome 17 sequence. The sequence working draft, however, provides evidence that supports clustered recombination breakpoints. BLAST analysis of the working draft sequence (http://www.ncbi.nlm.nih.gov/blast/blast.cgi?Jform=0, accessed 10/5/00) revealed that D17S33,

D17S1878, and D17S975 all map to BAC/PAC clones in contig ctg15917 within about 1800 kb of one another (http://genome.wustl.edu:8021/pub/gsc1/fpc_files/freeze_2000_06_15/MAP/17map). These data define a ~1800 kb region, or about 1% of the physical length of the chromosome, as the location of the centromeric recombination event in the leukemias of patients 1, 4, and 5. Lack of informative markers precludes determining if the recombination events in other leukemias also map in this region (Figure 2). Similar analysis of markers in the telomeric recombination interval revealed that D17S1830 and D17S1822 map to the same 173 kb BAC, but the region harboring D17S928 is yet to be sequenced.

Why might mitotic recombination be favored at these small chromosomal intervals in the ancestral leukemic clone? Perhaps, these intervals harbor recombination hotspots. Recently, meiotic recombination hotspots were identified in the paralogous NF1REP elements that flank the *NF1* gene (ref. 20 and Dorschner et al., unpublished data). Interestingly, the microdeletions in the leukemias of patients 9 and 10 are similar in location and extent to NF1REP-mediated germline microdeletions[19]. Whether both meiotic and mitotic microdeletions occur by a similar mechanism awaits the development of a junction fragment assay. Paralog-mediated recombination is a plausible explanation for the apparent clustering of recombination events in the leukemias with isodisomy. There are multiple families, each with multiple members, of paralogs on chromosome 17 that mediate rearrangements. These include at least 8 members of the NF1REP family[19], along with the CMT1A- and SMS-REP family of elements that mediate duplication and deletion events that cause Charcot-Marie-Tooth 1A, hereditary neuropathy with liability to pressure palsies, and Smith-Magenis syndrome[47-49]. Although they are known to occur by either unequal crossing over between chromosomes or by an intrachromosomal "looping out" [19,20,49,50], why these regions are predisposed to homologous recombination is not known. Perhaps these elements harbor motifs that are prone to double strand breaks, which stimulate homologous recombination in mammalian cells by several orders of magnitude[51,52].

Malignant myeloid leukemia in children with NF1

Are the LOH patterns similar simply because recombination is favored in certain regions or do they reflect the expression of loci or effects of mutagenic agents that may contribute to the development of malignant myeloid leukemias in children with NF1? Perhaps biallelic expression of a gene (or genes) on the q arm is essential for the clonal proliferation of neurofibromin-deficient hematopoietic cells. Therefore, LOH patterns at *NF1* are restricted to either a 1-2 Mb interstitial deletion or a large isodisomic segment of the q arm. This would predict that different chromosome 17 LOH regions and mechanisms would be found in NF1-associated solid tumors. To date, such analyses have not used a sufficient number of loci to test this prediction. We detected no correlations between extensive isodisomy or confined deletions and a parent of origin effect, leukemia type, or disease course. Thus, our data do not provide a simple explanation for the relative increase in the risk of leukemia in sons who inherit NF1 from their mothers[21]. There are no known imprinted genes on human chromosome 17 nor on mouse chromosome 11, which carries all the syntenic sequences with the exception of a handful of loci that are scattered among other mouse chromosomes[53]. Recently, noncontiguous loci showing LOH were observed in a kidney cell line treated with hydrogen peroxide, suggesting that oxidative damage can induce complex LOH patterns that are unrelated to tumor suppressor gene inactivation[54]. Whether oxidative damage increases the mitotic recombination rate or plays a role in development of the leukemias studied here is unknown.

Broad implications

A broad implication of our study is that interstitial isodisomy may be a frequent but previously unrecognized mechanism in human cancers. Previously, most LOH studies of tumors were restricted to a particular chromosomal region or arm and used a relatively low marker density, of which only a subset were informative. Mei et al.[55] determined that in 17 "genome-wide" LOH studies over the past 5 years, the average number of polymorphic microsatellite loci analyzed was 120, with 280 loci being the greatest number (average distribution of about 27 cM and 12 cM, respectively). Therefore, regions of interstitial LOH could have gone undetected or, if detected, were assumed to result from deletion. It is a common mistake to equate LOH with chromosomal deletion. Recently, automated allelotyping and the use of single nucleotide polymorphisms and high-density arrays are being employed for high resolution analysis of allelic losses and gains in tumors[54,56]. Interestingly, a study of chromosome 3p in lung cancer revealed multiple discontinuous regions of LOH, however, it is not known if these result from deletion or interstitial isodisomy[56]. Such high resolution studies will benefit greatly from the human genome sequence, which will determine the precise order of markers for an accurate evaluation of mitotic recombination events. Regions of LOH associated with partial or interstitial isodisomy will appear normal when analyzed by comparative genomic hybridization, making this approach of limited use for cancers where LOH preferentially results in isodisomy. It is noteworthy, that we found only a single report of germline interstitial isodisomy[58]; whether this is a reflection of low density marker studies or the rarity of such events is unclear.

By combining LOH studies in tumors with cytogenetic and/or molecular analyses to measure gene copy number, we have identified interstitial isodisomy for a common 60 Mb segment of chromosome 17q as a novel mechanism of LOH at the *NF1* locus. In addition, the apparent clustering of both isodisomic and deletion breakpoints implies the presence of regions prone to mitotic recombination. Sequence analysis and tissue specificity of such putative hotspots would contribute significantly to the poorly understood mechanism of mitotic recombination in mammals. Together, LOH and copy number analyses provide the opportunity to detect unique genetic mechanisms of somatic mutation, mitotic recombination-prone sites, putative modifying or imprinted genes, and/or correlations between tumor genotype and neoplastic transformation. In addition, mono- or bi-allelic expression from a locus (loci), other than the tumor suppressor gene itself, could affect the efficacy of putative therapeutic agents.

METHODS

Patients. Clinical descriptions, LOH and *NF1* mutation analyses have been reported previously for most of the patients [9,12,21]. Selected demographic and laboratory data are summarized in Table 1.

***NF1* gene dosage assay.** The *NF1* gene dosage assay is a quantitative, competitive PCR adapted from the method of Celi et al.[59] and performed as described previously[60]. Briefly, it measures the copy number of a segment of *NF1* exon 32 in genomic DNA by quantitating the amount of PCR product relative to that of a competitively amplified segment of a disomic control locus (*APP* on chromosome 21). Validation of the assay on genomic DNA from leukocytes demonstrated that disomy gave *NF1* gene dosage values of 0.98 ± 0.08 S.D., while monosomy (cells from subjects with germline *NF1* microdeletions) gave values of 0.45 ± 0.04 S.D. (S.D., one standard deviation). To approximate a 95% confidence interval, values indicative of germline disomy or monosomy were set at the mean ± 2 S.D. Therefore, *NF1* dosage values for disomy are 0.82 - 1.14 and for monosomy are 0.37 - 0.53.

Fluorescence In Situ Hybridization. Metaphase chromosome preparations of immortalized lymphoblastoid cells, derived from the malignant clone of patient no. 1, were prepared and hybridized as described previously[16]. The bacteriophage P1 probe P1-12, contains ~55 kb of sequence from *NF1* intron 27b[16]. BAC clone 1000G21 was identified by hybridization of the amplified product of the D17S928 locus (http://gdbwww.gdb.org/) to filter arrays of the RPCI-11 human male BAC library, segment 4 (Roswell Park Cancer Institute, Buffalo, NY). Hybridization signals were detected using a commercial system (Vector). Chromosomes were banded using Hoechst 33258-actinomycin D staining and counterstained with propidium-iodide and signals visualized by fluorescence microscopy using a dual band pass filter (Omega).

Cryopreserved bone marrow samples were thawed and cultured at $1x10^6$ cells/ml for 24 hr (90% RPMI 1640/10% fetal bovine serum, 100 U/ml penicillin, 100 µg/ml Streptomycin, 10 mM HEPES) at 37°C in 95% air/5% CO2. Following incubation, the cells were exposed to hypotonic KCl (0.75 M, 8 min, 37°C), fixed in absolute methanol:glacial acetic acid (3:1), and air dried on slides. *NF1* probes were P1 bacteriophage clone P1-9, which spans ~65 kb of the *NF1* gene including exons 2-11, and clone P1-12 (ref.24). Centromere-specific probes for chromosomes 7 and 17 (CEP®7-Spectrum Green™ and CEP®17-Spectrum Green™, Vysis, Inc., Downer's Grove, IL), and the PAC clone P263P1 (Genome Systems Inc., St. Louis, MO), were hybridized as controls. P263P1 was isolated by screening the PAC library using primers for D5S479, and contains an insert of 70 kb derived from 5q31. Labeled probes were prepared by nick-translation using Bio-11-dUTP (Enzo Diagnostics, New York, NY) or digoxigenin-11-dUTP (Boehringer Mannheim, Indianapolis, IN). Interphase FISH was performed as described previously[61]. Hybridization of probes labeled with either biotin or digoxigenin was detected with fluorescein-conjugated avidin (Vector Laboratories, Burlingame, CA) and rhodamine-conjugated anti-digoxigenin antibodies (Boehringer Mannhein), respectively. Nuclei were counterstained with 4,6,-diamidino-2-phenylindole-dihydrochloride (DAPI). The slides were randomized and examined by two observers in a blinded fashion, with 500 cells scored by each observer for each probe. The distribution of hybridization signals per nucleus for the CEP®17 probe was determined in bone marrow cells from healthy control individuals (N=10, Table 2).

Mapping LOH regions. Polymorphic loci were genotyped by PCR amplification as described [9,62] (http://gdbwww.gdb.org/). LOH at the *NF1* locus was evaluated by PCR analysis of at least one informative intragenic site including exon 5, intron 27B *Alu*I/*Alu*II, and intron 38 (ref. 31). LOH was determined by comparing the locus genotype in the patient's tumor DNA to that of peripheral blood DNA of the patient's parents. For patients no. 1, 4, 5, 9, and 10 normal tissue or an EBV-transformed cell line was available to confirm a constitutional genotype that included biparental inheritance of *NF1* alleles[21,63]. Segregation of alleles from parents to child for multiple informative loci on autosomes other than 17 was consistent with parentage as stated for each case (data not shown). Genetic distances are from the chromosome 17 sex-averaged map of the Center for Medical Genetics, Marshfield Medical Research and Education Foundation (http://www.marshmed.org/genetics/).

ACKNOWLEDGMENTS

We thank Virginia P. Sybert and Eric Sievers for referral of patient no. 1, Melvin H. Freedman for bone marrow samples, and Michael Dorschner for BAC1000G21. This research was supported in part by U.S. Army Medical Research and Materiel Command grant NF960043 (K.S.) and NIH grants PO1 CA40046 (M.M.L, K.M.S) and R0172614 (K.M.S.).

FIGURE LEGENDS

Figure 1. LOH at chromosome 17 loci in leukemic cells. Selected examples of LOH analysis in the tumor of patient 1 are shown. The loci, arranged in their unique order on the q arm of chromosome 17, document the interstitial nature of the LOH region. The flanking loci D17S33 and D17S928 retained heterozygosity, while intervening loci lost the paternal allele.

Figure 2. LOH at chromosome 17 loci in malignant myeloid cells of children with NF1. For each patient, a schematic of the chromosome 17 homolog that showed LOH is depicted. For patients 1-3, and 8 the maternal homolog is shown with the region of paternal isodisomy shaded. For patients 4-7, the paternal homolog is shown with the region of maternal isodisomy shaded. Hatched marks designate regions where a lack of informative loci precluded determining if the LOH region was interstitial in nature. For patients 9 and 10, the deleted regions are shaded with their parental origin indicated below. Loci that were informative in each patient are designated with a dash to the left of the chromosome; loci that were tested but not informative are not shown on the figure. Genetic map not drawn to scale, see marker intervals in cM on the right. Locus order and distances are from a sex-averaged genetic map (http://www.marshmed.org/genetics/) and from the analysis of a panel of somatic cell hybrids carrying segments of chromosome 17 (ref. 24,31,33). The unique order of q proximal loci D17S1294, UT172, NF1, and D17S1800 have been confirmed by physical mapping[19,64]. The unique order of other closely linked markers at q proximal (D17S959; D17S33, D17S1878, D17S975) and q distal (D17S836, D17S1806, D17S1822, D17S1930) cannot be determined due to the small sample size (188 meioses) used to construct this meiotic map (http://research.marshfieldclinic.org/genetics/Map_Markers/maps/IndexMapFrames.html).

Figure 3 (a-d). Fluorescence in situ hybridization of tumor cells. Metaphase spreads of immortalized lymphoblastoid cells of the malignant clone of patient 1 were hybridized with (a) *NF1* probe P1-12 and (b) BAC clone 1000G21 containing the locus D17S928. Each of 20 metaphase cells examined had signals on both chromosome 17 homologues, consistent with disomy at each locus. As expected, FISH of cells from a known *NF1* hemizygous individual with the probe P1-12 showed 48 of 50 metaphases with signals on only one chromosome 17 homologue (data not shown). The chromosome 17 homologs were identified by the Hoechst/actinomycin D staining, which reveals a Q-banding like pattern. (c) Dual-color FISH performed by co-hybridizing a digoxigenin-labeled *NF1* probe (P1-12), detected with rhodamine-conjugated anti-digoxigenin antibodies), and an α-satellite probe specific for the centromere of chromosome 7 (CEP®7) revealed monosomy 7 and disomy for the *NF1* gene in bone marrow cells from patient 3. (d) FISH analysis of myeloid leukemia cells with *NF1* (red triangle) and control probes. Probe 263P1 is a 70 kb PAC clone containing D5S479 (5q31) (yellow squares). CEP^R17 is a centromere-specific probe for chromosome 17 (green circles), and CEP^R7 is a centromere-specific probe for chromosome 7 (blue diamond). C1 is a cryopreserved bone marrow sample from a patient with AML-M4 in complete remission. Control samples C2-C5 are cryopreserved bone marrow samples from 4 children with myeloid leukemias that retained heterozygosity at the *NF1* locus. The mean distribution of signals (μ) for the chromosome 17 centromere-specific probe was determined by the interphase analysis of bone marrow cells from 10 healthy individuals.

Figure 4. LOH patterns and mechanisms in leukemic cells of children with NF1. (a) The two different patterns of LOH observed in the tumors analyzed are depicted. The interstitial isodisomic and deleted

regions can be of maternal or paternal origin. (b) A possible mechanism for double mitotic recombination during S/G2 leading to interstitial isodisomy in a progenitor cell. In this example, the germline maternal homolog carries the inactivated *NF1* allele (**X**) and the paternal homolog the normal *NF1* allele (*IIII*).

REFERENCES

1. Fearon, E.R. Human cancer syndromes: clues to the origin and nature of cancer. *Science* 278, 1043-50 (1997).
2. Tischfield, J.A. Loss of heterozygosity or: How I learned to stop worrying and love mitotic recombination. *Am J Hum Genet* 61, 995 -- (1997).
3. Cavenee, W.K. *et al.* Expression of recessive alleles by chromosomal mechanisms in retinoblastoma. *Nature* 305, 779- (1983).
4. Qian, F. & Germino, G.G. "Mistakes happen": Somatic mutation and disease. *Am J Hum Genet* 61, 1000-1005 (1997).
5. Friedman, J. & VM, R. Neurofibromatosis 1. Clinical and Epidemiologic Features. in *Neurofibromatosis. Phenotype, Natural History, and Pathogenesis* (eds. JM, F., DH, G., M, M. & VM, R.) 29-86 (The Johns Hopkins University Press, Baltimore, 1999).
6. Mulvihill, J.J. Malignancy: epidemiologically associated cancers. in *The Neurofibromatoses: A pathogenetic and Clinical Overview* (eds. Huson, S.M. & Hughes, R.A.C.) 487 (Chapman & Hall Medical, London, 1994).
7. Woodruff, J.M. Pathology of tumors of the peripheral nerve sheath in type 1 neurofibromatosis. *Am J Med Genet (Semin Med Genet)* 89, 23-30 (1999).
8. Colman, S.D., Williams, C.A. & Wallace, M.R. Benign neurofibromas in type 1 neurofibromatosis (NF1) show somatic deletions of the NF1 gene. *Nature Genet* 11, 90-2 (1995).
9. Shannon, K.M. *et al.* Loss of the normal NF1 allele from the bone marrow of children with type 1 neurofibromatosis and malignant myeloid disorders [see comments]. *N Engl J Med* 330, 597-601 (1994).
10. Xu, W. *et al.* Loss of NF1 alleles in phaeochromocytomas from patients with type I neurofibromatosis. *Genes Chromosomes Cancer* 4, 337-42 (1992).
11. Jacks, T. *et al.* Tumour predisposition in mice heterozygous for a targeted mutation in Nf1. *Nature Genet* 7, 353-61 (1994).
12. Side, L. *et al.* Homozygous inactivation of the NF1 gene in bone marrow cells from children with neurofibromatosis type 1 and malignant myeloid disorders. *N Engl J Med* 336, 1713-1720 (1997).
13. Sawada, S. *et al.* Identification of NF1 mutations in both alleles of a dermal neurofibroma. *Nature Genet* 14, 110-2 (1996).
14. Kayes, L.M., Riccardi, V.M., Burke, W., Bennett, R.L. & Stephens, K. Large de novo DNA deletion in a patient with sporadic neurofibromatosis 1, mental retardation, and dysmorphism. *J Med Genet* 29, 686-90 (1992).
15. Kayes, L.M. *et al.* Deletions spanning the neurofibromatosis 1 gene: identification and phenotype of five patients. *Am J Hum Genet* 54, 424-36 (1994).
16. Leppig, K.A. *et al.* The detection of contiguous gene deletions at the neurofibromatosis 1 locus with fluorescence in situ hybridization. *Cytogenet Cell Genet* 72, 95-8 (1996).
17. Wu, B.-L., Austin, M., Schneider, G., Boles, R. & Korf, B. Deletion of the entire NF1 gene detected by FISH: four deletion patients associated with severe manifestations. *Am J Med Genet* 59, 528-535. (1995).

18. Correa, C.L. *et al.* Molecular studies in 20 submicroscopic neurofibromatosis type 1 gene deletions. *Hum Mutat* 14, 387-93 (1999).
19. Dorschner, M.O., Sybert, V.P., Weaver, M., Pletcher, B.A. & Stephens, K. NF1 microdeletion breakpoints are clustered at flanking repetitive sequences. *Hum Mol Genet* 9, 35-46 (2000).
20. Correa, C.L., Brems, H., Lazaro, C., Marynen, P. & Legius, E. Unequal Meiotic Crossover: A Frequent Cause of NF1 Microdeletions. *Am J Hum Genet* 66, 1969-1974 (2000).
21. Miles, D. *et al.* Patterns of hematopoietic lineage involvement in children with neurofibromatosis, type 1 and malignant myeloid disorders. *Blood* 88, 4314-4320 (1997).
22. Stephens, K. *et al.* Preferential mutation of the neurofibromatosis type 1 gene in paternally derived chromosomes. *Hum Genet* 88, 279-82 (1992).
23. Jadayel, D. *et al.* Paternal origin of new mutations in von Recklinghausen neurofibromatosis. *Nature* 343, 558-9 (1990).
24. Kalra, R., Paderanga, D.C., Olson, K. & Shannon, K.M. Genetic analysis is consistent with the hypothesis that NF1 limits myeloid cell growth through p21ras. *Blood* 84, 3435-9 (1994).
25. Largaespada, D.A., Brannan, C.I., Shaughnessy, J.D., Jenkins, N.A. & Copeland, N.G. The neurofibromatosis type 1 (NF1) tumor suppressor gene and myeloid leukemia. *Curr Top Microbiol Immunol* 211, 233-9 (1996).
26. Morley, A.A., Grist, S.A., Turner, D.R., Kutlaca, A. & Bennett, G. Molecular nature of in vivo mutations in human cells at the autosomal HLA-A locus. *Cancer Res* 50, 4584-7 (1990).
27. Jeffreys, A.J., Tamaki, K., MacLeod, A., Monckton, D.G. & Neil, D.L., Armour, J.A.L. Complex gene conversion events in germline mutation at human minisatellites. *Nat Genet* 6, 136-145 (1994).
28. Giordano, M., Marchetti, C., Chiorboli, E., Bona, G. & Richiardi, P.M. Evidence for gene conersion in the generation of extensive polymorphism in the promoter of the growth hormone gene. *Hum Genet* 100, 249-255 (1997).
29. Collier, S., Tassabehji, M., Sinnott, P. & Strachan, T. A de novo pathological point mutation at the 21-hydroxylase locus: implications for gene conversion in the human genome [published erratum appears in Nat Genet 1993 May;4(1):101]. *Nat Genet* 3, 260-5 (1993).
30. Herman, J.G. *et al.* Silencing of the VHL tumor-suppressor gene by DNA methylation in renal carcinoma. *Proc Natl Acad Sci USA* 91, 9700-9704 (1994).
31. Schroeder, M. & Mass, M.J. CpG methylation inactivates the transcriptional activity of the promoter of the human p53 tumor suppressor gene. *Biochem-Biophys-Res-Commun* 235, 403-406 (1997).
32. Robinson, W.P. *et al.* Somatic segregation errors predominantly contribute to the gain or loss of a paternal chromosome leading to uniparental disomy for chromosome 15. *Clin Genet* 57, 349-58 (2000).
33. Dutly, F. *et al.* Seven cases of Wiedmann-Beckwith syndrome, including the first reported case of mosaic paternal isodisomy along the whole chromosome 11. *Am J Med Genet* 79, 347-53 (1998).
34. Gupta, P.K. *et al.* High frequency *in vivo* loss of heterozygosity is primarily a consequence of mitotic recombination. *Cancer Res* 57, 1188-1193 (1997).
35. Zhu, X. *et al.* Mechanisms of loss of heterozygosity in retinoblastoma. *Cytogenet Cell Genet* 59, 248-52 (1992).

36. Hagstrom, S.A. & Dryja, T.P. Mitotic recombination map of 13cen-13q14 derived from an investigation of loss of heterozygosity in retinoblastomas. *Proc Natl Acad Sci U S A* 96, 2952-7 (1999).
37. Itoh, N., Becroft, D.M., Reeve, A.E. & Morison, I.M. Proportion of cells with paternal 11p15 uniparental disomy correlates with organ enlargement in Wiedemann-beckwith syndrome. *Am J Med Genet* 92, 111-6 (2000).
38. Slatter, R.E. *et al.* Mosaic uniparental disomy in Beckwith-Wiedemann syndrome. *J Med Genet* 31, 749-53 (1994).
39. Sherwood, J.B. *et al.* Chromosome 4 deletions are frequent in invasive cervical cancer and differ between histologic variants [In Process Citation]. *Gynecol Oncol* 79, 90-6 (2000).
40. Abu-Amero, S.N., Ali, Z., Abu-Amero, K.K., Stanier, P. & Moore, G.E. An analysis of common isodisomic regions in five mUPD 16 probands. *J Med Genet* 36, 204-7 (1999).
41. Niederacher, D. *et al.* Patterns of allelic loss on chromosome 17 in sporadic breast carcinomas detected by fluorescent-labeled microsatellite analysis. *Genes Chromosomes Cancer* 18, 181-92 (1997).
42. Cappellen, D., Gil Diez de Medina, S., Chopin, D., Thiery, J.P. & Radvanyi, F. Frequent loss of heterozygosity on chromosome 10q in muscle-invasive transitional cell carcinomas of the bladder. *Oncogene* 14, 3059-66 (1997).
43. Tomlinson, I.P. & Bodmer, W.F. Chromosome 11q in sporadic colorectal carcinoma: patterns of allele loss and their significance for tumorigenesis. *J Clin Pathol* 49, 386-90 (1996).
44. de Nooij-van Dalen, A.G., van Buuren-van Seggelen, V.H., Lohman, P.H. & Giphart-Gassler, M. Chromosome loss with concomitant duplication and recombination both contribute most to loss of heterozygosity in vitro. *Genes Chromosomes Cancer* 21, 30-8 (1998).
45. Dib, C. *et al.* A comprehensive genetic map of the human genome based on 5,264 microsatellites [see comments]. *Nature* 380, 152-4 (1996).
46. Hattori, M. *et al.* The DNA sequence of human chromosome 21. The chromosome 21 mapping and sequencing consortium [see comments]. *Nature* 405, 311-9 (2000).
47. Reiter, L.T. *et al.* Human meiotic recombination products revealed by sequencing a hotspot for homologous strand exchange in multiple HNPP deletion patients. *Am J Hum Genet* 62, 1023-1033 (1998).
48. Potocki, L. *et al.* Molecular mechanism for duplication 17p11.2- the homologous recombination reciprocal of the Smith-Magenis microdeletion. *Nat Genet* 24, 84-7 (2000).
49. Chen, K.S. *et al.* Homologous recombination of a flanking repeat gene cluster is a mechanism for a common contiguous gene deletion syndrome. *Nat Genet* 17, 154-63 (1997).
50. Reiter, L.T., Murakami, T., Koeuth, T., Gibbs, R.A. & Lupski, J.R. The human COX10 gene is disrupted during homologous recombination between the 24 kb proximal and distal CMT1A-REPs. *Hum Mol Genet* 6, 1595-603 (1997).
51. Moynahan, M.E. & Jasin, M. Loss of heterozygosity induced by a chromosomal double-strand break. *Proc Natl Acad Sci USA* 94, 8988-8993 (1997).
52. Liang, F., Han, M., Romanienko, P.J. & Jasin, M. Homology-directed repair is a major double-strand break repair pathway in mammalian cells. *Proc Natl Acad Sci U S A* 95, 5172-7 (1998).
53. Beechey, C.V., Cattanach, B.M. & Selley, R.L. World Wide Web Site - Mouse Imprinting Data and References (URL: http://www.mgu.har.mrc.ac.uk/imprinting/implink.html). Vol. 2000 (MRC Mammalian Genetics Unit, Harwell, Oxfordshire., 2000).

54. Turker, M.S. *et al.* A novel signature mutation for oxidative damage resembles a mutational pattern found commonly in human cancers. *Cancer Res* 59, 1837-9 (1999).
55. Mei, R. *et al.* Genome-wide detection of allelic imbalance using human SNPs and high-density DNA arrays. *Genome Res* 10, 1126-37 (2000).
56. Wistuba, II *et al.* High resolution chromosome 3p allelotyping of human lung cancer and preneoplastic/preinvasive bronchial epithelium reveals multiple, discontinuous sites of 3p allele loss and three regions of frequent breakpoints. *Cancer Res* 60, 1949-60 (2000).
57. Girard, L., Zochbauer-Muller, S., Virmani, A.K., Gazdar, A.F. & Minna, J.D. Genome-wide allelotyping of lung cancer identifies new regions of allelic loss, differences between small cell lung cancer and non-small cell lung cancer, and loci clustering. *Cancer Res* 60, 4894-906 (2000).
58. Martin, R.A., Sabol, D.W. & Rogan, P.K. Maternal uniparental disomy of chromosome 14 confined to an interstitial segment (14q23-14q24.2). *J Med Genet* 36, 633-6 (1999).
59. Celi, F. *et al.* Determination of gene dosage by a quantitative adaptation of the polymerase chain reaction (gd-PCR): rapid detection of deletions and duplications of gene sequences. *Genomics* 21, 304-310 (1994).
60. Maruyama, K., Leppig, K. & Stephens, K. A gene dosage PCR assay for rapid and sensitive identification of patients with NF1 gene deletion. *Am J Hum Genet* 57S, A219 (1995).
61. Le Beau, M.M. *et al.* Cytogenetic and molecular delineation of a region of chromosome 7 commonly deleted in malignant myeloid diseases. *Blood* 88, 1930-1935 (1996).
62. Leppig, K. *et al.* Familial neurofibromatosis 1 gene deletions: cosegregation with distinctive facial features and early onset of cutaneous neurofibromas. *Am J Med Genet* 73, 197-204 (1997).
63. Luna-Fineman, S., Shannon, K.M. & Lange, B.J. Childhood monosomy 7: epidemiology, biology, and mechanistic implications. *Blood* 85, 1985-1999 (1995).
64. Shen, S. *et al.* Refined mapping of the human serotonin transporter (SLC6A4) gene within 17q11 adjacent to the CPD and NF1 genes. *Eur J Hum Genet* 8, 75-8 (2000).

Table 1. NF1 gene dosage in bone marrows of NF1 children with malignant myeloid disorders.

Patient No.	Sex	Age at Onset	Diagnosis	Origin of *NF1* mutation	LOH at *NF1* Locus	*NF1* Gene Dosage Value[a,b]	Predicted *NF1* Gene Copy No.[a]
1	M	9 mo	MPS	*de novo*	maternal	0.99	disomy
2	M	10 mo	AML	paternal	maternal	0.93	disomy
3	M	24 mo	monosomy 7	unknown	maternal	0.96	disomy
4	M	14 mo	JMML	maternal	paternal	0.86	disomy
5	F	30 mo	JMML	maternal	paternal	0.94	disomy
6	M	10 mo	JMML	maternal	paternal	0.87	disomy
7	M	5 mo	monosomy 7	maternal	paternal	0.90	disomy
8	F	18 mo	MPS	paternal	maternal[a]	0.85	disomy
9	M	5 yr	JMML	maternal	paternal	0.57	monosomy
10	M	19 mo	monosomy 7	*de novo*	maternal[a]	0.48	monosomy

[a] Data from this study.

[b] Measured in unfractionated bone marrow cells, except patients 3, 9 for whom leukemic cells in peripheral blood were used.

Table 2. Interphase fluorescence *in situ* hybridization analysis of bone marrow samples.

Patient[+]	Chr. 17	Number of Hybridization Signals					Control*	Number of Hybridization Signals				
		0	1	2	3	≥4		0	1	2	3	≥4
3	Cep®17	0	6	87	3	4	Cep®7	0	88	12	0	0
	P1-12	1	13	80	6	0	263P1	0	9	88	2	1
4**	Cep®17	0	88	12	0	0						
	P1-12	0.5	13	78	8	0.5	263P1	0.4	7	92	0.6	0
5	Cep®17	0	88	12	0	0						
	P1-12	0.4	6	90	2.6	1	263P1	0.2	4.8	93	0.5	1.5
6**	Cep®17	0	88	12	0	0						
	P1-12	1	9	76	12	2	263P1	0	15	84	0	1
10	Cep®17	0	88	12	0	0						
	P1-12	4	29	67	0	0	263P1	0	3	97	0	0
C1[†]	Cep®17	0	88	12	0	0						
	P1-12	2	5	89	2	2	263P1	0	7	90	1.5	1.5
C2[†]	Cep®17	0	88	12	0	0						
	P1-12	0.5	7	86	5	1.5	263P1	1.6	6	88	3	1.4
C3[†]	Cep®17	0	88	12	0	0						
	P1-12	0	9	85	3.4	2.6	263P1	0	8	89	2	1
C4[†]	Cep®17	0	88	12	0	0						
	P1-12	0.5	9.5	85	4	1	263P1	0.5	17	82	0.5	0
C5[†]	Cep®17	0	88	12	0	0						
	P1-12	0	5	94	1	0	263P1	0	3	96	0.8	0.2
Control[¶]	Cep®17	0	88	12	0	0						
N=10	Mean	0.15	4.5	95	0.24	0.15						
	S.D.	0.19	0.79	0.83	0.25	0.16						

*Probe 263P1 is a 70 kb PAC clone containing D5S479 (chromosome band 5q31 ; Cep®17 and Cep®7 are centromere-specific probe for chromosomes 17 and 7, respectively. [†]Patients no. 3-6, and 10 are described in Table 1. C1 is a cryopreserved bone marrow sample from a patient with AML-M4 in complete remission. C2-C5 are cryopreserved bone marrow samples from 4 children with myeloid leukemias that retained heterozygosity at the

NF1 locus. **FISH of *NF1* probe P1-9 revealed two signals in 86% (patient 4) and 95% (patient 6) of cells examined. ¶The distribution of signals for the chromosome 17 centromere-specific probe was determined by the interphase analysis of bone marrow cells from 10 healthy individuals.

Table 3. Genetic mechanisms leading to somatic inactivation of tumor suppressor genes

Constitutional heterozygosity at tumor suppressor	LOST		RETAINED
Tumor Genotype	Monosomy	Isodisomy	Heterodisomy
Single Locus Affected	• intragenic deletion • illegitimate non-homologous recombination	• gene conversion	• compound heterozygous mutations • methylation → transcriptional silencing
Multiple Loci Affected	• multilocus deletion • nondisjunction → chromosome loss • unbalanced chromosome abnormalities →e.g., translocation, isochromosome	• nondisjunction, chromosome loss, reduplication → chromosomal isodisomy • single homologous recombination → partial isodisomy • double homologous recombination → interstitial isodisomy	

[a]References [2-4,13,52-54]

FIGURE 1

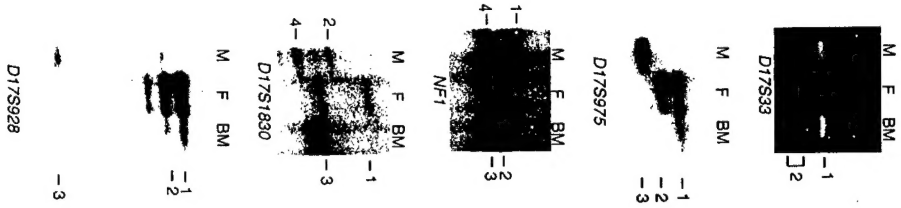

FIGURE 2

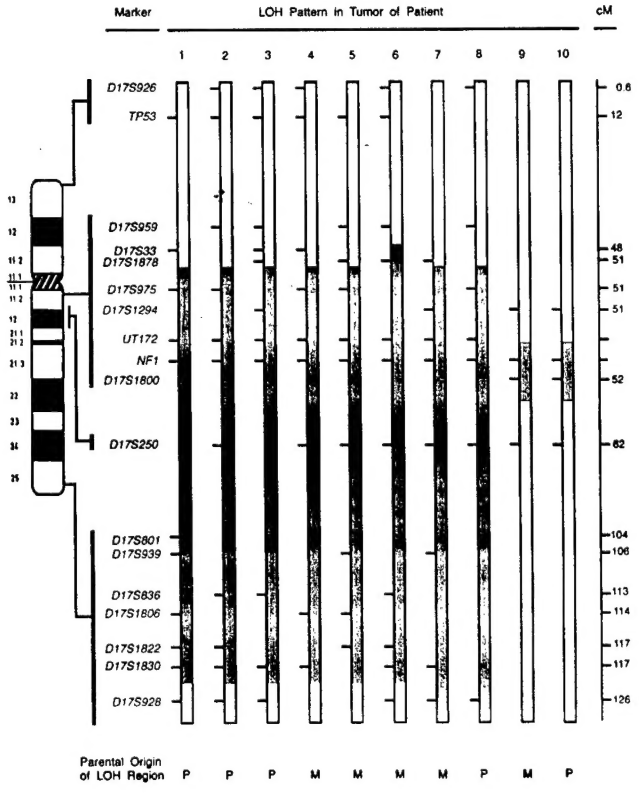

-FIGURE 3

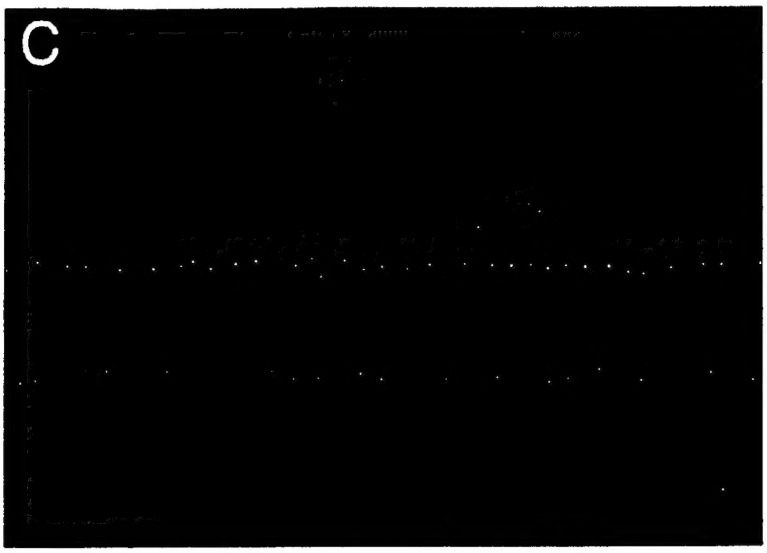

A

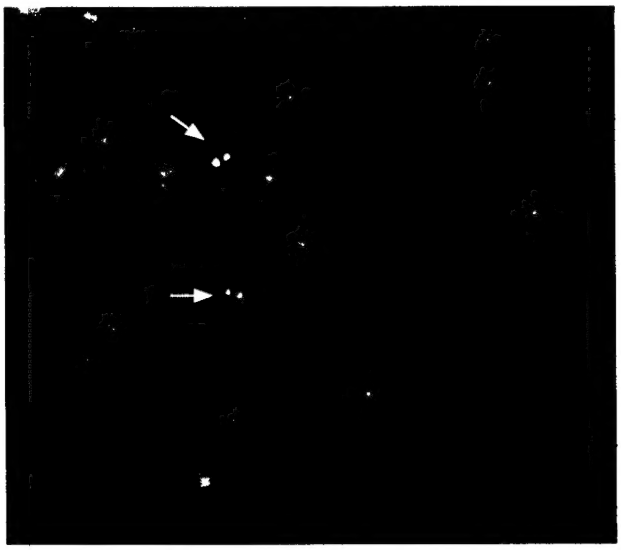

B

FIGURE 3D

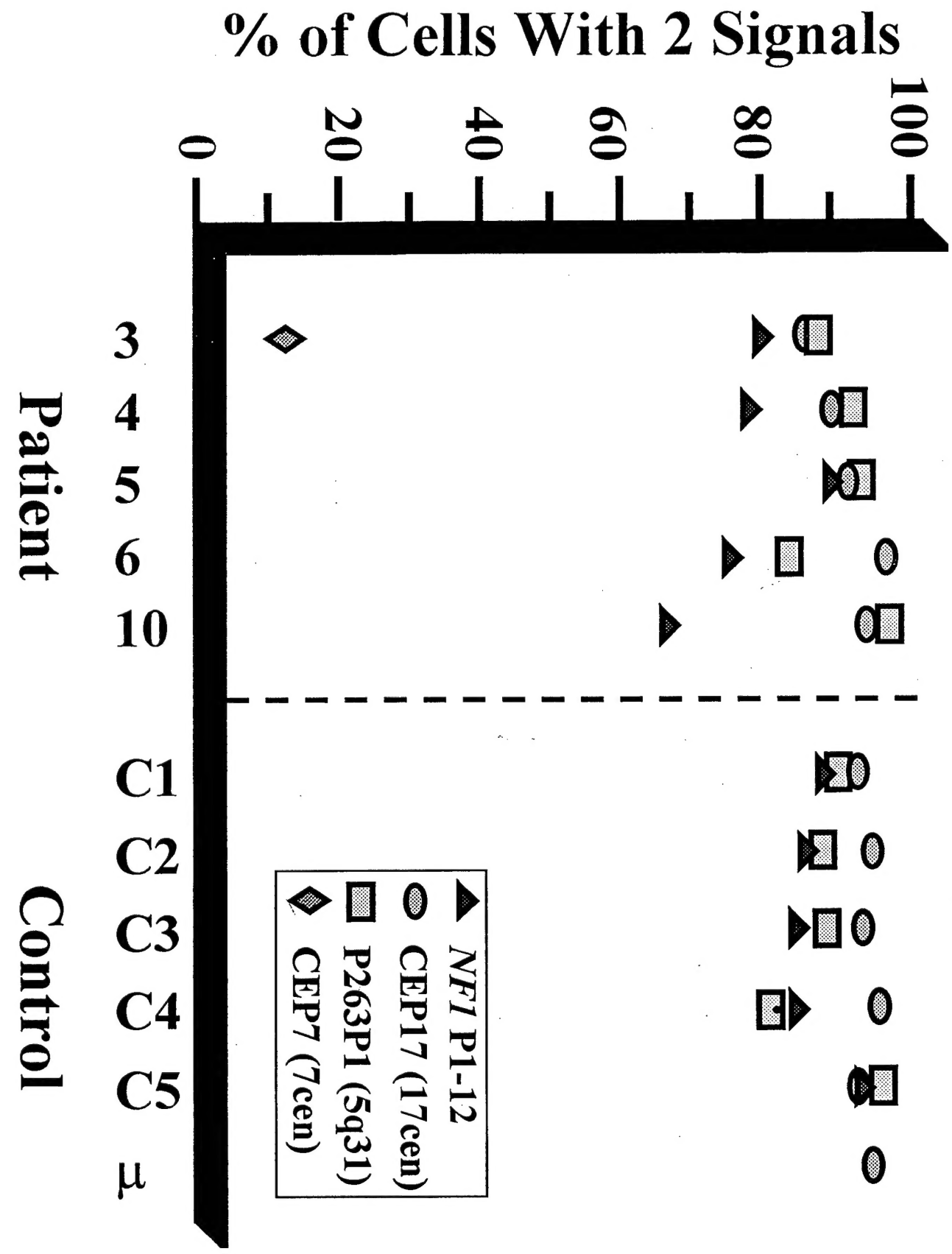
% of Cells With 2 Signals
0
20
40
60
80
100
Patient
3
4
5
6
10
Control
C1
C2
C3
C4
C5
μ
NF1 P1-12
CEP17 (17cen)
P263P1 (5q31)
CEP7 (7cen)

FIGURE 4

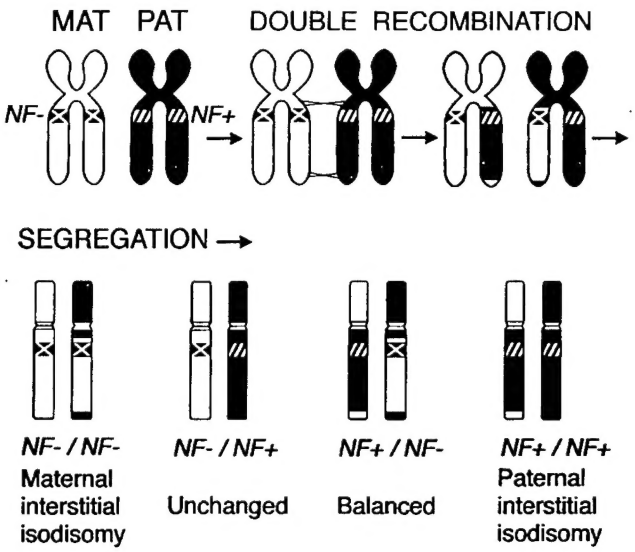
MAT
PAT
DOUBLE RECOMBINATION
NF-
NF+
SEGREGATION →
NF- / NF-
Maternal interstitial isodisomy
NF- / NF+
Unchanged
NF+ / NF-
Balanced
NF+ / NF+
Paternal interstitial isodisomy